Implementation of hiPSC-ECs in thrombosis-on-a-chip devices

João Pedro da Silva Simão

Thesis to obtain the Master of Science Degree in

Biological Engineering

Supervisors: Hugo Johan Albers

Prof. Cláudia Alexandra Martins Lobato da Silva

Examination Committee

President of the Committee: Prof. Jorge Humberto Gomes Leitão

Supervisor: Prof. Cláudia Alexandra Martins Lobato da Silva

Member of the Committee: Prof. Tiago Paulo Gonçalves Fernandes

October 2018

Preface

The work presented in this thesis was performed at the BIOS Lab-on-a-Chip Group, MESA+ Institute for Nanotechnology of the University of Twente (Enschede, The Netherlands), during the period February-August 2018, under the supervision of Hugo Albers (MSc, PhD Candidate), and within the frame of the Erasmus programme. The thesis was co-supervised at Instituto Superior Técnico by Prof. Cláudia Lobato da Silva.

I declare that this document is an original work of my own authorship and that it fulfils all the requirements of the Code of Conduct and Good Practices of the Universidade de Lisboa.

Acknowledgements

I want to start by expressing my gratitude to my supervisor in BIOS, Hugo Johan Albers, for all the knowledge, all the productive and unproductive discussions, all the support you were able to give me in the six months of my stay in the Netherlands. Experiments would not always go our way and the work would not always be perfect, but you would always have some guidance and a friendly “Bom dia, senhor!” for me. And as I told you on the last day I was there, I consider you a mentor, but also a friend. Obrigado.

I would also like to thank every member of the BIOS and the Applied Stem Cells Technologies groups, for trying to help me each time I had some work-related problems, for introducing me to the Dutch culture, and for making me feel welcome in the University and the Netherlands. And a special appreciation to Prof. Andries van der Meer for the valuable suggestions and meetings, which helped me to improve my workplan and experiments, and to Prof. Albert van den Berg for receiving me at BIOS.

I would like to thank my supervisor in Instituto Superior Técnico, Prof. Cláudia Lobato da Silva, for the help with all the guidelines and doubts about the written report and the submission of the thesis.

To my family, for being the pillar that kept me up when I felt down and for making me who I am today. To my mother, for always being there, for all the help, for every call, for all the motivation you were able to give me, even without knowing how important it was. To my father, for all the attempted jokes and playful tone, all the daily emails with photos from past family trips for me to remember to keep going. To my brother, for all the laughter and for being one of my best friends, even if you’ve never heard me say it. To my grandparents, for always caring and checking on me, whether I am in Portugal or in the Netherlands. Without all of you, this would not have been possible.

To all my friends, from my oldest ones in Almada to my newest ones in Porto, a big “thank you!” for the joy, the “catch-up” messages, the fun meals, the reunions. To my friends in Lisbon, my second family, for all the support throughout these last five years. We have experienced more that I will ever be able to describe, and you were always there for me. To Abreu, because “Somos nós contra o mundo”, and we won. To Lourenço, because “Quando se é-se bom, é-se bom”, and we are. To Jacinto, because “Se olharmos para estes anos, já vivemos bastante”, and we did. To Ana, to Cátia, for all the moments, for the late nights, for your endless friendship. And for the rest of the group (you know who you are), for the greatest adventures, for Portimão, for Paredes, for the Interrail, for the EBEC. Thank you.

To everyone I mentioned here, and to everyone who was not listed but also contributed to my work, I express my deepest gratitude. Part of my achievements are also yours.

João Simão, October 2018

Abstract

Thrombosis, characterised by the undesired formation of blood clots within blood vessels, is one of the most important human vascular diseases and remains a major worldwide cause of myocardial infarction and stroke. However, its multifactorial nature and physiological and genetic-related variability make research more difficult, and classical animal and *in vitro* models fail to accurately recapitulate *in vivo* human thrombogenesis. Rapid advancements in the field of microfluidics have recently brought promising results to this area of research, with devices of growing complexity and simpler processes of fabrication being developed. In parallel, the growth of human induced pluripotent stem cells (hiPSC) technology has also been predicted as a major step in scientific research and drug testing, representing a limitless source of human cells with patient-specific properties. Here, we aim at combining microfluidics with hiPSC technology to create patient-specific thrombosis-on-a-chip devices which can be used in research on the disease. Implementation of hiPSC-derived endothelial cells (hiPSC-EC) in the microchip was achieved and optimised and comparison between hiPSC-EC and human primary cells (HUVEC) displayed a more elongated, arterial-like morphology of the former. HiPSC-ECs were also hypothesised to have more plastic shear responsiveness than HUVECs, after nuclear alignment was observed when flow was present in the channel. During blood perfusion experiments in the microfluidic channels, hiPSC-EC presented similar characteristics to human primary cells (HUVECs), with comparable response to the inflammatory agent Tumour Necrosis Factor-α and reproduction of *in* vivo haemostatic mechanisms of platelet aggregation and fibrin deposition.

Keywords: Thrombosis-on-a-chip, Human induced pluripotent stem cells (hiPSC), Human Umbilical Vein Endothelial Cells (HUVEC), Microfluidics, Blood perfusion, Endothelium

Resumo

A trombose é uma doença vascular que se caracteriza pela formação de coágulos em vasos sanguíneos, sendo a principal causa de enfartes do miocárdio e acidentes vasculares cerebrais. Apesar do seu reconhecido impacto, a sua natureza multifatorial, em que se associam variabilidade genética e fisiológica, fazem com que os modelos animais e sistemas *in vitro* clássicos não reproduzam o processo de trombogénese de uma forma fidedigna. O progresso recente no campo da microfluídica tem permitido o desenvolvimento de plataformas mais realistas com resultados prometedores nesta área. Simultaneamente, o desenvolvimento da tecnologia de células estaminais pluripotentes humanas induzidas (hiPSC) tem representado um avanço fundamental na investigação científica, oferecendo uma fonte ilimitada de células humanas com características específicas de cada paciente.

O presente trabalho visa combinar a microfluídica com a tecnologia de hiPSC, de forma a criar dispositivos de *thrombosis-on-a-chip* individualizados que representarão um avanço na investigação futura da doença. Nesse sentido, desenvolveu-se e otimizou-se o processo de implementação de células endoteliais derivadas de hiPSCs no dispositivo. Quando comparadas com células primárias humanas (HUVEC), as hiPSCs assumiram uma morfologia mais alongada e próxima da arterial. A observação de um alinhamento nuclear das hiPSC-ECs na presença de fluxo parece também apontar para uma maior capacidade de resposta ao *stress* mecânico. Durante a realização de testes de perfusão sanguínea no dispositivo, as hiPSC-ECs mostraram ter a capacidade de responder ao agente inflamatório Tumour Necrosis Factor-α e reproduzir as fases principais da hemostase (agregação de plaquetas e deposição de fibrina), observadas em células primárias humanas.

Palavras-chave: Trombose-em-chip, Células estaminais pluripotentes humanas induzidas (hiPSC), Células endoteliais humanas da veia umbilical (HUVEC), Microfluídica, Perfusão sanguínea, Endotélio

Table of contents

List of figures

List of acronyms and abbreviations

2D: Two dimensional
3D: Three dimensional
ADP: Adenosine diphosphate
AJ: Adherens junctions
ATP: Adenosine triphosphate
bFGF: Basic fibroblast growth factor
CAD: Computer-aided design
CAM: Cell adhesion molecule
CD: Cluster of differentiation
CD41: Integrin alpha 2b
DAPI: 4′,6-diamidino-2-phenylindole
$DiOC_6$: 3,3'-Dihexyloxacarbocyanine Iodide
DVT: Deep vein thrombosis
EC: Endothelial cells
ECGM: Endothelial cell growth medium
ECM: Extracellular matrix
FACS: Fluorescent-activated cell sorting
FIX: Factor IX, antihaemophilic factor B
FV: Factor V, proacclerin
FVII: Factor VII, proconvertin
FVIII: Factor VIII, antiheamophilic factor A
FX: Factor X, Stuart-Prower factor
FXI: Factor XI, thromboplastin antecedent
GFP: Green fluorescence protein
hiPSC: Human induced pluripotent stem cell
hiPSC-EC: Human induced pluripotent stem cell-derived endothelial cell
HUAEC: Human umbilical arterial endothelial cell
HUVEC: Human umbilical vein endothelial cell
ICAM-I: Intercellular adhesion molecule 1
JAM: Junctional adhesion molecule
MACS: Magnetic-activated cell sorting
NF-κB: Nuclear factor B
PAR: Protease activated receptor
PDMS: Polydimethylsiloxane
PECAM: Platelet-endothelial cell adhesion molecule
PECAM-1: Platelet-endothelial cell adhesion molecule 1
RBC: Red blood cell

RFP: Red fluorescence protein
RIP: Receptor interacting protein
SERPIN: Serine protease inhibitor
TF: Tissue factor
TJ: Tight junction
TNF-α: Tumour Necrosis Factor-α
TNFR1: Tumour Necrosis Factor Receptor type 1
TNFR2: Tumour Necrosis Factor Receptor type 2
tPA: Tissue plasminogen activator
TRADD: TNF-R1-associated death domain
TRAF2: TNFR-associated factor 2
uPA - urokinase plasminogen activator
VCAM-I: Vascular cell adhesion molecule 1
VE-cadherin: Vascular endothelial cadherin
VEGF: Vascular endothelial growth factor
VT: Venous thrombosis
vWF: von Willebrand Factor
ZO-1: Zona occluden-1
ZO-2: Zona occluden-2

Motivation and context of the project

Thrombosis is an acute, severe condition affecting the vascular systems of thousands of people worldwide[1]. The disease is characterised by the undesired formation of a blood clot within a blood vessel and can lead to fatal cardiac arrests and strokes, remaining one of the most threatening but still inefficiently targeted pathologies known[2]. Most literature on thrombosis is either based on studies with animal models, which show distinct features from humans' systems and whose use in scientific studies carry several ethical issues, or inaccurate *in vitro* techniques, which are still not able to fully mimic complex conditions within human blood vessels and realistically address the disease[3,4].

However, recent advances in the fields of microfluidics and stem cells' technology promise to shed new light on the complex mechanisms of thrombogenesis and to take an important step towards thrombosis treatment. As more innovative protocols and techniques for microfabrication and microchips' designing are developed, more reliable become the artificial *in vitro* structures and conditions created to mimic natural human microenvironments. Already developed microchips with microchannels mimicking both healthy and injured, stenotic vessels[5,6] (characteristic of thrombotic situations), allow real time visualisation of the distinct stages of thrombogenesis and therefore further our understanding of vascular pathologies.

As one of the main cellular components of the vascular system, the implementation of endothelial cells in said microchannels is pivotal to study blood vessels and their intricate interactions *in vitro*. The use of standardised cell lines, such as human umbilical vein endothelial cells (HUVEC), is the most common approach in research, mainly due to their price and practical methods of isolation[7]. However, as generic cell lines, they do not exhibit the specific features and behaviour of each patient's cells, and much of the variability inherent to the already reported genetic component of thrombogenesis[6] cannot be considered in these studies. Thus, research undertaken with these cell lines, although useful and practical, will always be generic, and conclusions reached will not be accurately addressable (regarding treatment for specific patients). To overcome this issue, many authors have been predicting the implementation and the regulated, widespread use of human induced pluripotent stem cells-derived endothelial cells (hiPSC-EC) in microchips to be the next major breakthrough in this field[4,8]. The introduction of hiPSC-EC in these microdevices is expected to allow for patient-specific evaluation of the disease and its causes (including genetic factors) and mechanisms, improving diagnosis and drug targeting and testing[9].

Following that line of thought, this work aims at combining human induced pluripotent stem cells derived endothelial cells (hiPSC-EC) with thrombosis-on-a-chip devices (previously designed and developed at BIOS-Lab on a Chip Group, University of Twente), with the ultimate goal of advancing towards patient-specific analysis of the disease and its treatment. It explores the possibility of implementing, maintaining and testing hiPSC-EC within the aforementioned device, in conditions mimicking those of real human blood vessels, including human blood perfusion. Morphology and performance of hiPSC-EC when exposed to the inflammatory factor Tumour Necrosis Factor-α (TNF-α, reported to promote thrombogenesis[10]) and arterial shear rate were compared to those of HUVECs (presently used in the microchips) and are described in the present report.

I. Introduction

1. Vascular system

1.1. Structure and physiology

The vascular system, or circulatory system, is one of the most complex and multifunctional biological systems in a living organism. It encompasses the heart, a blood pumping organ, and all the vessels which transport blood to and from all the organs of the body with the ultimate goal of maintaining cellular homeostasis[11,12] (fig. 1).

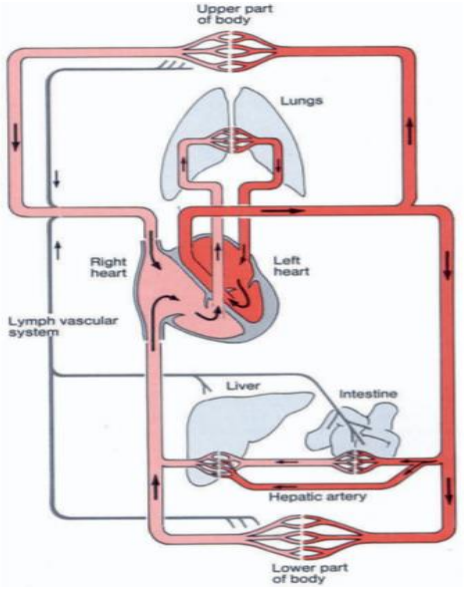

Figure 1 - Schematics of the circulatory system. Vessels with oxygen-enriched blood are represented in dark red, exhausted blood (with low O_2 concentration) are light red. Taken from [11]

These vessels can be grouped according to their functions and characteristics in: arteries, transporting blood from the heart to the rest of the body; veins, which carry blood from the different organs to the heart; secondary vessels (capillaries), present between main vessels, and whose function is to support the distribution of blood throughout the entire organism[11,13] and enable the exchange of nutrients with tissue cells[12].

The complex closed circuit formed by the blood vessels create two distinct systems of blood circulation: the systemic circulation and the pulmonary circulation. The systemic circulation is the section responsible for the transport of oxygen-enriched blood from the left ventricle of the heart to the cells of the rest of the body and then back into the right atrium of the pumping organ. The pulmonary vessels, on the other hand, form the path for exhausted blood to be carried from the right ventricle of the heart to the lungs, where it is fuelled with O_2, continuing its way back to the left atrium[11] (fig. 1).

Cellular homeostasis is maintained due to the nutrient transference and waste removal processes enabled by the vascular system. Systemic circulation provides new oxygen and nutrients to the cells, essential for the maintenance of their normal metabolic activity and functions. These are transferred through processes of diffusion, filtration and osmosis from blood to cells. The systemic vessels also

allow for the removal of waste products and carbon dioxide formed during their metabolism, that would otherwise create a toxic environment for the tissues. Blood is taken back into the heart and then (through the pulmonary circuit) to the lungs, where it is resupplied with oxygen.

1.2. Types and anatomy of blood vessels

The generic structure of arteries and veins is similar: the lumen, the hollow space where the blood flows, is surrounded by tissue, the vessel wall. The vessel wall is divided in three main layers: tunica intima (or tunica interna), the one in contact with blood, encompasses the endothelium and a thin basement membrane (formed by collagen and elastic fibres); tunica media, the middle layer, which is formed by smooth muscle cells and provides support to the vessel structure; tunica externa (or adventitia), the external layer, composed of connective tissue, fibres, and, in larger vessels, a small network of secondary vessels (usually called vasa vasorum) providing support to the main one.

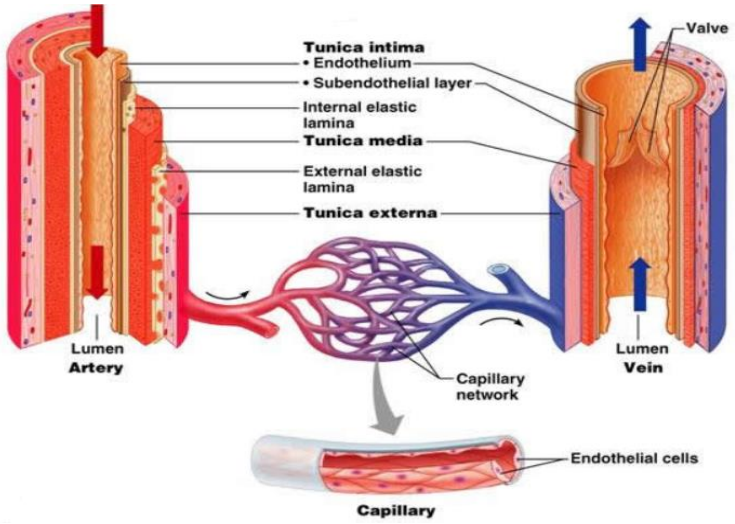

Figure 2 – Schematics of the structure of the vessel wall of a typical artery (left) and vein (right) and of the capillary network. The elastic membrane can be seen in the tunica intima of the artery, much more developed than in veins. The difference in size of the tunica media can also be observed. Adapted from [14]

Although the basic structure is the same, some differences are observed between the vessel walls of arteries and veins (fig. 2). Due to its function of transporting the blood out of the heart to the rest of the body, arteries' tunica media is more developed, presenting a thicker layer of smooth muscle and elastin. Therefore, these vessels can withstand higher pressures and help to regulate blood flow, after the fluid has been pumped away from the heart. On the other hand, veins, which do not possess a thick tunica media (less pressure), can transport and hold more blood than the arteries. Veins also present special features to counter the effects of backflow, venous valves, which help the regulation of the correct blood flow to the heart[12]. Differences in vessels' structure and function translate into differences in shear forces exerted on the cells. While typical shear rates in veins range between 100 and 250 s^{-1}, arteries' have higher values of 1000-5000 s^{-1}, corresponding to values of shear stress ranging from 1 to 10 dyne/cm^2 in veins and 10 to 50 dyne/cm^2 in arteries, to which cells adapt differently[4,15].

Smaller capillaries of the vascular system have different structure and function from main vessels. Since their role is to enable the exchange of nutrients and waste products between circulating blood and tissue cells around the vessel, they do not possess the complex structure of transporting channels (arteries and veins), as seen in fig. 2. Due to their size and function, the usual ratio between endothelial surface and blood volume in capillaries is 100 to 500 times higher than in the other vessels[16].

1.3. The endothelium and endothelial cells

All blood vessels in the human body are covered by a simple, squamous wall of epithelial tissue: the endothelium. Lining the inside part of this ubiquitous structure is a one-cell thick layer of endothelial cells, whose main function is to maintain vascular homeostasis, creating a bridge between the circulating blood and the environment outside the channel[17]. In the past, endothelial cells were considered a simple physical barrier[18] with selective permeability, showing no other complex purposes or interactions[19,20]. However, it is now recognised that these cells are involved in several mechanisms related to vascular genesis, nutrients transference and essential interaction with other relevant types of cells, such as smooth muscle cells and fibroblasts[18,20]. They are also the first line of contact with blood cells and molecules, and have the ability to respond to changes in blood composition or flow and promote the main mechanisms of defence against threats and injuries of the vessels' walls[19].

1.3.1. Selective barrier function and extracellular connections

The ability of the endothelial layer to selectively exchange materials with circulating blood is mainly enabled through the regulation of the cells' membrane permeability, cytoskeleton and cell-cell junction molecules[21]. Molecules present in blood are able to cross the endothelium and reach surrounding tissues via two main routes: the intercellular route, mediated by cell junctions located in between cells, or the transcellular route, crossing the membrane and cytoplasm of endothelial cells.

1.3.1.1. Intercellular route

Endothelial cells are usually connected to their neighbours by intercellular junctions formed by specialised molecules. These cell-connecting bridges have a certain degree of permeability, depending on the junction type and existent proteins, and are essential to the endothelium barrier function[21,22]. The integrity and tightness of the formed connections can also be temporarily modified in response to physical or biological signals[23].

Intercellular junctions between endothelial cells are considered to encompass four different types of structures (fig. 3): adherens junctions, tight junctions, gap junctions and discontinuous endothelium (or fenestrations).

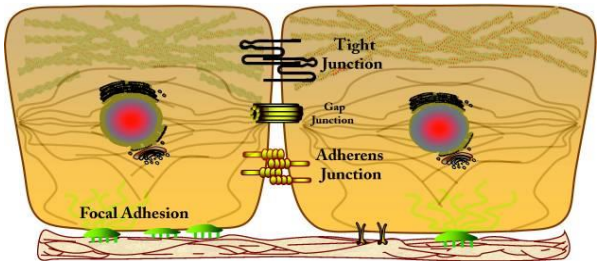

Figure 3- Structures involved in the adhesion and connections between adjacent endothelial cells. Tight junctions, gap junctions and adherens junctions are involved in cell-cell connection and focal adhesion molecules for cell-extracellular connection. These molecules are all connected through cytoskeleton filaments within the cell. Taken from [21].

However, only the first two types are thought to have a determinant role in selective permeability[21]. Gap junctions, consisting of six connexins in each side of the junctions (twelve in total), form open channels connecting the cytosol of the involved cells. They enable the passage of ions and small molecules, contributing for cell-cell communication but not directly to the selective barrier function[24]. Discontinuous endothelium and fenestration appear in certain specific tissues (e.g. kidney and liver) and are large gaps in between cells that allow for the passage of large molecules. However, they do not have a determinant role in permeability regulation in blood vessels and are not present in normal vascular endothelial layers[21].

Adherens junctions (AJs) are the most common intercellular connection structures and are responsible for the permeability (and impermeability) of the endothelium to large proteins and other macromolecules (the mean pore size is around 3 nm)[21]. The most relevant and studied integrant protein of the AJs is the vascular endothelial-cadherin (VE-cadherin)[21,25]. These endothelial-specific proteins are linked to actin filaments of the cell through catenins (fig. 4) and bind to other VE-cadherins of the adjacent cell through their extracellular domains (calcium-dependent homophilic interaction[24]). In spite of VE-cadherin's main role in AJs, other proteins, such as platelet-endothelial cell adhesion molecules (PECAM) and junctional adhesion molecules (JAMs), also contribute for the stability of these intercellular bridges.[21,22]

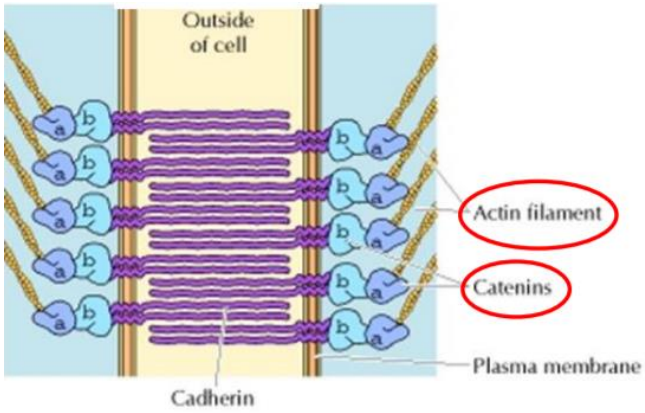

Figure 4 - Schematics of VE-cadherin composed-adherens junctions. Cadherins are linked to catenins on the one side, which connects them to actin filaments of the cell, and to other cadherins' extracellular domain on the other side, binding both cells together. Taken from [24]

Tight junctions (TJs), more common in certain types of specialised tissue (e.g. blood-brain barrier)[21,26], have smaller pore sizes (around 1 nm) and therefore can regulate the entrance of smaller molecules

(including ions)[21]. Two main types of transmembrane proteins, occludins and claudins, compose the structure of TJs (fig. 5). These proteins are linked to the cells' cytoskeletons via specialised proteins α-catenin, zona occluden-1 and zona occluden-2 (ZO-1 and ZO-2)[21,24], the latter also involved in signalling pathways of the cell. JAM-A protein is also reported to be present in TJs, both to promote the stability of the structure and the regulated interaction between the junction's molecules and the cytoskeleton[27].

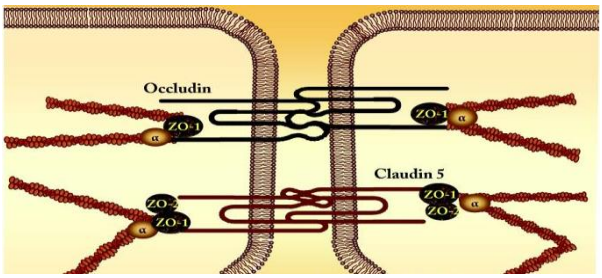

Figure 5- Schematics of a tight junction. Occludin, Claudin are the main proteins forming the junctions, which are stabilised by ZO proteins and α-claudin, connected to the cell's filaments. Adapted from [21].

1.3.1.2. Transcellular route

Transference and transport of molecules through the endothelial cells represents the other main mechanism of nutrient exchanging between blood and body tissues. It is mostly relevant for regulating the permeability to large macromolecules, which are otherwise excluded by adherens and tight junctions[21].

This route involves a three-step mechanism: endocytosis of the molecule at the endothelial luminal interface (in contact with blood), transcytosis inside the cell and exocytosis at the opposite side, the basolateral membrane. The entire process is supported by the formation of vesicles which mediate the endocytosis step and surround the target molecules throughout the entire process, until their exocytosis is terminated. Membrane invagination and vesicle formation happen after caveolin-1, a structural protein, is phosphorylated and oligomerise (with other caveolins) together with lipids and signalling molecules to form caveolae, an enclosed structure, which will then evolve into the necessary enclosed vesicle. Accessory proteins dynamin and intersectin-2 and signalling protein RAS are essential to terminate endocytosis (fig. 6). Docking and guidance of the recently formed vesicle (with the target macromolecule inside) are mediated through (v)-SNARE-(t)-SNARE binding mechanism, and ATP-driven motor molecules will enable its movement through the cell cytoplasm[21]. After reaching the basolateral membrane, fusion of the vesicle with the membrane will allow for the exocytosis of the desired molecule, which will the reach tissues. In certain situations, the process is reported to take advantage of vesiculo-vacuolar organelles (VVOs), structures which can form channels inside the cell and that will provide a path for macromolecules to be transported through the cytoplasm[28,29].

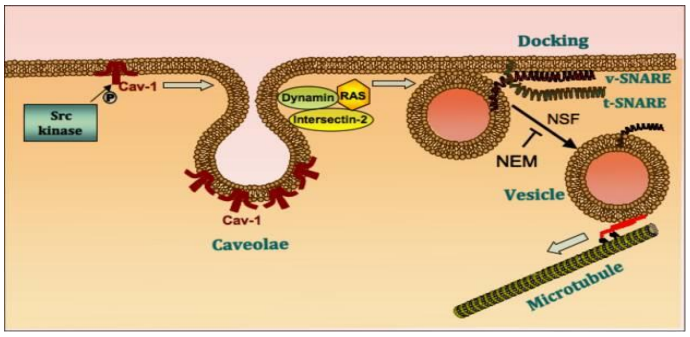

Figure 6 – Process of transcytosis, involving vesicle formation, through phosphorilation of caveolin-1 and its aggregation, and docking and transport inside the cell, mediated by the v-SNARE-t-SNARE mechanism and microtubule attachment. Taken from [21].

1.3.1.3. Cell-Extracellular Matrix adhesion

The integrity and permeability of the endothelial layer is not only kept through cell-cell interaction but also through the connections established between its basolateral membrane and the vessels' extracellular matrix (ECM)[21]. These are the bonds that avoid cell detachment and fix the endothelium to the vessel, and are essential for cells to be able to interact with the surrounding environment[30]. Cell-ECM adhesion is mainly achieved through structures named focal adhesions, small lipid raft domains whose main component are integrins. Integrins are transmembrane glycoproteins with two distinct subunits (α and β) that form the link between the cell's cytoskeleton (intracellular domain) and ECM proteins (e.g collagen and fibronectin) outside the cell[21,24] (fig. 7).

Different integrins with specific combinations of α/β subunits will interact with different ECM proteins[21,24,31]. For instance, the cell-ECM collagen bond is made when the heterodimers α_1 and β_1 or β_2 are present and the bond to fibronectin is achieved through the combination of subunits α_5 and β_1[21,31].

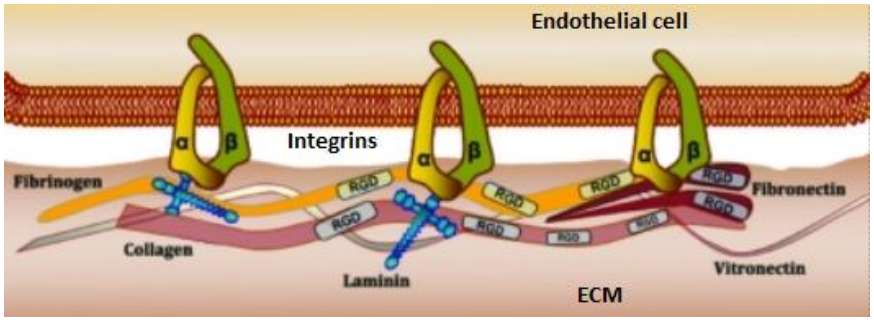

Figure 7 - Schematics of the bond between integrins and ECM proteins in focal adhesion structures. Most integrins will bind to the arginylglycylaspartic acid (RGD) area of matrix proteins. Adapted from [21].

Focal adhesions are also reported to be part of relevant signalling pathways, since integrins are able to play important roles in cell-ECM communication due to their privileged location[32]. Bonding between the cell's integrins and ECM proteins will also protect the tissues from leakage of blood cells and molecules, supporting the maintenance of homeostasis within and around blood vessels[21,32].

1.3.2. Important endothelial cells specific markers: vWF, PECAM-I, ICAM-I and VCAM-I

The state of the endothelium in a given moment highly influences the environment within a blood vessel and alterations to its equilibrium can either be the cause or the effect of different pathologies affecting human systems. The endothelial phenotype is regarded as a reliable, indicator of the state of the endothelial cells and can be characterised by certain surface markers which, together with certain specific proteins and other biomarkers, are involved in signalling and responding to injury by triggering inflammatory processes[16].

Specific endothelial cells markers are widely used *in vitro* (and were used in the present work), not only for identification and characterisation of the cells' phenotype, but also for measurement of the effects of pathologic agents[33]. Cells adhesion molecules (CAMs) of the endothelium surface are also frequently used in purification processes of populations of ECs[34]. Although dozens of molecules are deemed to be good indicators of ECs' identification, as extensively reviewed by Goncharov et al.(2017)[16], some of the most important in research nowadays are von Willebrand Factor (vWF), platelet-endothelial cell adhesion molecule 1 (PECAM-1), intercellular adhesion molecule 1 (ICAM-I) and vascular cell adhesion molecule 1 (VCAM-I)[16,33]. VE-Cadherin, a constituent of adherens junctions, is also used as a marker for endothelial cells[35].

VWF is a glycoprotein produced in endothelial cells' Weibel-Palade bodies[,25], which are specific endothelial organelles that can also be considered important ECs' markers[16]. This protein plays a major role in blood coagulation mechanisms[2,37] (further detailed in the section 2.2 of the Introduction) and has also been reported to be involved in vessel sprouting processes[38].

Even though vWF is an important EC marker, cell adhesion molecules encompass the majority of specific EC molecules taken advantage of to identify and characterise the endothelial phenotype. These molecules play various important roles in the essential interactions which ECs naturally establish in their microenvironment, both with other cells (of homo- and heterophilic nature) and the ECM.

Platelet endothelial cell adhesion molecule 1 (PECAM-1), also known as CD31, is a transmembrane homophilic protein, mainly expressed in endothelial cells and hematopoietic-derived cells[16,39]. It is involved in the maintenance of the integrity of the endothelium and the vessel, being required for the adhesion of leukocytes and their transendothelial migration upon detection of inflammation signals[39]. Due to the ubiquity of the endothelium and the role of CD31 in inflammation response, this CAM has been studied as a potential target for drugs and therapies[16]. Furthermore, Riccieri et al.'s publication[40] on the release of CD31's extracellular domain during apoptotic events and its presence in circulating blood of patients afflicted by severe vascular diseases (e.g. myocardial infarctions), together with another angiogenic and inflammatory factors, highlights its promising usefulness as a marker for the identification of certain human diseases.

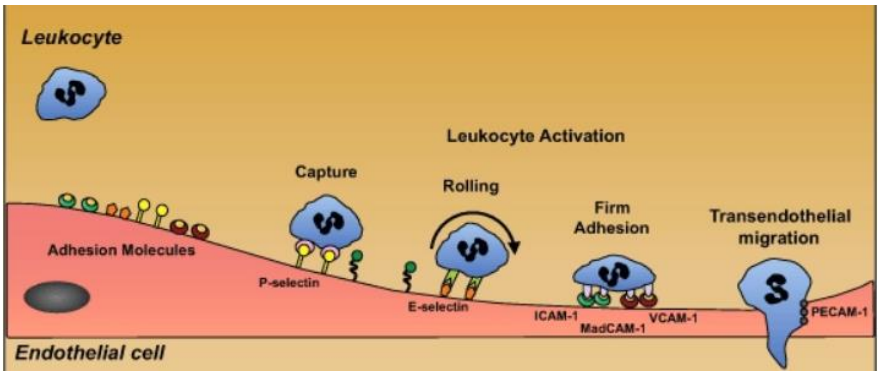

Figure 8 – Simplified schematics of the adhesion cascade of leukocytes and the role of main adhesion molecules of the surface of ECs. Taken from [41].

ICAM-I and VCAM-I, also known as CD54 and CD106, respectively, are two of the most important CAM in ECs. They are transmembrane proteins, not only involved in the vascular firm adhesion of leukocytes after their capture[41] (fig. 8) but also in mechanisms of signalling and response to injury[16,41]. The upregulation of ICAM-I is a well-described marker of cell injury and inflammation – activation of ECs leads to pronounced increases in its expression levels upon inflammatory stimuli[10,16,34].

The functions of these molecules (related to inflammatory responses) make them important players in *in vivo* mechanisms of defence and in *in vitro* research on diseases and drug targeting. Their role in the development of vascular diseases will be further highlighted in the following sections.

2. Haemostasis and vascular diseases: etiology and research on thrombosis

2.1. The basis of haemostasis

Haemostasis is the natural process which maintains the normal blood flow and blood vessels' condition in our body. This is achieved through coagulation mechanisms and plugging of injured vessel walls, together with a highly regulated balance between procoagulant and anticoagulant factors present in blood. Haemostasis is closely related to the coagulation cascade, a mechanism to achieve clot formation and strengthening after the initial plugging.

The mechanism of haemostasis is usually considered to have two separate simultaneous steps which work simultaneously[42] for the same goal: primary haemostasis, mainly related to platelets summoning, activation and aggregation in the site of injury; secondary haemostasis, is characterised by conversion of fibrinogen into fibrin and its further polymerisation and aggregation to strengthen the clot[2,37]. Perception of a blood leakage related to endothelial injury triggers this intricate two-step mechanism, which will be activated to repair said injury and revert the vessel back to its previous state of equilibrium.

2.2. Primary haemostasis: platelet activation and aggregation

Von Willebrand Factor (vWF) is a large multimeric protein, present in soluble state in plasma[37,43] and in an immobilised state in the subendothelial matrix[44]. Although immobilised vWF plays a clearer role in haemostasis than its soluble counterpart, both have been reported to be of relevance during clotting mechanisms[43]. They both support the initiation of haemostatic processes[45].

When under high shear conditions and after exposure to circulating blood (due to cell injury), immobilised vWF is able to bind with high affinity to collagen via its A3 domain[43] and to platelet receptors GPIbα via its A1 domain[43]. This will promote platelets capturing and enable their initial adhesion to the site of injury, which is then stabilised by the bond of platelets receptors GPVI and GpIa/IIa38 to exposed collagen[46]. Intracellular signalling mechanisms of platelets triggered by these interactions will then instigate conformational changes and the release of agonist molecules. While conformational changes themselves will activate other receptors and integrins and expose them to vWF and collagen, thereby reinforcing platetelet-endothelium adhesion and promoting platelet-platelet interactions, the release of agonists will induce the recruitment of more circulating platelets to the local[37,43].

Activated platelets' release of agonist molecules is one of the main events of primary haemostasis. The initiation of this process, with the release of molecules such as ADP, thromoboxane A2 and serotonin[37] will trigger a positive feedback mechanism, attracting and binding nearby circulating platelets to the haemostastic plug, promoting its propagation and strength. Soluble vWF has been reported to have influence during this recruitment stage, by binding to the first formed layer of platelets and promoting platelet-platelet interaction and consequent aggregation[43].

2.3. Secondary haemostasis & the coagulation cascade

The secondary haemostasis process encompasses a sequence of steps that is triggered upon vessel injury with the ultimate goal of fibrin formation and its deposition in the growing clot. Fibrin is an insoluble protein, originated by the cleavage of fibrinogen, which is naturally present in human blood plasma[47]. Fibrin's properties are unique and essential for haemostasis: it is capable of forming a viscoelastic polymer, with the ability to create stiff, durable networks while maintaining enough plasticity to endure unfavourable dynamic conditions (e.g. arterial shear) without degradation or rupture[47,48].

Tissue factor (TF) exposure is deemed to be one of the main initiators of the secondary haemostasis mechanism. TF is a quiescent membrane receptor, present in extravascular tissues and not exposed to the blood under healthy conditions. When injury occurs and its exposure is promoted, the receptor fulfils its role as a cofactor of circulating protein proconvertin (Factor VII, FVII) and activates this molecule ($FVII_a$), in the presence of calcium (Ca^{2+})[49]. The $FVII_a$-TF- complex is then able to convert the inactive Stuart-Prower factor (Factor X, FX) to its active form, FX_a, and is also involved in the activation of antihaemophilic factor B (Factor IX, FIX). Activation of these factors will trigger the initiation of a biological mechanism named extrinsic coagulation pathway[37].

When activated, FX binds to proacclerin (factor V, FV) through a calcium-mediated bond[50], forming a FX_a-FV_a complex, which some authors name prothrombinase[2]. This complex has a central role in secondary haemostasis, since it is able to convert the quiescent clotting factor prothrombin (factor II) to thrombin, the protease responsible for catalysing the conversion of fibrinogen (factor I) to fibrin[2,47] (through cleavage of two pairs of peptides in the central nodule of fibrinogen molecules[47]).

The small amounts of thrombin initially formed through the previously described stage (extrinsic pathway) not only initiate fibrin formation but also promote the activation of plasma thromboplastin antecedent (factor XI, FXI), which is expressed by activated platelets on the site of injury[2]. FXI_a then interacts with previously mentioned FIX (involved in the initiation of secondary haemostasis) and promote the activation of larger amounts of the clotting factor. Together with the quantities of FIX which had been activated when TF was exposed, this influx will, in the presence of antiheamophilic factor A (factor VIII, FVIII), result in the activation of more FX, which in turn increase the production rate of thrombin, and the cycle restarts[2,37]. This complex positive feedback mechanism will continuously supply the necessary amounts of fibrin, which will polymerise and form a strong scaffold to support platelets adhesion and the clot structure. Fig. 9 shows the simplified schematics of the secondary haemostasis sequential process.

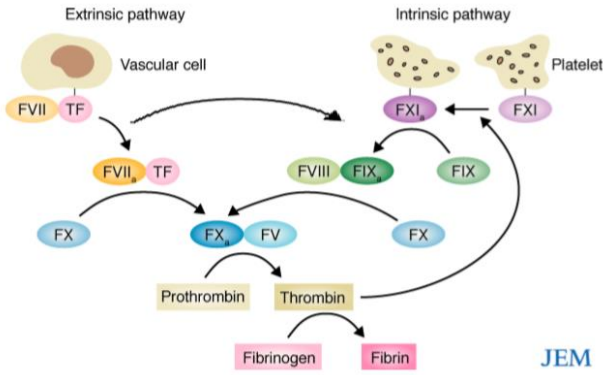

Figure 9 - Schematics of the secondary haemostasis process, culminating in the formation of fibrin. The extrinsic and intrinsic pathways work in cooperation to allow for clots strengthening in response to injury. Adapted from [2].

As a secondary but equally important function thrombin also influences the mechanism of primary haemostasis. The presence of the serine protease promotes platelet activation by cleavage of two protease activated receptors (PARs) on platelets, PAR1 and PAR4[37]. Once cleaved, these receptors enable signalling pathways involved in reshaping of platelets and integrin activation. This effect, together with expression of FXI by activated platelets, are the main points at which primary and secondary processes are intertwined. These points of connection lead to the enhanced activation of the two positive feedback loops (platelet recruitment and thrombin formation), which are both essential for the rapid and efficient creation the haemostatic plug to counter the injury and start the repair of the endothelium.

Finally, it is important to understand the importance of calcium in the haemostasis mechanisms. Not only is the ion pivotal for the formation of several of the complexes formed between coagulation factors during secondary haemostasis[50] (as described above), but it is also involved in platelet activation and recruitment, being one of the molecules that enables the release of agonist molecules by platelets[51]. Thus, the presence of Ca^{2+} in blood is essential in coagulation and its capture by external components result in strong anticoagulant effects. Binding Ca^{2+} in blood to prevent its action during haemostasis is the most frequently applied method when human blood is to be used in *in vitro* experiments (e.g. adding citrate solutions to the drawn blood, which react with Ca^{2+} and avoid coagulation in the tubes)

2.4. Down-regulation of the coagulation cascade

As the endothelium is repaired and the vessel wall returns to its healthy state, it becomes necessary to reduce and eventually stop the triggered positive feedback loop of secondary haemostasis.

The control of this process is achieved with the triggering of several mechanisms, of which the two most important ones are: activation of serine protease inhibitors (SERPINs), which function is to inhibit various activated factors of the coagulation cascade[52,53]; induction of the protein C pathway, a mechanism which results in the cleavage of cofactors VIIIa and Va, preventing their action in the cascade and disturbing secondary haemostasis[54].

SERPINs are a superfamily of proteins, with a highly conserved core structure involved in their function of tight regulation of coagulation and inflammatory processes. The mechanism of action of SERPINs focus on irreversibly binding and distorting the target protease, leading to its inactivation[53,55]. Of the serine protease inhibitors that act to control this process, antithrombin plays a leading role by inhibiting thrombin and factor Xa. Furthermore, if heparin or heparan sulphates are present in circulating blood, this inhibitory action will also be extended to factors IXa and XIa of the cascade[52].

The protein C pathway, on the other hand, results in the cleavage of factors Va and VIIIa. Protein C is a serine protease which, when activated, binds to the two cofactors and leads to loss of their function, cutting down prothrombinase formation and interfering with secondary haemostasis mechanisms[54].

2.5. Fibrinolysis: the removal of formed clots

The anticoagulant, down-regulation mechanisms are essential for avoiding exacerbated clotting events within the blood vessel. However, they only terminate coagulatory mechanisms and prevent the indefinite growth of the clot but are not responsible for the removal of its previously established structure, strengthened by platelet adhesion and the deposition of a polymerised fibrin network. The prolonged existence of the clot can lead to more problems that the injury itself, since altered flow patterns and channel occlusion can lead to ischemia in major organs and other problems inside the vessel[2] (detailed in the next section).

The physiological process of clot disintegration and removal is named fibrinolysis. This mechanism encompasses the action of three main serine proteases, which are usually found in blood in their inactive state (zymogens or proenzymes[37,56]). Two of these, tissue plasminogen activator (tPA) and urokinase plasminogen activator (uPA) are located on the surface of the fibrin mesh formed on the clot area and are able to bind to circulating plasminogen[56,57]. TPA and uPA are then able to efficiently catalyse the conversion of plasminogen (the zymogen) to plasmin (active state), an important fibrinolytic protease. The efficiency of the conversion of plasminogen to plasmin by tPA and uPA has been reported to be increased by at least 2-fold in the presence of fibrin[56]. This is one of the regulators of fibrinolysis and supports the controlled use of the mechanism, only triggered when depositions of fibrin come in contact with these proteases.

Plasmin is able to actively cleave fibrin and break down the polymer strings previously formed around the clot. The resulting soluble products are removed by the circulating blood and the clot starts its natural, slow disintegration[37,57].

Fibrinolysis is also tightly regulated by the action of other enzymes in circulating blood. Not only its upregulation is necessary to terminate coagulatory processes but also its down-regulation after the clot is removed, or else fibrin deposition mechanisms would be impaired in case of another injury occurs. This regulation is supported by enzymes of the SERPINs family, which inhibit plasmin action (the case of the alpha-2-antiplasmin enzyme) and plasminogen conversion through inhibition of tPA and uPA

actions (plasminogen activator inhibitor 1 and 2). Thrombin activatable fibrinolysis inhibitor, although not a SERPIN, have also been reported to play an important role in fibrinolysis control[37,52].

2.6. When haemostasis fails: vascular diseases

The haemostatic mechanisms are sensitive, tightly regulated biological pathways that can be disturbed by inherited or acquired factors. Impairment of this complex system and of the balance between procoagulant and anticoagulant factors will either lead to overcoagulation and vessel occlusion (if the former are abnormally favoured) or spontaneous or excessive loss of blood (if the latter are overproduced).

Bleeding disorders, of which the main examples are haemophilia A and B and von Willebrand disease, are usually related to genetic, inherited factors. These are connected to deficiencies in the production of coagulant factors of the haemostatic process. Haemophilia A is related to deficiencies of factor VIII, while Haemophilia B is characterised by shortage of factor IX. Both factors play an important role during normal secondary haemostasis, enabling the positive feedback mechanism that leads to the strengthening of the blood clot[37]. On the other hand, von Willebrand disease is related to deficiency in the von Willebrand factor production. This condition strongly affects the ability of platelets to adhere to exposed endothelium on the site of injury and start the coagulation process[37,58]. Bleeding problems can also be related to problems in platelet molecules and membrane receptors or even with receptors of collagen in the vessel wall[37].

Bleeding conditions, although threatening, affect less people worldwide than overcoagulation-related disorders, which lead to a higher number of deaths every year and continue to be poorly understood. The connection of thrombotic events with a set of inherited, genetic factors (named thrombophilia[59]) has been a main target of scientific studies but the mechanisms behind the development of these diseases are far from being fully understood. These thrombophilic states can lead to vessel blockage or weakening, or even to damaged valves in veins. These problems can, if serious, result in nutrient and oxygen shortage or accumulation of waste products in cells and will possibly provoke complete stoppage of other systems[13,59]. More on thrombosis will be discussed in next sections of the Introduction.

Moreover, conditions resulting from reduction or blockage of blood supply to the brain (also known as strokes) or to the heart (coronary artery or ischaemic heart disease, resulting the in commonly called myocardial infarctions or heart attacks) accounted for more than 15 million deaths worldwide in 2016, according to a World Health Organization study[1] (fig. 10). According to this same study, these two pathologies have showed the highest numbers amongst the leading causes of deaths for at least the last 15 years.

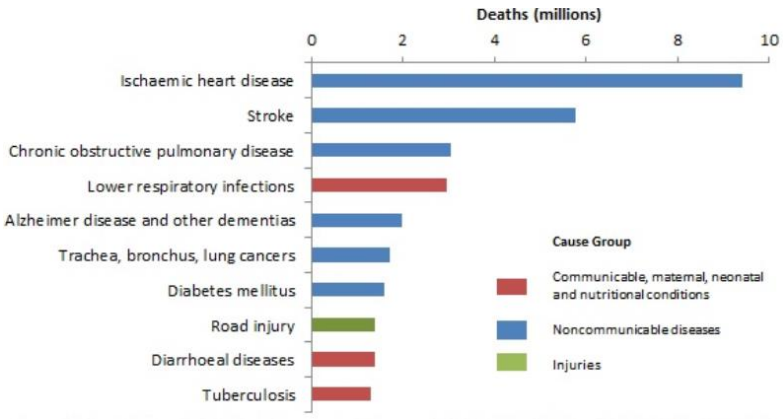

Figure 10 - "Top 10 global causes of death, 2016", data made available by World Health Association. Ischaemic heart disease and stroke lead the main causes of death worldwide. Taken from [1].

2.7. Thrombosis: a silent killer

Thrombosis is characterised by the undesired formation of a blood clot, also designated thrombus, in a blood vessel[2,60]. This condition is deemed to be one of the most common affecting the vascular system and has remained the primary cause of strokes and heart attacks worldwide for years[1]. Furthermore, studies show that 25% of every thrombosis cases result in the patient's sudden death[4].

Formation of thrombi in the blood stream not only directly reduces blood flux in the affected vessel, originating further injuries, but can also have an effect on other organs different from the primary focus of injury[61]. This is a relatively common and threatening situation since, if detached, embolus (the designation of a loose clot) can travel the blood stream (embolization) and create blockages in other systems.

In 1856, Rudolf Virchow described for the first time three important factors for thrombogenesis which came to be known as the Virchow's triad: hypercoagulability, blood stasis and endothelial damage[4,62,63]. Although a first general description, the triad's elements have been regarded as the pillars of the disease's formation. However, a revised, more complex and broader version of this classification has been recently considered as more studies and information on thrombosis are published: blood-borne factors, vessel wall dysfunction and the fluid dynamics within the vessel, as well as some genetic-related factors, are to be considered in thrombogenesis[4,6]. This is a more explanatory version of the triad, in which "fluid dynamics" not only encompasses blood stasis but also other relevant flow patterns, and in which genetic factors are introduced as of great relevance for thrombosis' formation[6,64].

Although thrombosis has remained a leading cause for human death for years, and even though extensive research on the matter has been conducted, the exact mechanisms and causes of thrombogenesis are yet to be accurately described and targeted. This is mainly due to the complexity of its origin and development stages, whose causes, as previously explained, are multifactorial and highly dependent on the environment within each specific affected vessel and on individual genetic factors[4,6,64].

2.7.1. Types of thrombosis

Distinct classifications of thrombosis have been described, depending on the type of the affected blood vessel: arterial thrombosis, if it occurs in arteries; venous thrombosis, in the thrombus is formed in a vein[60]. Microvascular thrombosis is frequently regarded as a distinct third type of thrombosis, in the cases in which minor vascular vessels (capillaries) are the focus of injury[4].

Arterial thrombosis is deemed to be closely related to atherosclerosis development, a disease characterised by the formation of a solid plaque within an artery, which may harden over time. These plaques, composed of fat, cholesterol, calcium and other blood components [65], tend to form in areas of stagnant flow in the vascular system (vessel branching or bending[4]), interfering with the natural haemodynamics inside the channel and narrowing the artery's passage (fig. 11).

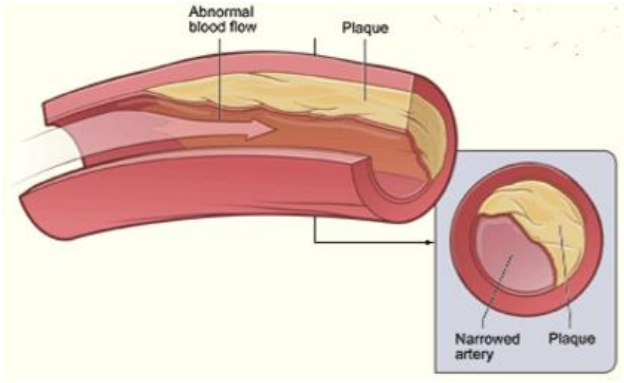

Figure 11 - Representation of an artery with a formed atherosclerotic plaque. The inset image shows a cross-section of the injured artery, partially occluded by the plaque structure. Adapted from [65].

After erosion or rupture of this solid formation, an inflammatory reaction occurs, increasing cytokines' release which, together with the perception of altered blood flow patterns, will induce platelets' recruitment to the site[66,67]. Although a natural defence and recovery mechanism of the body to avoid further injury, the aforementioned aggregation of platelets will further exacerbate the occlusion of the channel and the consequent decrease of the blood flow in the target vessel[4,67]. The abnormal narrowing of that body channel, a process called stenosis, will therefore result in a reduction of the oxygen-enriched blood supply to the rest of the body and consequently in an oxygen shortage in main organs or limbs (ischaemia). Thromboembolisation can also stand as a severe consequence of arterial thrombus formation, if thrombus detaches from the site[68] and travels in the bloodstream to other locations.

Venous thrombosis (VT), the other main type of thrombosis, can occur in different types of veins throughout the body and can be further characterised as such (e.g. deep vein thrombosis, renal vein thrombosis, etc). Among these, deep vein thrombosis (DVT) is the most common and studied pathology, leading some authors to use VT and DVT interchangeably.

The factors that contribute to the origin and development of VT are usually described by the classic Virchow's triad[4]. Although this historic attribution and description are still in use, it is now considered that both hypercoagulability and stasis are more relevant for the formation of VT than endothelial damage[68], since venous thrombi have been reported to be mainly composed of fibrin and red blood cells

(RBCs) and less of platelets, in opposition to arterial thrombi[37]. Furthermore, valves of the venous system are deemed the most probable focus site of thrombogenesis, due to abrupt shear stress conditions, blood stasis and hypoxic environment, which are regarded as key factor to promote thrombus formation and the associated embolic process [4,62]. DVT is regarded as the primary origin of the third most common disease of the circulatory system (after the aforementioned stroke and myocardial infarction), venous thromboembolism[68]. This condition leads, in turn, to further injuries in other organs. Pulmonary embolism, characterised by the blockage of blood vessels in the lungs, is one of the most serious and common consequences of venous thromboembolism[68].

2.8. Models of research on thrombosis

2.8.1. The classic models: animal models and macro in vitro models

Classically, thrombosis and its causes and consequences have been studied using various *in vivo* and *in vitro* methods. These represent the gold standard of thrombosis research and have led to several significant breakthroughs regarding the disease.

2.8.1.1. Animal models

Animal models represent the *in vivo* models to study thrombosis and have been a widespread, useful tool to understand some of the mechanisms and molecules involved in the development of the disease[4,69]. In fact, in their extensive literature review on animal models used for research on venous thrombosis alone, Levi et al.(2007)[70] reported a total of 18 different animal species represented on past published studies.

Although other well-known classic animal models are present in some publications (such as the zebra fish or rabbits), mice and rats are undoubtedly the most frequently used in research on thrombosis. Small animals are usually preferred to bigger ones due to their availability, lower cost (e.g. with maintenance and reagents used) and the reduced ethical issues that arise from their use. However, bigger animals, such as pigs, primates and dogs, are still used and represent well-established models of the disease, since their physiology, disease mechanisms and genetics are closer to those of humans[3].

Amongst larger animals, non-human primates were once the main model for research on thrombosis, due to their haemostatic mechanisms' similarities to those of humans[71]. However, due to the laws for protection of the used species (risk of extinction) and higher costs of maintenance, their use was drastically reduced in the last decades. Thus, pigs have gained popularity in this area of research as a simpler alternative and are now the main large animal model used thrombosis, since they result in lower costs of maintenance and require lower levels of expertise to work with. In addition, they have human-like cardiovascular anatomy, haemodynamics and wound healing processes[3]. The porcine model is also reported to develop atherosclerotic lesions naturally, without the need of genetic manipulation[72]. These two models, although less frequently used in research than murine models, still stand as more

representative models of the human pathology (fig. 3) and are preferentially used to test therapeutic solutions and drugs' *in vivo* effects before human clinical trials[3].

Murine models are an easy-handling, readily available and cost-effective alternative to larger animals. They are not only used for research on new components and mechanisms that may be relevant in thrombosis[4], but also frequently regarded as an *in vivo* model to easily confirm conclusions drawn from *in vitro* methods[3,70]. Furthermore, their established genetic data[4] and the wide range of genetically modified strains of mice reported in literature[73] provide a great opportunity to individually test the importance of each player (e.g. platelet receptors or coagulation cascade factors) in thrombogenesis.

However, limitations when working with mice are also heavy. Due to their different biological system, mice are not naturally prone to develop atherosclerosis[3] and consequent thrombotic events. Thus, genetic modifications are required, and physical or chemical agents must be added if murine models are to be used. Although relatively easy to work with, these are induced artificial factors that will not accurately mimic the causes and steps of human thrombogenesis. In addition, vessels and haemodynamics of rodents are distinct from those of humans and species-related differences such as platelet count (reported to be four times higher in mice than in humans) or platelets' volume (double the size in humans) will always have to be considered when interpreting conclusions reached in these studies[3,4,70].

These models have been useful when studying the mechanisms of the disease, since they can reproduce the high complexity of the vascular system and thrombosis development itself. However, biologic, physiologic and genetic differences between mice and humans cannot be overcome and as such, these do not stand as fully representative of the human disease.

2.8.1.2. In vitro models

Research on thrombosis is also made through *in vitro* experiments. Systems used aim at mimicking as closely as possible the conditions found in the human vascular system, such as the wall shear and blood flow within the different blood vessels. The parallel plate flow chamber and the cone-and-plate viscometer are the main classical apparatus for *in vitro* research on the disease. Whilst the former is composed by a rectangular cavity through which the blood is transported with the support of constant flow pumps, the latter consists of a conic insert rotating above a plate with the sample.

Parallel plate flow chambers are rectangular-shaped structures, consisting of two parallel plates, one on top of the other (but not in contact)[74]. A hollow, narrow (millimetre or centimetre magnitude[4]) gap is left between them. In the device, target cells are cultured in the inside surface of the top plate, which is usually transparent (e.g. glass slide or coverslip) and the fluid of interest is perfused through the space between the plates[74] (fig. 12). Flow rates are applied using constant-flow pumps, capable of providing the necessary laminar flow.

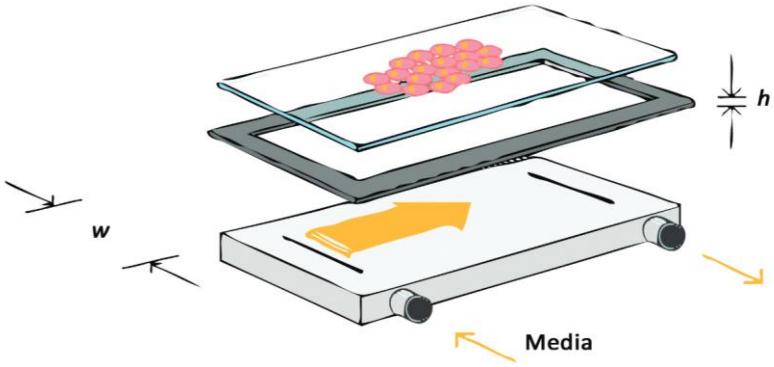

Figure 12 - Parallel plate flow chamber schematics. Cells are seeded in the inside surface of the top plate, in contact with the fluid of interest (e.g. media), to analyse the response of the cells and interaction with different molecules. Taken from [74].

This system is able to offer a relatively controllable environment to study both the effects of shear stress on attached cells and on molecules in suspension (in the circulating fluid) and the biological interactions between the former and the latter. Several systems have been reported that use certain endothelial or ECM proteins (e.g. vWF or collagen) to line the top surface, with the goal of studying their interaction with circulating blood and its cells[75]. The use of parallel plate flow chamber to study platelet interactions in coagulation[76] and the pathways of leukocyte adhesion to the endothelium under flow[74] are some of the relevant examples of the importance these models have had in research.

Cone and plate viscometers were once mainly used to measure viscosity of biological fluids[77]. They are composed of a conic structure rotating above a flat surface, with the gap between them full of the fluid under study (fig. 13). Due to the movement of the conic part of the viscometer, Couette flow (fluid movement resulting from the forces the liquid within withstands for being in between a moving and a stationary surface) is created inside. Although not being the original area of focus of cone and plate viscometers, the characteristic flow pattern and the imposed shear stress made them great candidates for research with blood and cell suspensions[78].

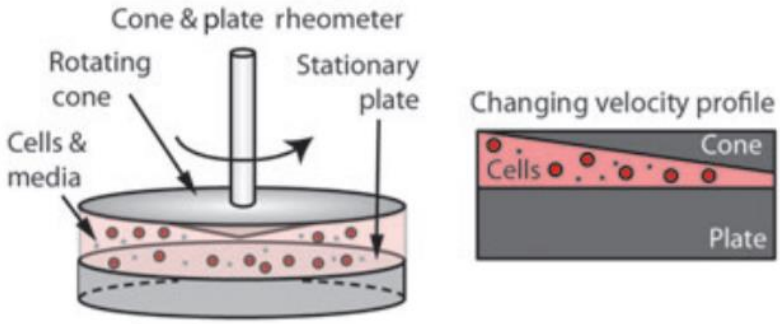

Figure 13 - Cone and plate viscometer. The fluid of interest is introduced in between a rotating conic surface and a stationary, flat surface. A velocity profile is created, changing linearly along the structure (from the angle tip to the side wall) and applying shear stress to the cells. Taken from [78].

The rotation applied can be controlled by the operator and the conic surface-flat surface angle enables a liner change in velocity and height of the fluid, which will induce uniform shear stress along the surface (from the tip of the angle to the side wall). Girdhar and Bluestein (2008)[77] report that the system is easily

programmable to reproduce arterial flow and shear patterns and can be used in real-time microscopy to follow morphological changes in cells and the interaction between different types of cells in blood (under physiologically-relevant shear stress conditions). Thus, studies with cone and plate viscometers have been useful to understand the effects of shear stress and fluid movement in blood cells' morphology and interactions.

These *in vitro* models have, nonetheless, several limitations related to human vessels' anatomy and physiology. Neither parallel plate flow chambers nor cone and plate viscometers are flexible, easily changeable structures, and they do not allow for accurate, vessel-like complex features to be tested[65]. In addition, only cells in suspension or in two dimensional (2D) monolayers can be studied, and no natural three dimensional (3D) structures can be reproduced (e.g. humans' vascular lumen). Finally, as macro *in vitro* models, both methods require large amounts of blood, cells and expensive reagents to be able to even remotely mimic human organism's micro-environments[53]. As so, they represent expensive, time and resources-consuming, low-throughput models of research, and their use has gradually decreased with the development of a new, promising, more efficient area: microfluidics.

2.8.2. Innovative models: microfluidics

2.8.2.1. Development of microfluidic fabrication and materials

Microfluidics is the area of study that encompasses all models and technology that allow manipulation of reduced amounts of fluids (10^{-9} to 10^{-18} litres) in small channels (of tens of micrometres) built in specific devices[79]. These found application in various distinct areas from molecular analysis and separation to cell culturing, mainly due to the ability to accurately control samples and molecules using small volumes of reagents.

The first microfluidic chips were developed with materials used in the microelectronics field, like silicon and glass, using techniques of photolithography and etching of the surfaces. These materials have important, useful properties that made them promising for the development of microfluidics (e.g. negatively charged surfaces and clean surfaces after the etching step)[79]. However, they are expensive and require cleanroom-mandatory, complex techniques to seal and work with and, as such, are time and resources-consuming. To counter those disadvantages, polymers slowly became the most frequently used material for structuring the base of microfluidic platforms[79–81].

Polymers are less expensive, simpler materials to work with. Their fabrication processes require no complex techniques like etching (they can easily be moulded) and sealing only require one-step, well characterised techniques. Although their surfaces are not as advantageous and naturally useful (they have to be treated and well controlled) and in spite of their lack of stability at high temperatures and when in contact with certain organic solvents, they will work in the majority of the designed experiments within the biological areas of research[80]. Due to their fabrication process, they are also less time-consuming and will result in higher throughput comparing to silicon and glass microchips.

Amongst several polymers used, polydimethylsiloxane (PDMS) is undoubtedly the best-established material for the fabrication of microfluidic devices. PDMS is an optically transparent, silicon and carbon-based, soft elastomer. Easily moulded into shapes capable of having micron scale features in it and cured at low temperatures, the nontoxic composition and surface can provide a good structure for cell attachment and enable its use in *in vivo* implants. As with other polymers, sealing and surface treatment techniques are simple and well-described.

Soft lithography comprise a set of techniques developed with the growth of the microfluidics use in the fields of biology and chemistry, with the goal of providing a versatile, inexpensive and experimentally convenient method for laboratories to be able to create their own devices. These techniques all rely on a mould to transfer a set of geometric features, using flexible organic materials, instead of the classic materials used in microelectronics. From soft lithography, the rapid prototyping procedure was developed[81]. The method can be divided in two main stages, one of rapid fabrication of a master mould with a thin film of photoresist (with the desired features for the device) and the other one of replication moulding, the fabrication of an elastomer stamp (usually PDMS) as a negative replica of the features of the master mould. Creation of the device always implies the creation of the device's design in a computer-aided design (CAD) program, where format and dimensions are set. The final wafer that will be used as the mould for PDMS chips is then obtained from the original computer-aided design (CAD) design through several steps of photolithography. Photolithography is a mechanic process that allows the transference of certain geometric features of a photomask to a solid surface (wafer) made of silicon. The first step is to obtain a transparency, the photomask, with this design on it (for instance, with an imagesetter). Photolithography techniques then create a layer of photoresist on top of a silicon wafer, using the photomask as the mould. This results in a resistant, durable wafer featuring a positive relief of the original CAD design[80]. Replica moulding is then used to obtain the final PDMS microchip. This step involves the pouring of the elastomer on the wafer, which is then curated (e.g. at 60 ºC for PDMS chips), generating a negative replica of the master's features. Surface treatment of the PDMS and sealing of the chips finalise the process of the microfluidic device fabrication. PDMS' hydrophobic properties make surface activation necessary for processes using aqueous solutions. This can be achieved through air plasma treatment. Exposing the surface of PDMS to air plasma induces the introduction of polar silanol groups (fig. 14), which make it more hydrophilic and therefore suitable for experiments with the biological solutions and suspensions used. Furthermore, this activation is responsible for PDMS' ability to easily bond irreversibly to glass (and some other materials) through the formed silanol groups[80,81].

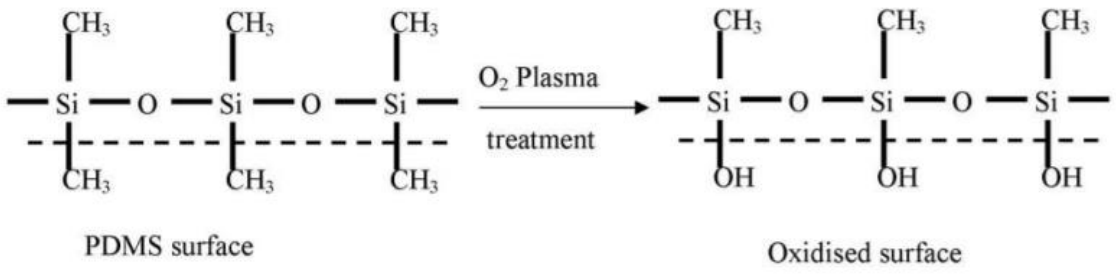

Figure 14 – Oxidation of the PDMS surface during air plasma treatment of the microfluidic device. Taken from [82].

Rapid prototyping and replica moulding allow for the reduction of costs and time for designing and fabricating new microfluidic devices, that can promptly be used in biological experiments.

2.8.2.2. Microfluidics advantages in thrombosis research

Microfluidic devices are becoming the main model of research regarding thrombosis. The highly controllable, low-cost nature of microfluidics are some of the most attractive generic features for scientists working in this area[83]. However, this model of research has some other specific perks which make them the first-choice platform for the development of research on vascular diseases nowadays.

As described before, classical *in vitro* models of research on thrombosis, such as the parallel plate flow chambers and the cone and plate viscometers, are not able to correctly mimic human vessels complex geometries and require large amounts of expensive, human materials (e.g. blood and cells). Microfluidic devices can overcome both obstacles. Microfluidic channels make the development of cellular 3D, enclosed, vessel-like structures possible, with small amounts of reagents required[5,6,10]. Complex geometric designs of real human vessels have been reproduced through 3D printing techniques[6] and the fabrication of stenotic channels resembling occluded, thrombotic vessels are also easily made with small, no time-consuming changes in the design of the microchip[5]. The high number of channels, low amounts of materials and less time spent in the fabrication processes when compared to macro *in vitro* models also result in higher throughput and repeatability.

Microfluidic models have also been replacing *in vivo* models as the most important platform for studying thrombogenesis. Data provided by research on microdevices is directly interpreted as human-specific, since human cells are used to line the microchannels and human blood can be used in perfusion experiments in the platform[5,6,10,84]. Furthermore, since no ethical issues arise from the direct use of these platforms, part of the obstacles of working on vascular diseases' research are surpassed.

However promising, microfluidic devices also present some possible disadvantages comparing to the aforementioned alternative methods: small channels offer higher resolution but can also make detection more demanding and, most important, are susceptible to blockage from particles[85] which may interfere with the results.

Continuous advances in this area promise to support a more accurate analysis of thrombosis and all the components involved in the development of the disease. Microfluidic models with growing complexity and detail are being developed with the goal of mimicking the human vascular environment as closely as possible[57]. Channels lined with endothelial cells are used to reproduce blood vessels design and behaviour, such as the constant laminar flow (characteristic of microfluidic devices), and to allow easy manipulation of shear stress, flow, concentration of agents and other important conditions that are thought or proved to be linked to the development of vascular diseases[53].

2.9. Main methods for inducing thrombogenesis *in vitro*

In principle, the environment within a blood vessel (*in vivo* or *in vitro*) should neither be pro-coagulatory nor prothrombotic, and spontaneous creation of thrombogenesis should not exist. Thus, the ability to recreate thrombosis in *in vitro* and *in vivo* models depends on the introduction of one of the factors known to influence thrombogenesis[4,86]: vessel wall dysfunction, through the application of chemical or physical factors or, alternatively, via direct alteration of the channel's configuration through the physical induction of stenosis.

Animal models are frequently divided into three different groups, if solely considering the mechanisms used to trigger the desired thrombotic events[86]: models of physical induction of stasis or stenosis in the vessels; models of application of ferric chloride ($FeCl_3$); models of electrolytic stimulation.

For complete stasis and incomplete stenosis models, mice undertake surgery to reduce blood flow in the desired vessel (usually, the inferior vena cava for venous thrombosis[86,87] and the carotid artery for arterial thrombosis[5]). In complete stasis of the vena cava, blood flow is completely blocked, inducing rapid development of thrombotic events[87,88]. However, the lack of blood flow in these experiments limits the potential to test the effects of therapeutic agents on the model[86,87]. As such, incomplete stenosis is the most frequently used technique to physically induce thrombosis development, with reported success in mimicking several features of the human disease[89,90]. Some authors report stasis and stenosis models to induce thrombotic events of different natures, recapitulating distinct aspects of thrombogenesis and, as such, defend that none of the methods is more accurate or recommendable than the other[90]. Parallel methods can be used in arterial thrombosis models, as described by Westein et al.[5], who described an *in vivo* murine model of arterial thrombosis, after using a micromanipulator-controlled needle to create a stenotic lesion in the animal's carotid artery.

Vessel wall dysfunction is achieved through two types of processes: introduction of inflammatory agents, of which $FeCl_3$ is the most frequent in murine models[5,86], or application of electrolytic stimulation[91]. Exposure of vessel walls to ferric chloride results in endothelial damage[86] and consequent denudation of the cell layer[90]. On the other hand, application of direct current to the vessel (the electrolytic model), results in the local formation of free radicals, which will interfere with normal cellular processes and lead to endothelial activation and thrombi development[81,] . These techniques present simpler, more easily reproducible approaches than the induction of physical stenosis in mice[85,86]. However, due to rapid thrombi formation and introduction of external, non-physiological agents, both methods are considered by certain groups as having disputable pathophysiological relevance for research on human thrombogenesis[86].

With the growth of *in vitro* microfluidic devices, a turn towards two of the methods was observed: partial stenosis of the channel and the introduction of inflammatory agents became the most used techniques. The introduction of stenotic obstacles in microfluidic channels only require simple alterations of the design of the device, in contrast with the necessary complex surgical procedures in animal models[5,6].

Regarding chemical induction of thrombogenesis, the most frequently used inflammatory agent for inducing injuries of *in vitro* endothelium is Tumour Necrosis Factor alpha (TNF-α)[10,92]. This is an

inflammatory cytokine produced during human physiological response to acute inflammation and that has relevant roles in mediating anti-tumour and infection responses. However, its release can lead to cell injury, vessel dysfunction and interfere with coagulation processes. TNF-α has been reported to upregulate the expression levels of endothelial receptors and adhesion molecules (such as ICAM-I) in *in vitro* experiments with diverse endothelial cell lines and promote the rapid *in vitro* thrombi formation[10,34]. Various concentrations of TNF-α solutions have been used to induce thrombi formation, depending on the platform, cells and goal of the experiment. The more usual concentrations range from 5 ng/mL[10,84] to 50 ng/mL[92] of the agent; exacerbated effects, including cell death and monolayer degradation have been observed at higher concentrations.

The mechanism of action of TNF-α has been extensively researched and reviewed[93,94]. The two main receptors for TNF-α, TNF receptor type I (TNFR1) and type II (TNFR2), have distinct intracellular domains, resulting in different pathways of response to the inflammatory cytokine. TNFR1, the main focus of research, possess a TRADD (TNF-R1-associated death domain protein), which together with TRAF2 (TNFR-associated factor-2) and death domain kinase RIP (receptor interacting protein) mediate pro-apoptotic and pro-inflammatory signalling pathways. Although the mechanism of response is not yet fully understood, the activation of the nuclear factor B (NF-κB) pathway, through deactivation of its inhibitor (IκB), may be responsible for the expression of other pro-inflammatory cytokines (e.g. interleukin-1) and for influencing the apoptotic processes that are characteristically induce by high concentrations of TNF-α. Schematics of the mechanism can be seen in fig. 15.

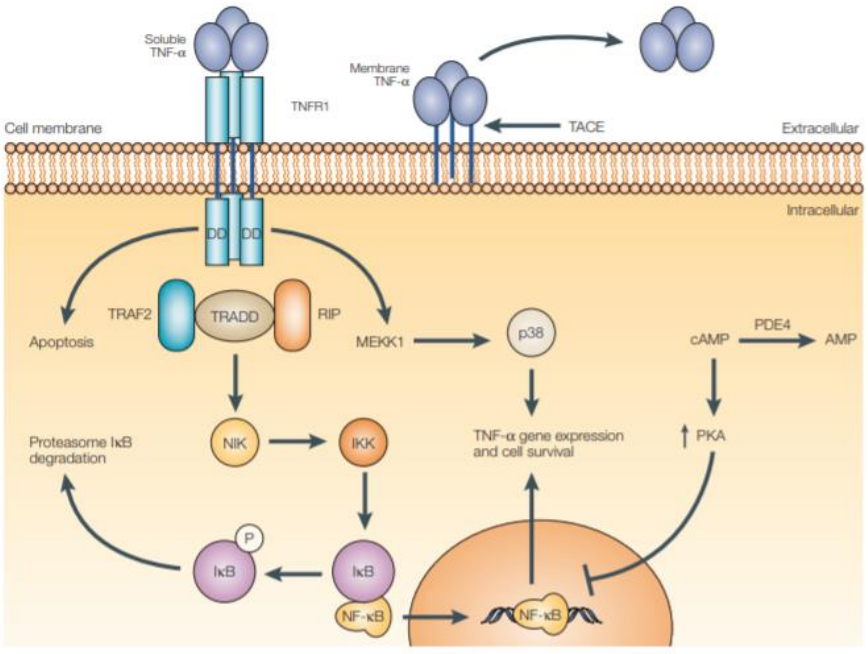

Figure 15 - Schematics of TNF-α interaction with TNFR1 in the ECs' surface and the activated pathways induced by this bond. TRADD, TRAF2 and RIP are activated and induce several pro-inflammatory and pro-apoptotic mechanisms, one of the main ones being the activation of NF-kB and of second messengers (e.g. cAMP) promoting further inflammatory responses. Taken from [93].

2.10. *In vitro* modelling of the endothelium

2.10.1. Human umbilical venous endothelial cells

Human umbilical venous endothelial cells (HUVECs) are the most frequently used endothelial type of cells in research. HUVECs popularity is due to two important factors: on the one hand, the availability, price and simple protocols of isolation of these cells and, on the other hand, the endothelial characteristics that make them suitable models of the endothelium[7].

HUVECs are isolated directly from human umbilical cords. Diverse protocols have been optimised and reported to yield several thousands of cells for each human umbilical cord[95,96] . HUVECs present cobblestone-like morphology in static conditions[6,97] and are able to grow into a full monolayer of cells, either *in vivo* or *in vitro*, or be differentiated into 3D spheroid cultures[98]. This venous primary cell line has been reported to express many known endothelial cell markers[34] (e.g. ICAM-I and VCAM-I) and signalling molecules (e.g. NO[7]). Furthermore, they have the ability to respond to several physiological stimuli of chemical (e.g. high levels of glucose[7]), physical (e.g. high shear[97]) and pathological (e.g. TNF-α[10,34]) nature. Co-cultures of HUVECs with other types of human cells to mimic real *in vivo* interactions[99] and 3D *in vitro* structures of vessel networks[100] have already been developed and support the dynamism of HUVECs as models of the human endothelium.

However, important differences between HUVECs and other ECs have been described in literature and led to the categorisation of this cell line as the most important model on general behaviour and properties of ECs, but not under specific conditions or for pathological studies[95], in which their advantages are outshone by the possible loss of information on the realistic response of human ECs. Authors have encountered diverse challenges regarding distinct responses of *in vitro* cultured HUVECs and *in vivo* ECs in the presence of certain molecules[7] or even drastic differences in expression levels of relevant glycoproteins and receptors between HUVECs and the cells whose behaviour they are meant to reproduce (e.g. in studies of the blood-brain barrier[101]). In addition, as a standardised cell line, HUVECs do not offer the possibility to take into consideration individual, genetic variability of the endothelium, thus failing to perform in areas in which patient-specific characteristics would be of great value (mostly related to medical and drug screening applications).

This led researchers to look for alternative cell lines for modelling the *in vivo* endothelium and reproducing it in *in vitro* experiments. Human induce pluripotent stem cells-derived endothelial cells (hiPSC-ECs) have recently gathered great attention from the scientific community as a possible promising alternative to limiting factors of primary cells' use in research.

2.10.2. Human induced pluripotent stem cells-derived endothelial cells

Human induced pluripotent stem cells (hiPSC) have been one of the most acclaimed breakthroughs in the biological and medical fields of the last decades. HiPSCs are human pluripotent stem cells which are obtained through *in vitro* reprogramming of adult somatic cells, in the presence of certain specific

transcription factors. After this reprogramming step, hiPSC can be differentiated into different types of adult cells of the human body and present a virtually limitless source of human cells for research and use in patient-specific medical applications.

Several protocols have been designed for optimising the reprogramming method originally developed by Takahashi and Yamanaka (2006)[102], who demonstrated that mice hiPSC could be obtained from fibroblast cultures with the introduction of factors OCT3/4, Sox2, c-Myc and Klf4. Malik and Rao (2013)[103] clearly organised these methods in three main categories: single cassette reprogramming vectors (with lentiviral vector sequences incorporation), reprogramming by nonintegrating viruses (adenovirus and Sendai Virus) and nonviral reprogramming methods (mRNA or miRNA transfection, PiggyBac transposon integration and introduction of minicircle vectors or episomal plasmids). Of those, Halaidych et al.(2018)[34] pointed out the particular importance of the Sendai virus-based reprogramming method in the generation of hiPSC from skin fibroblasts, nasal epithelial cells, peripheral blood mononuclear cells and cells from human urine.

Generation of endothelial cells from hiPSC (hiPSC-ECs) for research on main vascular diseases has also been the focus of several groups. The presently used strategies for differentiation of hiPSC into ECs follow one of three main methods: stromal cell co-culture, embryoid body differentiation or 2D monolayer differentiation[104] (fig. 16). Of those, the latter is currently the most successful reported strategy for EC-differentiation[8].

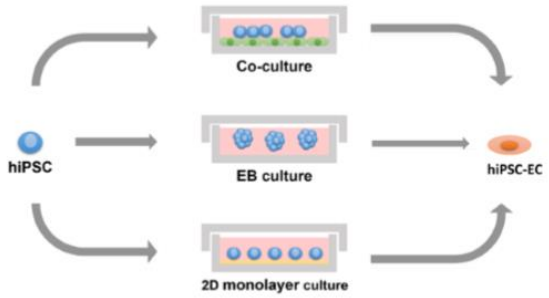

Figure 16 – Schematics of the three main categories of methods to generate human endothelial cells from hiPSC: co-culture with stromal cells; embryoid bodies culture and differentiation; 2D monolayer culture and differentiation. Taken from [104].

Stromal co-culture, now outpaced by the growth of the other two methods, involve culturing hiPSC with stromal cells (usually murine), which influence the undirect differentiation of the former into ECs (mixed with hematopoietic cells[105], smooth muscle cells and other murine stromal cells[104]). The low frequency of differentiation and the resulting mix of different cells (including murine) led to the decay in its use.

Embryoid body differentiation involves the development of 3D aggregates of hiPSC and their spontaneous differentiation into adult cell lineages (usually directed into ECs by the addition of specific growth factors). This process is thought to recapitulate some of the early human embryonic development stages and has been reported to result in robust induction of ECs, which are then purified via fluorescent-activated cell sorting (FACS) or magnetic-activated cell sorting (MACS) using specific EC markers and enriched in EC-favourable monolayer cultures[104].

Protocols using 2D monolayer differentiation have been the most successful techniques for achieving high yields of differentiated ECs (more efficient differentiation with higher yield of ECs[106,107]). The method implies the addition of specific factors at specific stages of hiPSC development in a matrix-coated culture plate, which will first direct them towards a mesoderm specification phase and ultimately towards an endothelial specification phase[8,104]. A combination of the factors Activin A, Bone Morphogenetic Protein-4 (BMP4), and Basic Fibroblast Growth Factor (bFGF) is usually applied during mesoderm differentiation, while vascular endothelial growth factor (VEGF) is added for EC differentiation[8].

Several studies using the expression of endothelial markers as a method for confirming the identity and characteristics of ECs derived from hiPSC have been published[34,108,109], usually measuring expression levels of some of the EC specific molecules described previously (section 1.3.2 of the Introduction), such as CD31 or vWF. A number of authors reported physiological-like levels of these markers in hiPSC-EC, and some revealed an inclination towards arterial and embryonic natures in most of tested cell lines and protocols[34,108], while others indicated that they displayed an intermediate nature, with the expression of venous and arterial markers[109,110]. Furthermore, authors such as Ikuno et al. (2017)[110] and Tan et al. (2013)[111] stated the possibility to control arterial-venous fates of hiPSC during and after EC differentiation stages through the different supplementation of small molecules and growth factors in the medium. Studies describing hiPSC-EC displaying some venous or lymphatic EC-specific markers are, nonetheless, still a minority and the efficient induction of these types of EC specification stand as an obstacle to overcome[8].

Halaidych et al. (2018)[34] published a study on the detailed characterisation of multiple hiPSC-EC lines, to conclude about batch-to-batch and line-to-line variability, and on their comparison with human primary ECs (HUVECs, HUAECs and human dermal blood ECs, HDMECs) in diverse functional assays. The expression of EC surface markers and gene expression profiling assays displayed a mixed arterial and embryonic-like nature, as previously reported in literature[108]. In contrast with their CD34+ hiPSC-EC line and tested primary cells, their CD31+ hiPSC-EC line also demonstrated enhanced barrier functions and less responsiveness to barrier disrupting agents, e.g. histamine or thrombin[34]. Both upregulation of ICAM-I in presence of the inflammatory agent TNF-α and leukocyte adhesion during inflammatory response assays was more pronounced in primary cells (HUVECs) than in hiPSC-EC, indicative of differences in response to injury between these cell lines. Furthermore, vWF basal levels were also lower in hiPSC-ECs. These results suggest several important differences between hiPSC-ECs and primary cells. In addition, they also showed consistent results between independent batches of hiPSC-EC, although some differences were found when comparing different lines (CD31+ and CD34+ isolated cell lines). Finally, the assays suggested that hiPSC-ECs possess the ability to reproduce endothelial barrier function and to respond to pro-inflammatory factors. However, some relevant differences in terms of receptors' upregulation and levels of coagulation proteins (vWF) may be indicative of possible future discrepancies when recreating the dynamic environment of human vessels and the development of vascular diseases (when comparing hiPSC-EC and primary cell lines).

Overall, hiPSC-ECs represent a promising approach in vascular research and drug targeting, offering human endothelial cells phenotype with patient-specific characteristics. Yet, methods for their

differentiation and implementation are still not standardised and quality control assays still are not well-developed[8,34,109]. Even though hiPSC-ECs consistently display key features of human ECs, some teams showed relevant differences between these cells and diverse primary human cell lines regarding the expression and production of important *in vivo* EC molecules, such as pro-inflammatory receptors (e.g. VCAM-I), essential factors of coagulation processes[34] (e.g. vWF) and stress response proteins (e.g. PAI-1[109]). This can be a limitation in studying and modelling certain human conditions. Thus, more investigation on the subject and the standardisation of reprogramming and differentiation methods is still necessary before full the establishment of hiPSCs technology.

3. Thrombosis-on-a-chip: in pursuit of Personalised Medicine

The thrombosis-on-a-chip project aims at creating a microfluidic device that models human thrombosis accurately. The device should be able reproduce human blood vessels' environment and *in vivo* thrombogenesis stages, enabling the design of complex, realistic, vessel-like geometries and the use of human cells. The long term, ultimate goal is to build a reliable, dynamic *in vitro* model, which can be used in research on the disease and eventually be applied to medical purposes, allowing the patient-specific evaluation of each drug's and treatment's effects. For that end, the implementation and standardised use of hiPSC as patient-specific sources of human cells are considered the next big game changer – and a step towards the personalised medicine paradigm. Personalised Medicine represents a new hope to research on human diseases, bringing improved drug targeting and patient-tailored therapies to the table[112].

Although both highly threatening for human life, arterial thrombosis has been a bigger focus of research than its venous analogous. This is probably related to scale differences and higher complexity of venous thrombosis, which still makes the disease harder to reproduce in microfluidic devices[4]. However, some work on the subject has been developed, and research on clot propagation mechanisms and embolisation[113] and on the effects of wall shear rates on venous clot formation and composition[114] have been performed using microfluidics.

In arteries, atherosclerosis and its close relationship with the development of thrombotic events have been studied for decades. The advancements in the field of microfluidics have, however, brought new opportunities to the area, both confirming with human cells previous conclusions taken from studies with animal models and enabling the use of realistic vessel-like geometries.

Microfluidic channels designed with stenotic areas mimicking atherosclerotic plaques have been tested, and results were promising for research on the disease. Westein et al.(2013)[5] successfully performed blood perfusion with recalcified human whole blood on microfluidic channels fabricated with one-sided stenotic obstacles of different sizes, resulting in 20%, 40%, 60% or 80% of lumen occlusion (fig. 17).

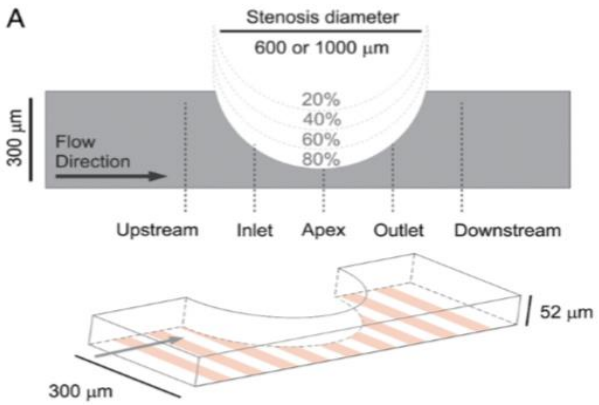

Figure 17 - Design of the microfluidic channels fabricated by Westein et al. to study the influence of stenotic obstacles on flow dynamics and thrombogenesis. different levels of occlusion (20%, 40%, 60% and 80%) were tested. Taken from [5].

The authors' goal was to conclude about the previously hypothesised[115,116] influence of plaque-induced flow dynamic alterations on the platelet aggregations processes during arterial thrombogenesis. In parallel to the microfluidic experiment, Westein et al. (2013) also used an *in vivo* murine model, upon physical induction of local stenosis in the carotid artery with a micromanipulator-controlled needle and activation of the endothelium with ferric chloride[5]. With their work, they not only demonstrated both *in vivo* and *in vitro* thrombi development in stenotic vessels – showcasing the large potential of microfluidics in research on thrombosis – but also showed that areas downstream of stenotic injuries are indeed more prone to thrombi formation. Furthermore, the authors were able to describe the increased relevance of the presence of soluble and endothelial vWF in promoting these aggravated pathological events during atherothrombosis and confirmed the role of shear rate gradients[67] and altered flow patterns[115,116] in platelet aggregation. In their work, it is suggested that endothelial cells also directly contribute to stenosis-induced platelet aggregation due to increased levels of vWF secretion and accumulation in areas of near-vascular occlusion, as Ni et al.(2000)[117] had observed in mice.

To overcome limitations related to standard 2D microfabrication methods, which produce simple, rectangular channels not allowing for fully representative configurations of blood vessels, the reproduction of more complex 3D geometries of human vessels has recently been the focus of some groups' work. Costa et al.(2017)[6] described and published a method for recreating *in vitro* microfluidic models of real 3D human vessels' designs, using thoracic computed tomography angiography (CTA) data from real anonymised patients. The microchip's complex design was fabricated using 3D printing, offering a more accurate replication of human vessels' architecture (fig. 18A and B) compared to that obtained using standard soft-lithography techniques[5,6].

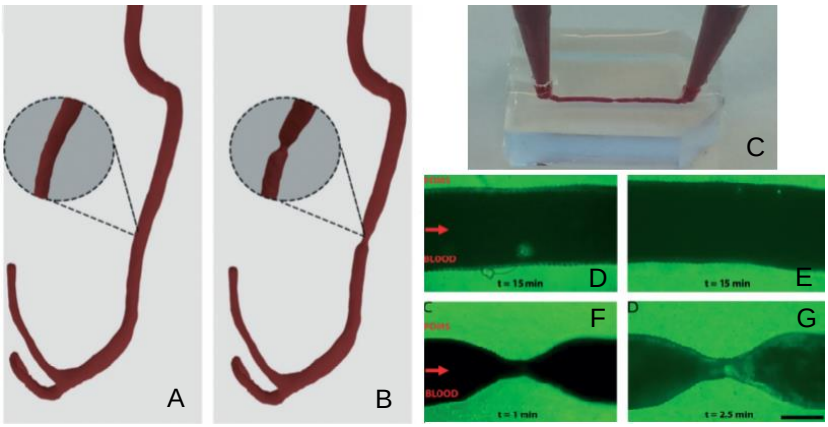

Figure 18 - Images of the work of Costa et al. in microfluidics. Modelling of vessel models were rendered and designs for healthy (A) and stenotic (B) channels were made. As a proof-of-principle experiment, fabricated 3D-printed devices were used in blood perfusion experiments (C) and differences in platelet aggregation within healthy (D, E, after 15 min) and stenotic (F, G, after 1 and 2.5 min) channels was observed. Taken from [6].

As proof-of-principle experiments, the authors then successfully tested these models with healthy and stenotic vessels during blood perfusion (fig. 18C, D, E, F and G), after endothelising the microchannels with human primary EC (HUVECs). After only 2.5 minutes of blood perfusion platelet aggregation was visible in the stenotic vessel (fig. 18F, G) but not in the healthy control (even after 15 minutes, fig. 18D, E), indicating the usability of the device in reproducing thrombogenesis. Due to the reproduction of the

natural shape of the vessels' walls and structures, the authors also suggest that the model can similarly be used for comparison of *in vitro* tests with *in silico* simulations on realistic fluid flow patterns within human vessels[6].

In another tone, Jain et al. (2016)[10] work was focused on demonstrating the ability to implement and test endothelial cells in the microfluidic chips and the potential clinical value of these devices. After endothelising and fixing the cells, the authors showed that the endothelium still retained expression of important ECs markers, such as vWF, ICAM-I and VCAM-I. They also reported that, after activation of the endothelial layer with TNF-α, platelet adhesion and further development of thrombosis was still observed in dynamic conditions, during blood perfusion (under flow at arteriole-like shear rate, 750 s^{-1}). Lastly, the device was used in preliminary tests to establish its adequacy for the detection of antiplatelet drug effects in healthy donors and patients already under antiplatelet medications. The pre-treated endothelium was perfused with blood containing different doses of antiplatelet drug abciximab (ReoPro®), from 0 to 100 µg/mL (the usual clinical range is 1 to 10 µg/mL). Results were similar to those obtained in previous studies on the inhibitory effects of abciximab on platelet adhesion, using flow cytometry analysis[118], which showed dose-dependent inhibition of adhesion and optimal effects at 10 µg/mL and higher. However, they were not in accordance with the results of conventional methods for assessing platelet function, like light transmission aggregometry (LTA[10]), which resulted in total inhibition of platelet aggregation at all drug concentrations tested. The authors believe that this indicated higher dynamism of the device in comparison with LTA, showing robust results with less time of operation and lower costs. Furthermore, due to fixation of the endothelium, the device can be stored and used in laboratories or as a point-of-care testing method. Although further investigation on the effects of fixation on coagulation mechanisms and on its suitability for medical application is needed, the endothelised chip demonstrated positive and promising results in a drug testing context, allowing for qualitative and quantitative analyses of prothrombotic responses of the cells and platelets.

4. Objectives

The microfluidics' field is reaching a point where designed devices can reproduce real patient's complex vessel geometries and where microchips for research on human diseases are beginning to be tested against assays used in clinical environment. In both sets, they are being successful and continue to display promising results. However, a point in common in publications of diverse groups working in the area is the belief that the implementation of hiPSC-EC stands as the next step towards a personalised, enhanced approach to the study of human disease. Differences between hiPSC-EC and primary cells have been identified in literature and conclusions of the work of Halaidych et al. (2018)[34] (on the lower levels of vWF, ICAM-I, etc in hiPSC-EC in comparison with HUVECs), Westein et al (2013)[5] (on the importance of vWF in thrombosis exacerbation) and others[97,108–110], seem to predict distinct responses of these cell lines in a prothrombotic context.

This work aims at combining hiPSC-EC with thrombosis-on-a-chip devices, with the ultimate goal of advancing towards patient-specific analysis of thrombosis and its treatment.

The specific objectives were to:

- Design and optimise protocols for the implementation of hiPSC-EC on thrombosis-on-a-chip devices
- Describe morphological differences between hiPSC-EC and HUVEC on-chip (under static conditions)
- Assess the capacity of hiPSC-ECs seeded on-chip to be tested under blood perfusion
- Compare the thrombogenic response between hiPSC-ECs and HUVECs in healthy conditions and after vessel wall dysfunction was induced (with TNF-α)

II. Materials and Methods

1. Microfluidic device fabrication

The microfluidic device used in the experiments throughout this report had already been designed in the BIOS Lab-on-a-chip group of the University of Twente, using specialised computer-aided design (CAD) software, and the master mould (silicon wafer) had already been fabricated prior to this work.

1.1. Rapid prototyping: chip design and wafer fabrication

The current project aimed at implementing and characterising hiPSC-ECs in the presence of blood perfusion and not at testing the effects of different flow patterns and geometries on thrombosis. Thus, the goal for the planned experiments was to have a simple, straight-forward design, resembling a human-vessel like structure but with no complex geometries.

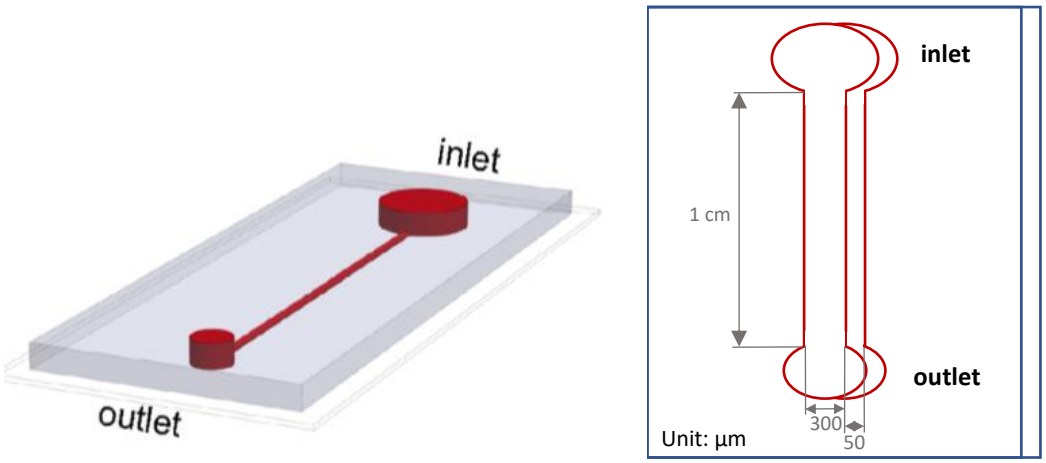

Figure 19 – Schematics of the design of the microfluidic device. Two reservoirs were designed 1 cm from each other, with a hollow, straight, rectangular chamber in between (the channel) with dimensions of 300 x 50 µm (width x height). The left picture was taken from [10] for representing a similar channel, although with different inlet and outlet reservoirs.

In fig. 19, two schematics of the microchannels of the chip can be observed (not to scale). The straight, rectangular channel where cells were to be seeded was designed to be 1 cm long (length), with dimensions of 300 x 50 µm (width x height). The channel, a hollow chamber, connects two hollow, circular reservoirs in the extremities: one to be used to introduce fluids in the microchannel (inlet); the other to be the outlet, from where fluids would exit the channel. These reservoirs, punctured by hole puncturing techniques after the PDMS curing step, were both approximately 1 mm wide.

A silicon master mould with the desired structures was fabricated by photolithography at BIOS. The master wafer was used for moulding polydimethylsiloxane (PDMS) microchips with the designed patterns by soft-lithography techniques[81].

1.2. Preparation of the PDMS and replica moulding

The PDMS elastomer used in BIOS laboratories, SYLGARD™ 184, is supplied as two separate components by Dow Corning. One of the components is SYLGARD™ 184 Silicone Elastomer Base, a liquid, viscous, silicon base, and the other one is a curing agent, which works as a catalyst for the cross-linking of PDMS (when mixed with the base). After mixing the two components, cross-linking will happen at relatively low temperatures (~60 ºC) after just two to three hours. PDMS will then solidify due to the reactions between the vinyl groups of the base and the hydrosilane groups of the curing agent.

The first step consists of mixing the base and the curing agent in a 10:1 (w/w) ratio in a disposable plastic tube. The tube should then be let for at least two hours in a vacuum desiccator, to avoid air humidity while the mixture is being degassed and the bubbles (formed during mixing) removed.

The previously fabricated silicon wafer can be placed in a glass Petri dish wrapped in aluminium foil (so that the PDMS does not come in contact with glass. When ready, the mixed, degassed prepolymer is then poured over the wafer and will naturally adapt its shape to the desired features of the wafer (as a negative replica of the wafer surface). Observed bubbles formed during the pouring step can either be removed manually with a small plastic pipette or by leaving the glass dish in vacuum for around 10 minutes. The latter was the preferred one for the experiments reported here.

Finally, the glass dish with the wafer and PDMS on top is cured at 60 ºC for at least 3 hours (Quincy Lab Inc. Model 10 Lab Oven), to ensure proper cross-linking and solidification of the polymer. After that period, the produced replica can be carefully removed from the master wafer and reservoirs can be punctured (e.g. using a borer or hole puncturing tool). Scotch tape was always taped to the sensitive surface (the negative of the wafer) to avoid dust from entering the channels.

1.3. Sealing and surface treatment of the PDMS chip

Glass slides (Thermo Fisher Scientific) to be used as the sealing surface of the microchip were rinsed with ethanol and isopropanol to remove possible biological residues and dust. PDMS chips were then placed at the plasma treatment chamber with the face of interest pointing upwards (to be activated), together with the clean glass slides. Immediately after the programme of plasma treatment ended, both activated surfaces (PDMS and glass) were brought to contact and the microchip was instantly, irreversibly sealed.

These steps were always done less than 30 minutes before the seeding of the cells, not only to reduce the probability of particles (e.g. dust) entering the channels but also to prevent loss of the treatment strength. The activated, oxidised surface of PDMS is easily and quickly reverted to its hydrophobic state if it stays in contact with air. Keeping the microchip in contact with polar liquids (e.g. Phosphate-Buffered Saline (PBS)) is important to prevent this.

1.4. Chip coating

Collagen is one of the main ECM proteins in the human blood vessels. Thus, for promoting the attachment and growth of human endothelial cells inside the channels of the fabricated microfluidic devices, rat tail collagen type I (Corning) was chosen as coating.

After plasma treatment, chips were taken to a laminar flow hood in a Microbiological Laboratory Class I (ML-I, Biological Safety) and collagen-I at 0.1 mg/mL was introduced in the inlet reservoirs. Collagen was slowly pushed through each channel, avoiding air bubbles formation, until a small droplet appeared on the outside of the outlet reservoir. Once the procedure was over, microchips were incubated at 37 ºC, 5% CO_2 (BINDER incubator) for 30 min to 1 h.

Some droplets of collagen solution should always be left on top of the reservoirs of the channels and, if possible, some PBS (Sigma Life Science) should be left on and around the device. This steps prevent drying of the device during incubation, which could interfere with the correct coating process.

2. Cell culture

2.1. HUVEC cell culture

HUVECs (Lonza, Pooled donor) were cultured in Endothelial Cell Growth Medium (ECGM, Cell Applications, Inc.). All the steps described were performed in a laminar-flow chamber and safety protocols were followed to avoid contamination of the equipment and cells and ensure the safety of the operator.

Cells were cultured in collagen-I coated T-75 flasks and grown at 37 ºC, 5% CO_2. Whenever high confluency was achieved (around 80%), cells were passaged to new T-75 flasks with fresh ECGM medium. For this step, the exhausted medium was removed from the flask, cells were washed with PBS and 0.05 % Trypsin (Gibco Life Technologies) was added for 5 minutes at 37 ºC, until cells detachment was confirmed (under the microscope). To deactivate the cell-dissociation agent, 7 mL of fresh medium was added to the flask and the cells were resuspended. The suspension was then centrifuged for 5 minutes at 390 x g (Allegra X-12R Centrifuge, Beckman Coulter). After that, the supernatant was carefully discarded. Around 1 mL (depending on the desired ratio for the cultivation of the cells) of fresh medium was used to resuspend the pellet of cells and around 10 mL were added to a new, coated T-75. Finally, the cell suspension was transferred to the new T-75 and incubated at 37 ºC and 5% CO_2.

2.2. HiPSC-EC cell culture

HiPSC were reprogrammed from human skin fibroblasts and differentiated into EC lines following previously reported protocol[119] (hiPSC-ECs were kindly provided to BIOS by the Leiden University Medical Center). HiPSC-ECs were cultured in Human Endothelial Cells Serum Free Medium (EC-SFM, Gibco) supplemented with platelet-poor plasma-derived serum, 1% (Hycultec), vascular endothelial

growth factor, 30 ng/mL (VEGF, R&D Systems) and fibroblast growth factor, 20 ng/mL (FGF, Miltenyi Biotec). All the steps described were performed in a laminar-flow chamber and safety protocols were followed.

Cells were cultured in 0.1% (w/v) gelatin coated T-75 flasks, according to the protocol of Orlova et al.[119]. and incubated at 37 ºC, 5% CO_2. When cells reached high confluency (around 80%) in the T-75 flasks they were passaged to new T-75 with fresh new EC-SFM full medium, following the same protocol of HUVEC except for the use of TrypLE (TrypLE™ Select (1x), Gibco) instead of trypsin as the dissociation agent.

3. Cell seeding of the microchips

Two different ways of seeding the microchips' channels with endothelial cells were used:

- To have a 3D, vessel-like structure (e.g. for blood perfusion), the bottom and the top half of the channel were seeded, meaning that the entire channel was lined with cells;
- For other purposes (e.g. morphology pictures) only the bottom part of the channel was seeded (to get a monolayer but avoiding two distinct planes of cells, making the pictures clearer).

The first steps of cell preparation were already described in more detail in the above sections. Briefly, cells were trypsinised (or dissociated with TrypLE), fresh medium was added, and a suspension of cells was obtained after centrifugation, removal of the supernatant and resuspension in ECGM.

Endothelial cells were seeded in the microchannels at around 15 x 10^6 cells/mL. The medium used for cell seeding and to culture inside the microchip was ECGM medium (for both types of cells), due to the necessary antibiotics. Cells were counted in a Luna Automated Cell Counter (Logos Biosystems) and the suspension was then carefully introduced in the inlet of the coated microchannels and the chip was incubated for 30 minutes at 37 ºC and 5% CO_2. A droplet of medium was left on top of the reservoirs and some PBS was be poured around the chip, so it does not dry.

After the incubation time, depending on the goal of the experiment, either the top part of the channel was also seeded (repeating the protocol but with the chip upside down in the incubator) or pipette tips with fresh medium were introduced in the inlets and empty tips in the outlet (promoting replacement of the medium throughout the day).

Pipette tips were replaced for new ones with fresh medium (or an inflammatory solution of TNF-α, see section 4.2 of Materials and Methods) at the end of the day. By then, the entire interior of the microchannels should already be lined with a monolayer of healthy cells.

4. On-chip experiments

4.1. Morphology tests

For observation and comparison of the morphologies of HUVECs and hiPSC-ECs, nuclear staining (NucBlue™ Live ReadyProbes, ThermoFisher Scientific) and VE-cadherin primary (Rabbit polyclonal, Abcam) and secondary (AlexaFluor 488 goat anti-rabbit polyclonal, Abcam) antibodies were used. To avoid photobleaching when working with the nuclear staining and secondary antibody, lights were turned off and, during incubation periods, Petri dishes containing the chips were wrapped in aluminium foil.

The cell-seeded microchannels were flushed with PBS to remove the medium and wash the cells and a prepared 4% buffered formaldehyde solution (Sigma) was introduced for cell fixation (20 min at room temperature). The channels were then flushed with PBS, for 10 minutes. The primary antibody solution, 1 µg/mL antibody in PBS with 1% bovine serum albumin (BSA, Sigma) was added to the channels and chips were incubated for 4 hours at 37 ºC or overnight at 4 ºC. PBS should be left on top of the chip to avoid drying.

After the incubation time, PBS was flushed through the channels and left in the channel for 10 minutes. The secondary antibody solution (10 µg/mL antibody in PBS) was added to the microchips and incubated for 1 hour at room temperature. The microchannels were then flushed with PBS once and the nuclear staining solution (2 drops/mL in PBS, according to the supplier) was added. After incubation for 30 minutes at room temperature and reflushing with PBS, cells were observed in an EVOS FL microscopy system (Invitrogen) with GFP (VE-cadherin) and DAPI (nuclei) filters

4.2. Inducing vessel wall dysfunction (factor of thrombogenesis)

Vessel wall dysfunction is considered one of the main factors promoting thrombogenesis and can be induced *in vitro* to analyse the development of the disease. TNF-α, an inflammatory cytokine reported to induce endothelial injuries, was used as the trigger for vessel wall dysfunction in the seeded microchips.

At the end of the devices' cell-seeding day, pipette tips were removed from the inlets of the channels and part of them were replaced with new pipette tips with fresh ECGM medium and the other part with a solution of 10 ng/mL TNF-α (Sigma-Aldrich) in ECGM medium. New empty pipette tips were introduced in the outlets to allow for the medium to be gradually replaced by the new solution. After a 16h exposure period (overnight), pipette tips were all replaced with ones with fresh medium.

The cells were then directly fixated or used in blood perfusion experiments, according to the planned experiments.

4.3. Whole blood perfusion with DiOC6 staining

To mimic as closely as possible the microenvironment inside a blood vessel, human whole blood was perfused through the cell-seeded channels of the microfluidic devices. Blood perfusion was conducted for 20 minutes and recorded using the side camera and software of a Leica DM IRM microscope. Citrated blood (to avoid coagulation in the tube) was provided by the Experimental Centre for Technical

Medicine (ECTM) of the University of Twente at the days of the experiments. The blood was used within the first 4 to 5 hours after being drawn from donors, to reduce possible degradation of the blood and time-dependent platelet malfunction.

The microfluidic chip was placed in a Petri dish taped to the microscope platform to assure it was not moved during the experiment. A BD Luer-Lok 3 mL syringe was connected to Tygon plastic tubing (VWR) with customised connectors and a customised L-shaped metal tip in the end. This equipment was flushed with washing buffer, a solution of HEPES (1M, Gibco), glucose (1%, Merck Millipore), BSA (1%, Sigma), CaCl2 (200 mM, Sigma) and heparin (0.1 µ/mL, Sigma), meant to prevent the blockage of the tubing due to clotting. The syringe was placed in a syringe pump (Harvard Apparatus PHD 2000 Programmable) and the metal tip was introduced in the outlet of the target channel of the microchip (the setup is shown in fig. 20). $DiOC_6$ staining solution (Life Technologies) for platelets was added to the blood (2 µg/mL), mixed by carefully inverting the tube three times and left for 10 minutes (incubation). A solution of MgCl2 (31.6 mM) and CaCl2 (63.2 mM) in HEPES, used as the recalcification buffer, was added at 1:10 (100 µl/mL) to the blood sample to allow for normal coagulation mechanisms. Immediately after, a 200 µL micropipette tip filled with the recalcified blood was introduced in the inlet reservoir and the pump set to the "Refill" mode with a flow rate of 7.5 µl/min, corresponding to a physiological arterial shear rate of approximately 1000 s^{-1} (present in human large arteries[5]). In this mode, the pump pulls the blood through the microchannel, where it contacts the *in vitro* endothelium, to the syringe.

$DiOC_6$ staining was observed with the GFP filter of the Leica microscope to follow real-time platelet aggregation.

Figure 20 – Pictures of the setup used for blood perfusion experiments. The microchip was placed inside a Petri dish on top of the microscope platform. The outlet was connected to a syringe placed on the pump. A pipette tip filled with blood was introduced in the inlet and the blood was pulled by the pump through the channel. A side camera connecting the microscope and the computer allowed for real-time record of the experiment.

4.4. Blood perfusion 2.0 (CD41, labelled fibrinogen, NucBlue, VE-Cadherin/P-selectin)

The second stage of blood perfusion on-chip involved observation of real-time platelet aggregation, the location of clots, their composition, and if platelets were being activated during the process. Lights in the laboratory were reduced to a minimum during the entire process to avoid photobleaching.

The protocol for blood perfusion was followed as described in the previous section with some differences. Fluorescently labelled fibrinogen (Alexa 647, Invitrogen) and CD41 labelled primary antibody (PE, Invitrogen) were directly added to the blood tube at 7 µl/mL and 10 µl/mL (incubation for 10 minutes), respectively, and carefully mixed before the recalcification step. To observe CD41-PE fluorescence in real time (platelet aggregation during perfusion), the BGR filter of the Leica microscope was chosen. After 20 minutes of perfusion, the chip was perfused with 50 µL of washing buffer at the same flow rate of the blood perfusion, to remove weakly attached particles from the channel. PBS was then slowly flushed through the channel and the staining protocol described in section 4.1, "Morphology tests", for VE-cadherin and nuclear staining were followed. In tests for platelet activation, VE-Cadherin primary antibody was replaced by P-Selectin labelled primary antibody (FITC, Santa Cruz) at 10 µg/mL in PBS with 1 % BSA. The rest of the protocol was followed as previously described.

Chips were analysed under the EVOS microscope. CD41-PE (R-phycoerythrin) fluorescence was observed with the RFP filter, fibrin (converted from labelled fibrinogen) with the Cy5 filter, nuclei with DAPI and VE-cadherin with the GFP filter.

5. Analysis of blood perfusion data

After blood perfusion, fixed and stained microchips were used to obtain endpoint measurements and data on platelet coverage and average clot size on healthy and injured HUVECs' and hiPSC-ECs' endothelial layers. Four fixed points of a channel (near the inlet, around 1/3 of the channel, around 2/3 of the channel and near the outlet) were chosen and pictures were taken (same points for all chips, regardless of the condition, to avoid operator's subjectivity). Considering the goal of this experiment, the RFP filter was used when taking the pictures.

The analysis of the channels was made so that the sections near the walls were not considered, since the flow near the edges of rectangular channels do not usually reproduce the reality of human cylindrical vessels[4]. Therefore, data from the first 50 µm in each side of the channels was discarded in this analysis. Only the middle 200 µm section was considered.

Platelet coverage was estimated using the triangle script of the software Matlab 2016b and surface area of the clots was determined with the regionprops script. Statistical analysis of the final sets of endpoint measurements of the platelet coverage data (four points per channel times the number of days of experiments – two days for untreated, three days for treated) was performed using the Student's *t*-Test with a significance level of 5%. This was made in Microsoft Excel software, using two distinct methods to confirm the results: the software's Data Analysis package and the direct Excel's function (t-test). For each healthy condition (HUVECs and hiPSC-ECs), data from two independent experiments was considered. For each diseased condition (HUVECs and hiPSC-EC exposed to TNF-α), three independent experiments were analysed.

6. Seeding of the microwells and tests with TNF-α

In tests with microwells, the same procedure already described for cell culture and seeding of the microchips was followed. After collagen-I coating the well surface, cells were seeded at 5 x 10^4 cells/mL (10000 cells/well, following previous protocols[34]). The final volume of each microwell was kept constant at 200 µL.

For tests on the effects of several concentrations of TNF-α on the EC monolayer of hiPSC-ECs and HUVECs, this agent was added at concentrations of 1, 2.5, 5, 10 or 50 ng/mL. As positive and negative controls, 70 % ethanol and ECGM medium were used, respectively. After introduction of TNF-α, wells were incubated at 37 ºC, 5 % CO_2 for 16 h. For tests on the effect of exposure time to TNF-α, cells in contact with the same listed set of concentrations were incubated for 19 h and 22 h.

After the incubation period, cells were washed with ECGM and fresh medium was introduced. Staining for F-actin and nuclei was performed following the method described in section 4.1 of Materials and Methods for fixation, followed by permeabilisation with a solution of Triton-X (0.3 %, Sigma) in PBS for 30 minutes at room temperature. ActinGreen™ 488 ReadyProbes™ (Thermo Fisher) and NucBlue were added to the microwells at 2 drop/mL of medium of each one of the staining solutions, the plate was incubated for 30 minutes at 4 ºC and cells were observed under microscopy (with the EVOS microscopy system).

III. Results and Discussion

1. Optimisation of hiPSC-ECs culture in T-75 flasks

The first goal of the project was to design protocols to successfully grow and implement hiPSC-ECs in previously designed thrombosis-on-a-chip devices.

HiPSC-ECs were seeded in T-75 flasks and their growth followed (fig. 21D, E and F) in parallel with HUVECs' growth (fig 21A, B and C).

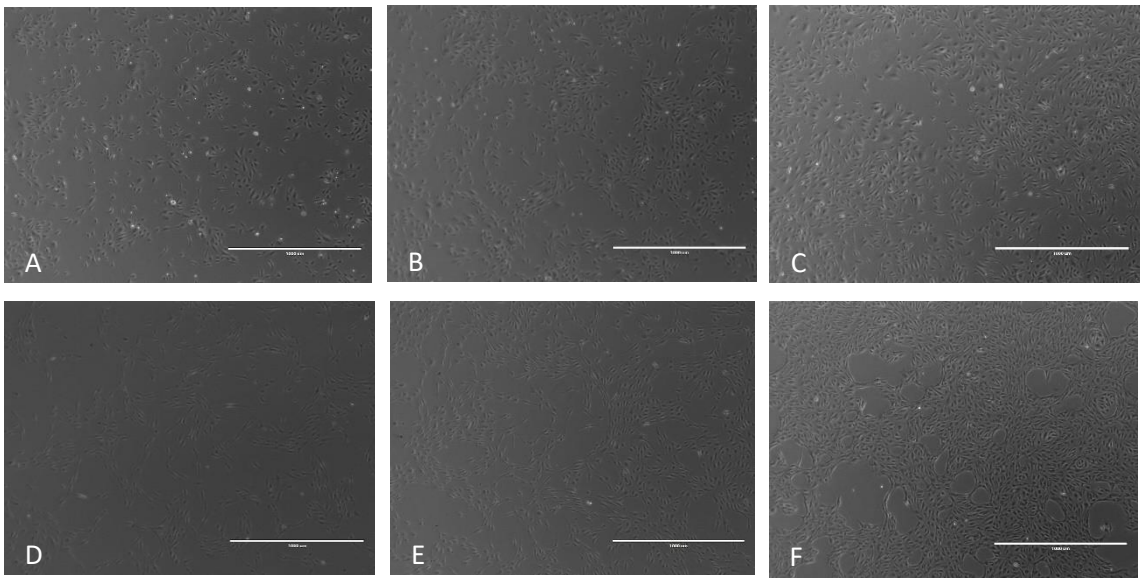

Figure 21 - Growth evolution of HUVECs (A, B,C) and hiPSC-ECs (D,E,F) in T-75 flasks. A and D were taken one day after seeding (at 1:6). B and E were taken two days after seeding. C and F were taken four days after seeding. Scale bars, 1000 µm

HiPSC-ECs grown in the T-75 displayed endothelial-cell-like morphology. However, it was noticeable that hiPSC-ECs presented a more elongated, spindle-shaped morphology when compared to the characteristic cobblestone shape of HUVECs. This is in agreement with the report of Belt et al.[120], who showed the spindle-like morphology of hiPSC-ECs growing in T-75 cultures and reported a shift into a more fibroblast-like morphology after prolonged culture.

In contrast with HUVECs, which were grown in collagen-I coated T-75 flasks, the culture of hiPSC-ECs was performed in 0.1 % (w/v) gelatin-coated flasks. This followed previously established protocols[119] which successfully achieved fully functional hiPSC-EC. However, there was no prior information pointing at the preferential use of gelatin over collagen as coating for hiPSC-EC growth. Although no further detailed characterisation was made, some attempts of cell seeding and culture with collagen-I coated T-75 flasks resulted in successfully cultured hiPSC-ECs, with no visible changes in growth or morphology. Although, more tests have to be carried out to be able to conclude about the most advantageous ECM coating for the flasks, hiPSC-ECs growth on both matrices seem to be adequate.

2. Cell culture on-chips: seeding densities and ECM coating

Several seeding densities were tested, with the goal of reaching an optimal value at which the channels with healthy, confluent monolayers of HUVECs and hiPSC-ECs could be used at the end of the same day they were seeded (which was relevant for the other planned experiments involving overnight exposure to TNF-α).

Previously developed protocols[10,92] had described the optimal seeding density of HUVECs in these devices to be between 5 x 10^6 cells/mL (below which cells would not be able to properly grow and create a stable monolayer) and 20 x 10^6 cells/mL (above which the cells would be overconfluent, resulting in cell death and unhealthy monolayers). To find a narrower range of values to reduce variability in the experiments that would follow, some channels were seeded at 5-10 x 10^6 cells/mL (fig. 22A) and others at 15-20 x 10^6 cells/mL (fig. 22B).

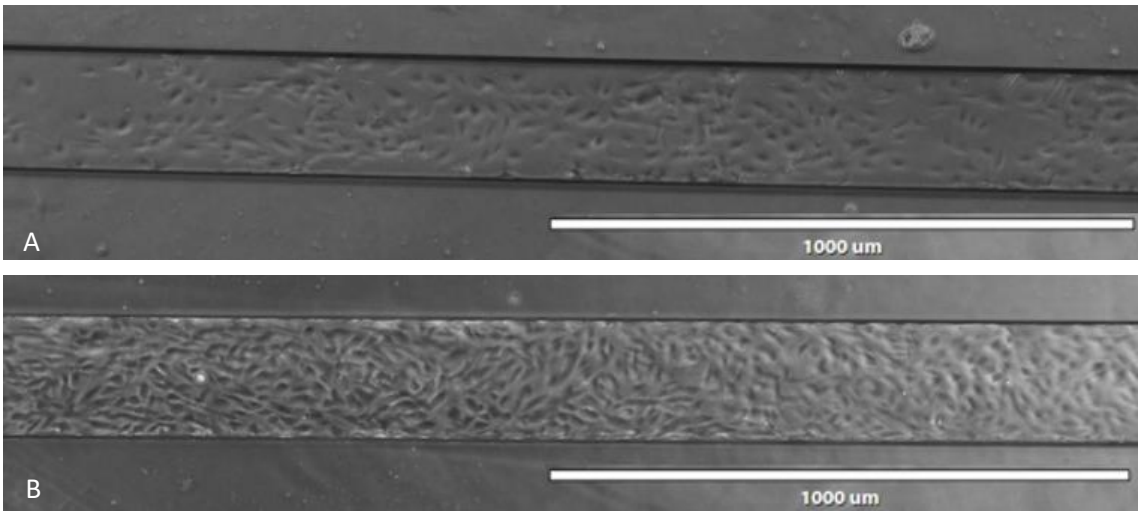

Figure 22 - Thrombosis-on-a-chip device's microchannels seeded with HUVECs. Pictures were taken around 5 hours after cell seeding. In A, the channel was seeded at around 5 x 10^6 cells/mL; in B, the channel was seeded at around 20 x 10^6 cells.

It was generally found that, after 5 hours, seeding densities below 10 x 10^6 cells/mL resulted in incomplete monolayers of attached cells (fig. 22A) which did not reproduce the epithelial layer of human blood vessels. On the other hand, seeding densities above 15 x 10^6 cells/mL (and bellow 20 x 10^6 cells/mL) mostly resulted in full monolayers of cells (both hiPSC-ECs and HUVECs), that could line the entire inner walls of the microchannels (fig. 22B). Yet, some of the channels with higher seeding densities (around 20 x 10^6 cells/mL) presented overconfluent layers with some cell death which could influence the result of the experiments. Thus, the seeding density deemed optimal for implementing hiPSC-ECs and HUVECs in the microfluidic devices in use was set to 15 x 10^6 cells/mL.

It is also relevant to mention that two ECM protein solutions for coating of the microchannels were tested: fibronectin-I and collagen-I. These are two main ECM proteins of human blood vessels' walls. While fibronectin was pointed as the coating to use by previous relevant protocols regarding implementation of hiPSC-EC in *in vitro* devices[121] , collagen-I had been the coating solution used in BIOS' thrombosis-on-a-hip devices for implementation of HUVECs and was going to be used for HUVECs in the present experiments.

After coating the microfluidic devices with fibronectin-I (50 µg/mL in PBS), and implementing hiPSC-ECs, gaps near the walls of the channels were noticed (where no cells were attached). Events of contraction and compaction of the coating layer by cultured cells have been reported[26,122] before and these were hypothesised as the cause of the observed gaps, since they were located near the edges and cells were still attaching in the centre of the walls. Tests with collagen-I at 0.1 mg/mL, the same concentration used for the implementation of HUVECs on-chip, resulted in the establishment of full monolayers with no visible gaps. Although some possibilities to avoid cells' ECM matrix (fibronectin-I) contraction have been described, such as the functionalisation of the interior walls with a glutaraldehyde solution, to strengthen PDMS-fibronectin interaction[26], in view of the results described it was decided that the use of collagen was preferential. This would not only provide a simpler (no need for further enhancements of ECM protein-PDMS interaction) but documented approach for coating *in vitro* platforms for the implementation of ECs[6,10] but also remove one of the possible exterior variables when comparing the results of tests with hiPSC-ECs and HUVECs on-chips (the type of coating solution).

3. Characterisation of hiPSC-ECs' morphology on-chips

The morphology of healthy hiPSC-ECs seeded in the thrombosis-on-a-chip device was analysed in order to verify if this cell line was able to present endothelial cell-like morphology inside the channels and retain the ability to form a human blood vessel-like full monolayer of cells. Furthermore, the comparison between hiPSC-ECs and HUVECs morphologies was expected to underline some relevant similarities and differences between cell lines and enlighten the authors about the implications of the arterial nature of this specific line of hiPSC-ECs, as reported by Halaydich et al.[34] when comparing it with other primary cell lines.

Pictures of a microchannel seeded with HUVECs and another one seeded with hiPSC-ECs are presented in fig. 23A and B, respectively. More detailed images of both cell lines are presented in fig. 24.

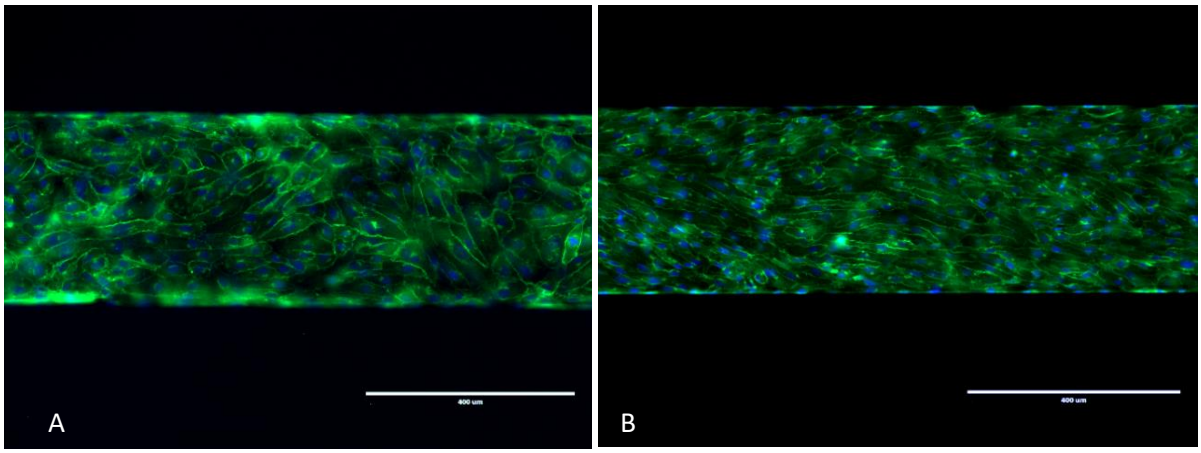

Figure 23 - Microchannels lined with an endothelium of HUVECs (A) or hiPSC-EC (B). A full monolayer of ECs is represented in both cases. Nuclei were stained with NucBlue, in blue (DAPI); adherens junctions with VE-cadherin antibody and AlexaFluor488 labelled secondary antibody, in green (GFP). Scale bars, 400 µm.

The first relevant observation is that both channels, although seeded with different cell lines and using slightly different protocols, resulted in full, apparently healthy monolayers of endothelial cells. However, differences in the organisation of the monolayer and the orientation and morphology of individual cells were visible, even with a low magnification (fig. 23).

The main distinct feature between the two channels was the general organisation and orientation of the cells that formed each monolayer. HUVECs show no alignment of nuclei or cytoskeleton and no changes to their typical cobblestone-like morphology, displayed in static environments (fig. 23A and 24A). This was expected, since no fluid perfusion experiments were performed before the pictures were taken.

However, under the same conditions, hiPSC-ECs created an organised, similarly aligned layer of cells (fig. 23B and 24B). They also show an elongated shape, with similar nuclear alignment. Since hiPSC-ECs were observed to have no special alignment during growth and even after reaching confluency in microwells (displayed in fig. 25D) under static conditions, and since no perfusion experiments had been performed and no shear had purposely been applied, the morphology depicted in fig. 23B was not expected. Two hypotheses to explain the observations were drawn: either cells were adopting the most efficient shape and distribution inside the channel, or enough flow was being created during seeding and medium replacement to induce these morphological changes. The hypothesis that an exterior factor was responsible for the observed reorganisation was supported by the fact that every hiPSC-EC in every seeded microfluidic device was aligned and elongated in a close-to-horizontal angle, never vertically. This may suggest that the observed phenotypic adaptation was not arbitrary and that it could be related to the direction which the fluids were taking inside the channel (causing mild shear stress to the cells), even at low flow rates. To test the hypothesis, the shear stress applied to the cells inside the channel was estimated (more detailed calculations can be found in Appendix I). Considering an approximate value for the dynamic viscosity of the medium of 7.5×10^{-3} dyne.s/(cm^2) and an estimated flow rate of 1.7 µl/min during medium replacement, from one pipette tip to the other, the shear stress was estimated to be of 1.7 dyne/cm^2 (venous shear) in the thrombosis-on-a-chip microchannels during these periods, and higher during seeding and blood perfusion. We can infer that, although for short periods of time, cells were exposed to these intermittent conditions (dynamic and static) for approximately 24h.

In vivo vascular endothelial cells are known to be exposed to at least two distinct types of mechanical forces: the shear stress due to blood circulation inside the channel and pulsatile movements of the vessel due to blood pumping[123]. It has been reported that the usual, healthy phenotypic response of the endothelial layers to arterial, laminar shear stress is the alteration of microtubule, filaments and actin structure, which are reorganised to align the cells in the direction of the flow[97,123]. However, when comparing the adopted morphology and alignment of hiPSC-EC, HUVECs and Human Umbilical Arterial Endothelial Cells (HUAECs) under flow corresponding to low, venous shear rate, Smith et al.[97] reported that HUVECs failed to realign as consistently as the other two cell lines, in agreement with the present results obtained for HUVECs.

Different groups reported observation of phenotypic alterations, characterised by elongation and cell alignment, in hiPSC-EC under dynamic conditions[97,124]. Shear stress is known to influence arterial

marker expression[125] in these cells, even at values as low as from 0.1 to 5 dyne/cm^2 (physiological shear stress of veins and venules[124]).

This is a possible explanation for the alignment and elongation of hiPSC-ECs observed in this work. Our morphology experiments also support Smith et al.[97] conclusion that hiPSC-ECs have more plastic shear responsiveness than HUVECs. To note that hiPSC-ECs' response to shear stress in their studies was closer to those of HUAECs, which also changed orientation and elongated under venous flow rate, than to those of HUVECs. This supports the idea of a more arterial-like nature of hiPSC-ECs. In fact, this responsiveness may represent a shared characteristic amongst arterial cell lines and not verified for venous ECs. However, it is still yet to be described if these alterations have any direct influence on the response of each cell line to dynamic perfusion of fluids (most importantly, human blood).

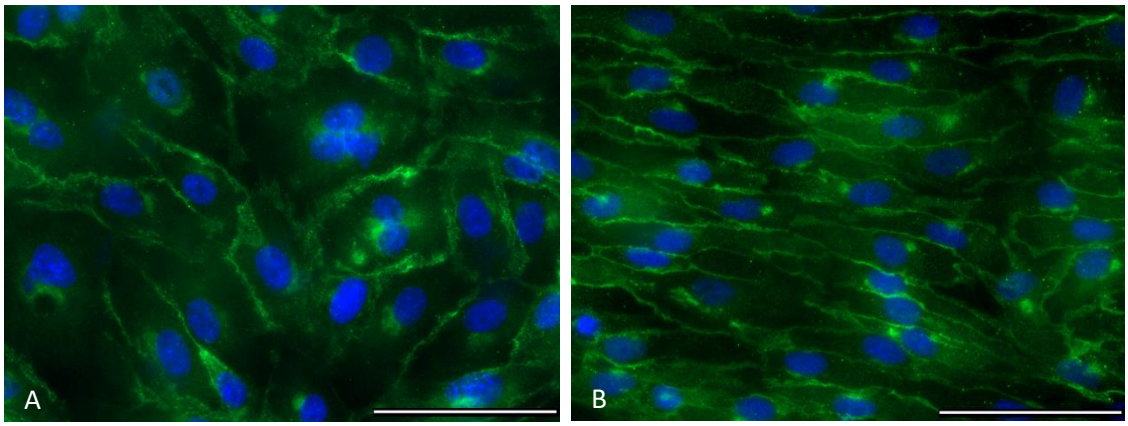

Figure 24 – High magnification imaging of the HUVECs (A) and hiPSC-ECs (B) endothelium. Morphologic differences can be noticed between the two cell lines. Nuclei stained in blue (DAPI), adherens junctions' VE-cadherin in green (AlexaFluor 488, GFP). Scale bars, 50 µm

Under higher magnification, however, other differences were noticeable when comparing HUVECs and hiPSC-ECs (fig. 24A and 2B, respectively). The analysis of the monolayer evidenced differences in the pattern of VE-cadherin labelling of cell-cell connections. In fig 24A, HUVECs present spread in-between cells staining, with blurred areas of VE-cadherin-labelled structures. Conversely, hiPSC-ECs labelled adherens junctions form thin, well-defined lines of cell-cell interactions. These observations are in agreement with those of Halaydich et al. (2018)[34], when culturing these cells lines in static conditions. They reported that their CD31+ hiPSC-EC line (the same used in the present experiments) presented highly organised adherens junctions and tight junctions (the latter were not stained in the present work) in junctional integrity tests, in contrast with HUVECs, which had apparently less organised and defined cell-cell connections.

Finally, and even though the two cell lines presented relevant morphological differences and distinct responsiveness to low shear stress, it was deemed that both adapted positively to the microchannels. Neither hiPSC-ECs nor HUVECs demonstrated visible signs of stress under microscopic analysis, showing full, healthy monolayers and intact cell-cell interactions.

4. Inducing endothelial injury

TNF-α is an inflammatory cytokine, whose uncontrolled release is known to promote endothelial injury and epithelial dysfunction, and upregulate several surface adhesion molecules (e.g. ICAM-I)[10]. Previously published experiments described 10 ng/mL of TNF-α in cell medium as a suitable concentration to induce endothelial cell injury in seeded microfluidic devices and recreate the development of thrombotic events, without leading to cell death[6,10]. However, little has been written about the effects of TNF-α (and concentrations to use) in cultures of hiPSC-ECs.

Microwell experiments were conducted to analyse the effect of different concentrations of TNF-α (0, 1, 2.5, 5, 10 and 50 ng/mL) and exposure times to the inflammatory agent (16, 19 and 22 h, selected according to distinct publications using different exposure times[10,34,126]) on the viability and morphology of cultured hiPSC-ECs. In parallel, HUVECs were also tested under the same conditions.

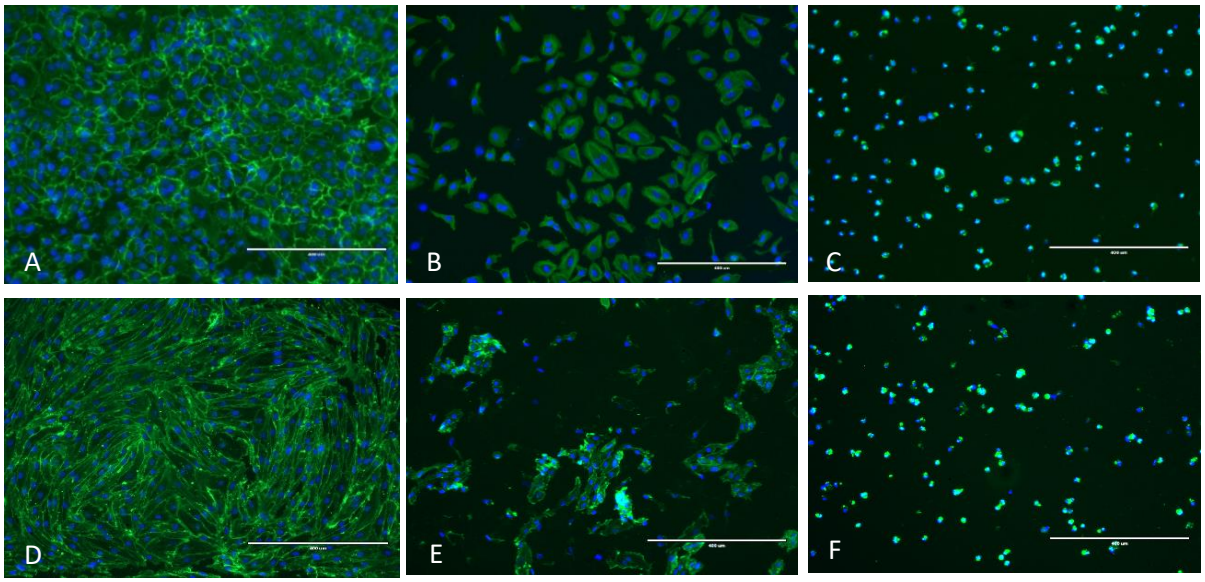

Figure 25 - Experiments on the effects of different TNF-α concentrations on HUVECs (A, B, C) and hiPSC-ECs (D,E,F) in microwells. Data is shown for the negative control, corresponding to null concentration (A, D), 2.5 ng/mL TNFα in cell medium (B, E) and 10 ng/mL TNF-α in cell medium. Cells were exposed for 16 h to the inflammatory agent. Nuclei stained in blue (DAPI), F-actin in green (AlexaFluor488, GFP). Scale bars, 400 µm.

As expected, the negative controls (0 ng/mL, fig. 25A and D) led to full monolayers, with no apparent disruption of the cells' structure and no evidence of cell death. On the other hand, at 50 ng/mL, all cells were dead (data not shown), due to the pro-apoptotic effects of TNF-α (described in section 2.9 of the Introduction). The results obtained for the other concentrations of TNF-α were, however, not expected. Only the concentration of 1 ng/mL led to an almost full, viable monolayer (data not shown), similar to the negative control. The TNF-α concentration of 2.5 ng/mL was found to severely injure both endothelial cells lines, leading to pronounced morphological alterations (fig. 25B and E, respectively) and cell death. The concentrations of 5 ng/mL (data not shown) and 10 ng/mL led to cell death (fig. 25C and F), with no viable individuals surviving the effects of the inflammatory agent.

To confirm that the expected effect was induced by TNF-α in cells seeded in microfluidic devices (and thus discard potential errors in the stock solution preparation), hiPSC-ECs and HUVECs cultured in microchannels were exposed to a 10 ng/mL solution of TNF-α in cell medium (fig. 26).

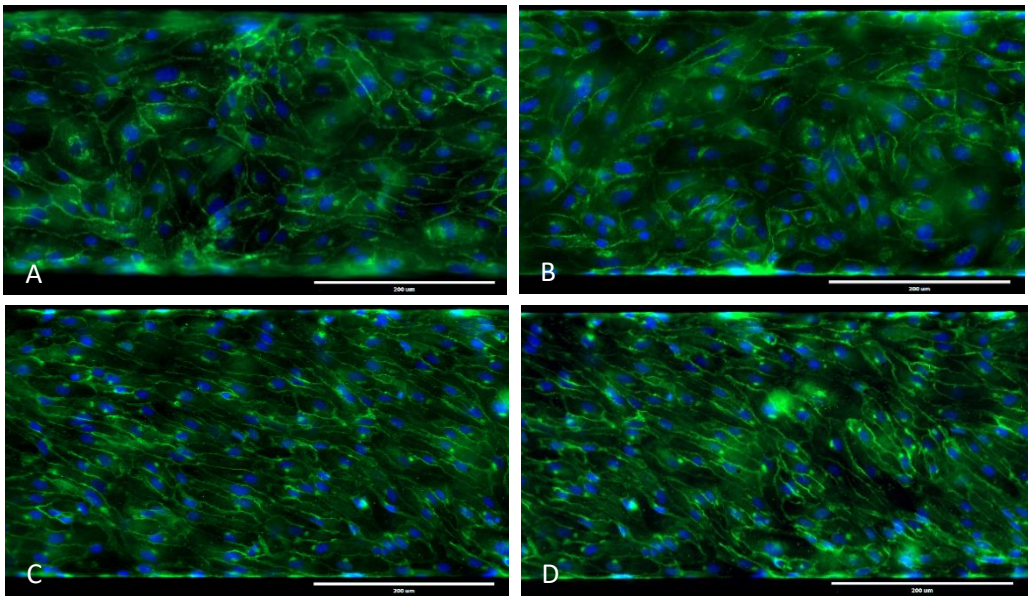

Figure 26 - Experiments to verify the effect of cell exposure to 10 ng/mL TNF-α in the microfluidic device (for 16 h). Untreated endothelium of HUVECs (A) and hiPSC-ECs (C) and their treated counterparts (B and D, respectively). Nuclei stained in blue (DAPI), adherens junctions' VE-cadherin in green (AlexaFluor 488, GFP. Scale bars, 200 µm.

As expected, no major morphologic changes were noticeable and cell death was not significative, following 16 h exposure to TNF-α (fig. 26B and D), comparatively to untreated cells (fig. 26A and C).

Two hypotheses were proposed to explain the different behaviour and response of the cells to the inflammatory agent between the two *in vitro* platforms

The first possible explanation was that, although the mass concentration of TNF-α was the same in both platforms (10 ng/mL), the number of molecules of the inflammatory agent reaching and interacting with each cell was different and higher in the case of ECs growing in microwells. To verify the validity of this hypothesis, the mass concentration of the TNF-α solution was converted to the ratio of the number of molecules of inflammatory agent added per each cell attached. Considering the volumes inside each platform at each moment, the seeding densities, and values of viability and attachment efficiency of around 100%, it was estimated that, in the microfluidic device, existed around 2.4×10^4 molecules of TNF- α/cell (see calculations in Appendix II). On the other hand, this ratio was estimated to be 7.1×10^6 TNF-α molecules/cell in the case of microwells. This represents a 300-fold difference between both platforms. This difference can possibly translate into a higher number of TNF-α molecules interacting with TNFR1 and TNFR2 EC's receptors in the case of the microwells, supposing these receptors are not saturated at 2.4×10^4 molecules of TNF-α/cell. A difference of this magnitude can result in a highly intensified inflammatory reaction and induce apoptotic responses to the presence of TNF-α in microwells, compared with cells in the microfluidic device.

Another dissimilarity between both *in vitro* models is the conditions imposed by each model on the attached cells. Dynamic and static environments can influence differently the intake rate of molecules and barrier mechanisms of cultured cells, as concluded by Santaguida et al.[127] when studying the blood-brain barrier *in vitro*. The adaptation of cells to the channels and the flowing pattern of the TNF-α solution during the first hour of exposure may have contributed to the observed differences in the response of the ECs (compared to the static environment cells experience in microwells). The exact mode by which flow influences the interaction between ECs and TNF-α is, however, still not studied, and would be an interesting point for further investigation.

Even though these hypotheses should be further tested, the most important conclusion for the present work is that exposure of cells to the same concentrations of the inflammatory agent TNF-α have drastically different effects on ECs, depending on the *in vitro* platform they are being tested in. Since microfluidic devices and dynamic, under flow experiments are presently considered to be the most realistic approaches to mimic human vessel microenvironments, the validity and reliability of microwells as a platform to reproduce any aspects of human vasculature in research are therefore questionable.

The other parallel set of experiments, created with the goal of testing the effect of exposure time to TNF-α on ECs, resulted in observations similar to those of fig. 25 (obtained after 16h of exposure), independently of the exposure time (data for 19h and 22h is not shown). Thus, this variable was deemed of less relevance for future tests and 16 h of exposure was set as the standard exposure time for the planned experiments of blood perfusion.

As a final experiment to try to confirm that the 10 ng/mL TNF-α treatment (for 16 hours) was actually inducing an inflammatory response in cells cultured in microchips, ICAM-I was labelled by immunofluorescence. TNF-α has been reported to upregulate the expression of ICAM-I in endothelial cells[10,34] as a result of its effect as an inflammatory cytokine. Thus, the expression levels of ICAM-I can be analysed to conclude about the action of the agent.

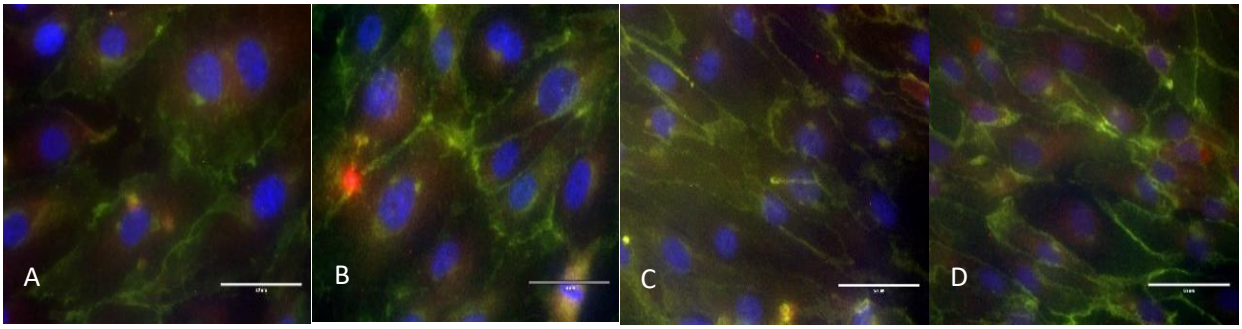

Figure 27 - Experiments on the upregulation of ICAM-I due to the presence of TNF-α. HUVECs' untreated (A) and treated (B) endothelium showed almost no difference. hiPSC-ECs' untreated (C) and treated (D) endothelium displayed differences in ICAM-I expression. Nuclei stained in blue (DAPI), adherens junctions' VE-cadherin in green (AlexaFluor 488, GFP) and ICAM-I in red (AlexaFluor 647, Cy5). Scale bars, 50 µm.

This experiment was developed as a one-time off test to check if TNF-α induced ICAM-I upregulation, allowing us to conclude about its effect on cell activation. Indeed, a higher Cy5 intensity in treated channels comparing to the healthy ones was expected, due to reported activation by TNF-α and

consequent ICAM-I upregulation[10,34]. Furthermore, treated HUVECs were also expected to display higher upregulation of the surface marker in comparison with the analogous TNF-α-treated hiPSC-EC channels, following the results of Halaydich et al.[34]. However, the observed results were deemed inconclusive, as differences between treated and untreated cells were not obvious (fig. 27) and further analysis of the levels of ICAM-I expression and more repetitions of the tests would be necessary.

Finally, previous successful experiments with this inflammatory agent in BIOS and the described literature was enough to consider that TNF-α is able to induce a response that would, in principle, be useful to create thrombogenesis-on-chip during blood perfusion. Thus, it was decided to continue with the planned blood perfusion experiments to confirm if differences between untreated and treated channels were noticeable under the desired dynamic conditions.

5. Whole blood perfusion: platelet aggregation in microfluidic devices

The lipophilic dye $DiOC_6$ is reported to enable platelets observation in blood perfusion[5,6], without promoting their activation (in contrast with some other labelling compounds). The dye was added to the blood before perfusion in the microfluidic device started. Fig 28A and B were taken 15 minutes into after initiating a blood run in untreated and TNF-α exposed hiPSC-EC-seeded channels, respectively.

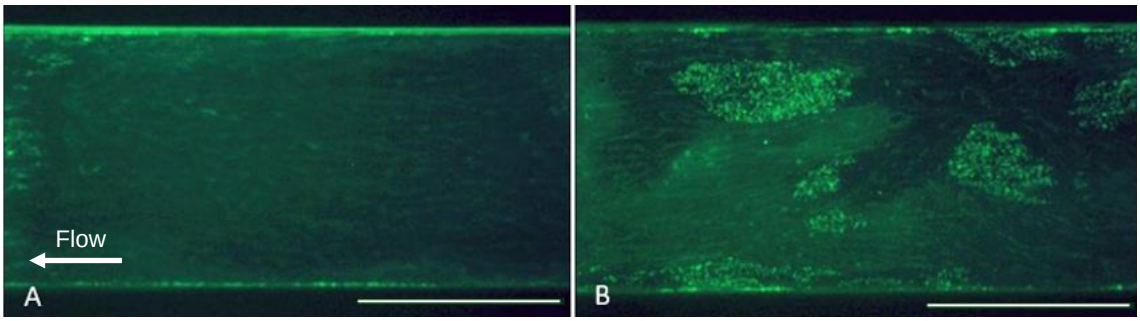

Figure 28 - Pictures of blood perfusion experiments (15 min after blood perfusion started) in microchannels with untreated (A) and treated (B) hiPSC-EC endothelium. Flow direction from right to left. Platelets were stained with $DiOC_6$. Scale bars, 200 µm.

Differences between channels were noticeable during and at the end of the blood perfusion experiments. Layers of $DiOC_6$-labelled platelets were observed in both channels, although with increased incidence and size in the channels previously exposed to TNF-α (fig. 28B). Platelets were adhering to distinct, apparently random sites of the channel, which could indicate that injury had occurred and that the objective of the experiment was reached. However, the structures observed presented the appearance of 2D platelet layers instead of the expected 3D clot-like configuration[84]. Indeed, the inflammatory process and platelet activation should create a mechanism of platelet recruitment to the site, that would not only fill the site of injury but also adhere to previously attached cells. Various iterations of this process during the first 15 minutes of the blood run were thus expected to result in a 3D platelet-based structure and not in widely spread 2D sheets of platelets. Two hypotheses were advanced as possible explanations for the observations.

The first hypothesis was that an inflammatory process was actually being triggered during the blood run due to TNF-α-induced endothelial injury, and platelets were just starting to adhere to the endothelium at the time the picture was taken. Thus, as in a stepwise process, platelets were first adhering directly to injured endothelium and only after would start overlaying each other. According to this hypothesis, the reason for the lack of observation of fully grown, 3D blood clots was merely the reduced amount of time that had passed from the point at which the injury had been noticed and pinpointed to the point at which the picture was taken. This hypothesis was supported by the low number of platelets that had adhered to the healthy endothelium (fig. 28A), in contrast with the high number of adhering platelets observed after TNF-α treatment of the cells (fig. 28B), which had been cultured and perfused following the same protocols. Therefore, the observations suggest that inflammatory processes were occurring in the treated channel and inducing the development of thrombi.

On the other hand, some platelet coverage was observed in the healthy endothelium and all observed structures, both in healthy and treated endothelium, were seen as 2D monolayers of platelets. Therefore, the alternative hypothesis is that platelet aggregation is only occurring at sites where gaps in the cells monolayer were formed during perfusion (or due to an incomplete monolayer at the start of the blood perfusion) and collagen was exposed, instead of developing as a consequence of endothelial injury. This could explain why platelets only adhered as a 2D sheet, i.e., as a full inflammatory process was not triggered, since no injuries were perceived, 3D clots were not formed, and platelets only adhered due to their natural ability to interact with ECM proteins from the vessel wall. In favour of this hypothesis, the format of the areas of platelet aggregation observed in fig. 28B is similar to the ones reported by Jain et al. (2018)[84], after the group perfused recalcified citrated human whole blood through a collagen-coated microfluidic device's channel with no cells seeding its walls (only exposed collagen).

Both hypotheses could be further discussed, and a conclusion reached, if additional staining procedures were used. Labelling relevant endothelial cell structures (using specific markers), such as the cytoskeleton (e.g. F-actin staining) or cell-cell junctions (e.g. VE-cadherin), would clarify the position of the cells in the channel and confirm or refute the second hypothesis. However, since $DiOC_6$ partially background-stained endothelial cells' structures (as observed in fig. 28), there would probably be interference with the new labels and no concrete, well-defined conclusions would be reached. For this hypothesis to be tested, it was considered that the $DiOC_6$ solution would have to be replaced by a platelet-specific label, without background staining of the endothelium and, at the same time, endothelial cells-specific labels would have to be added in future experiments.

6. Whole blood perfusion: platelet aggregation and activation, clot location and composition

To advance the knowledge about the possibility of creating the thrombosis-on-a-chip model, the same protocols for $DiOC_6$ blood perfusion experiments were used in the blood runs with labelled fibrinogen, integrin alpha chain 2b (CD41) and VE-cadherin antibodies and nuclear counterstain (Hoechst 33342). The three specific goals of the blood perfusion experiments using these staining protocols were:

- To prove that 3D clots formed during blood perfusion were located on top of cells and not only on gaps of the monolayer (with exposed collagen coating) – using nuclear and VE-cadherin labels for mapping the position of the seeded ECs and CD41 for following platelet aggregation.

- To confirm that platelets were achieving an activated state and thrombogenesis-on-chip was occurring – using CD41 and P-Selectin labels for platelets and nuclear counterstaining for the endothelium.

- To analyse the 3D structure and clot composition (in terms of platelets and fibrin) and compare them with reported *in vivo* and *in vitro* arterial clots.

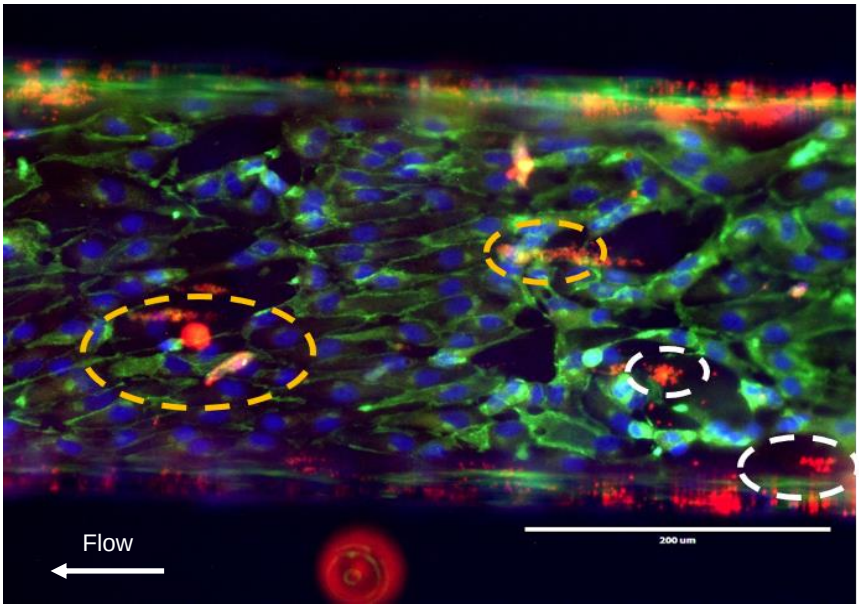

Figure 29 - Fluorescent staining of a treated hiPSC-EC channel after blood perfusion for 20 minutes. Nuclei stained in blue (DAPI), adherens junctions' VE-cadherin in green (AlexaFluor 488, GFP) and platelets' CD41 in red (PE, RFP). Dashed lines indicate points of platelet aggregation. Scale bar, 200 µm.

The approach used (labelling platelets and endothelial structures - adherens junctions and nuclei), allowed to conclude about the locations of the blood clots formed during blood perfusion. In fig. 29, several points of platelet aggregation (inside dashed lines) can be observed in the channel.

On the one hand, platelets adhering to gaps without endothelial cells (clots identified in white) can be seen, as previously discussed. Gaps in the monolayer were not expected following previous observations of healthy on-chip monolayers (fig. 23) and could either be related to the adaptation to the sudden change in shear stress, to the exposure to TNF-α or to some flaws in the monolayer originally formed during seeding (which may have been enhanced by shear stress and the inflammatory agent). Even though this was not the original goal of the experiment, confirming that platelets are indeed adhering to exposed collagen of the coating layer was of relevance, since it showed that platelets from the human whole blood used in the experiment are keeping their ability to interact with ECM proteins *in vitro* and aggregate on the exposed ECM layer, as it happens in real, severe vessel injury situations (i.e., during haemostatic plug formation).

On the other hand, it is also possible to observe zones of platelet aggregation on top of endothelial cells (clots identified in orange, in fig. 29). In fig. 30 it is observable that the signal corresponding to CD41-labeled platelets overlays and crosses the organised green lines corresponding to cell-cell connections (identified through VE-cadherin), instead of gaps in the monolayer. This strongly suggests that cells are becoming injured after exposure to the inflammatory agent and that it is possible to develop thrombosis-on-a-chip with hiPSC-ECs by inducing vessel wall dysfunction.

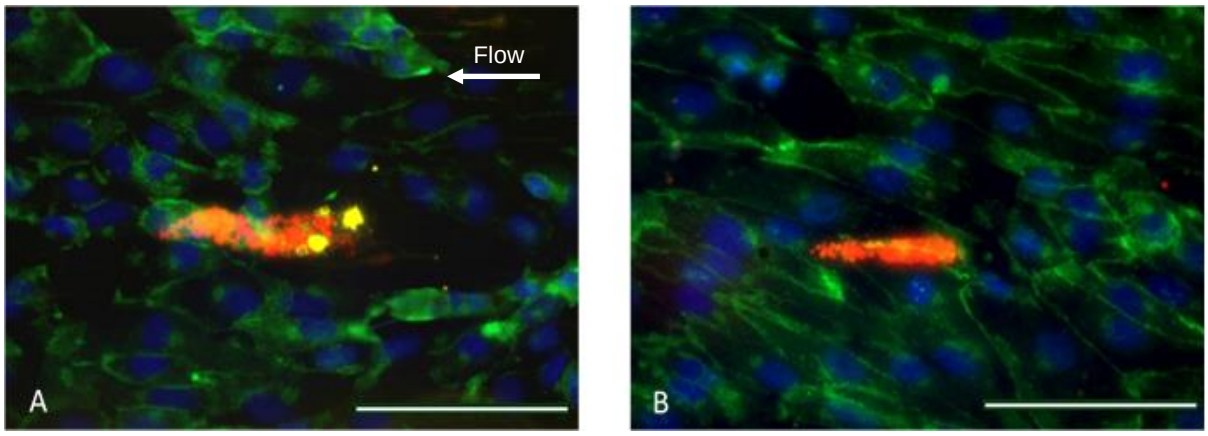

Figure 30 - Close up images of clots forming on top of hiPSC-EC cells. Nuclei stained in blue (DAPI), adherens junctions' VE-cadherin in green (AlexaFluor 488, GFP) and platelets' CD41 in red (PE, RFP). Scale bars, 50 µm.

After observation of fig. 30, two interesting and intertwined features of the clots forming on top of ECs were noticeable: the common orientation of the aggregations and their teardrop-like shape (better observed in the second picture). The observed adopted orientation was most probably related to the direction of the flow during blood perfusion, at arterial shear rate. It can be seen that it is similar to that of the seeded hiPSC-ECs, supporting the idea that both cells and the clots are influenced by the flowing of fluids inside the channel. The teardrop-shaped configuration, as described by other groups in previous publications [10,84], is also influenced by the laminar flow patterns introduced during perfusion. Jain et al. (2018)[84], performed an experience using video microscopy within a similar microfluidic channel, and concluded that this clot morphology was characteristic the dynamic environment created inside the channels. The author also adds that this binding behaviour has been reported to happen in *in vivo* situation, in which the small aggregates of platelets not only grow in size and volume but also slowly

move downstream of the main core of the clot, along the surface of the endothelium, creating a tail-like structure, easily observed in fig. 30B.

Hence, given the discussed observations, the dynamics of platelet-endothelium binding and of the blood clots' development in the studied thrombosis-on-a-chip device is suggested to reproduce the analogous events occurring in humans.

To further support this hypothesis, the occurrence of the two main stages of *in vivo* haemostasis was assessed in the channels: platelet activation and fibrin deposition. It is known that the activation of the platelets adhering to the site of injury represents an essential step during *in vivo* primary haemostasis mechanisms, promoting the recruitment of more platelets to build the clot. In this work, with the goal of analysing if the circulating platelets were effectively being activated in the induced coagulatory process, the antibody for a marker of platelet activation, P-Selectin[5,128], was added.

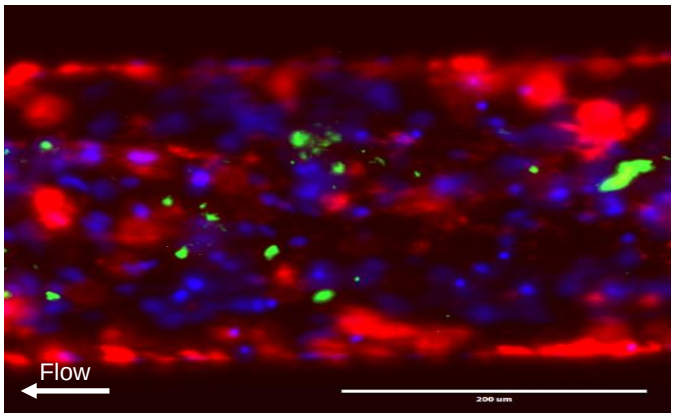

Figure 31 - Fluorescent staining of a TNF-α treated hiPSC-EC channel after blood perfusion for 20 minutes. Nuclei stained in blue (DAPI), platelets' P-Selectin in green (AlexaFluor 488, GFP) and platelets' CD41 in red (PE, RFP). Scale bar, 200 µm.

Fig. 31 shows a general view of part of the channel where spots of green fluorescence, corresponding to labelled P-Selectin, are visualised. With higher amplification and after splitting the GFP and RFP channels (fig. 32), P-Selectin was found to be exposed in areas where platelets (marked with CD41

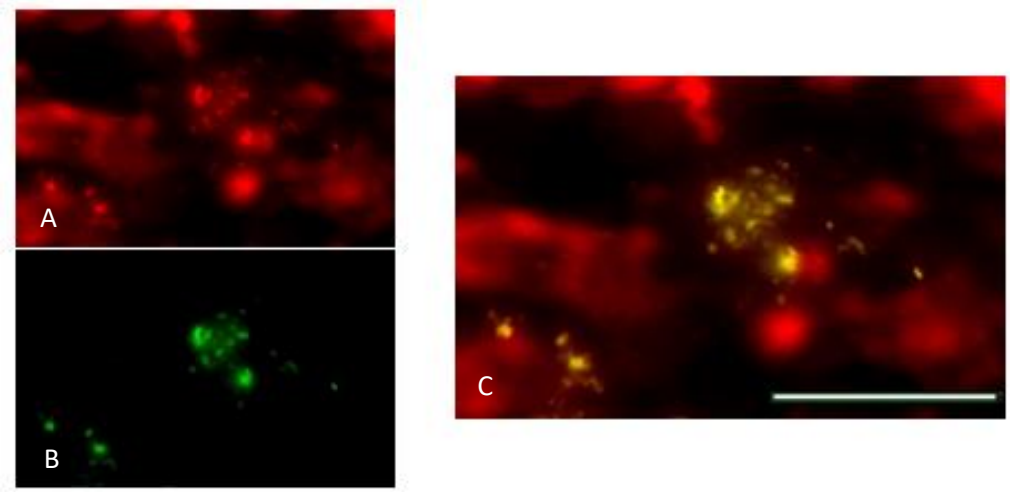

Figure 32 - Close up images of fluorescently labelled clots and activated platelets in an endothelium of hiPSC-ECs. RFP channel (CD41, image A) and GFP (P-Selectin, B) were merged together to confirm overlay (C). Scale bars, 50 µm

antibody, in red), were aggregating and where thrombus masses were growing, suggesting that a part of these blood cells were in an activated state.

Thus, the most important conclusion of this experiment is that platelets circulating in the channel (whilst blood is being perfused) seem to be capable of displaying markers of activation and adhere to sites where other platelets are aggregating. As previously described (see section 2.2 of the Introduction), this is an essential part of *in vivo* mechanisms of haemostasis and thrombogenesis and represents an argument in favour of the authors' goal of recreating *in vivo*-like thrombotic development in microfluidic devices with an *in vitro* hiPSC-EC endothelium. However, since this was a one-off experiment, more independent tests will have to be undertaken to derive solid conclusions on the activation of platelets inside the channels.

As a last goal, this work aimed at analysing the composition of the clots formed during blood perfusion. Labelled fibrinogen was added to the blood vessel before the start of the experiment, with the objective of verifying if it would be converted to fibrin and be involved in the triggered coagulation mechanisms.

Fibrin was consistently observed to be present around and in the blood clots formed in the channels during blood perfusion (fig. 33), creating a mesh to support the adhesion of platelets and increase the strength of the structure.

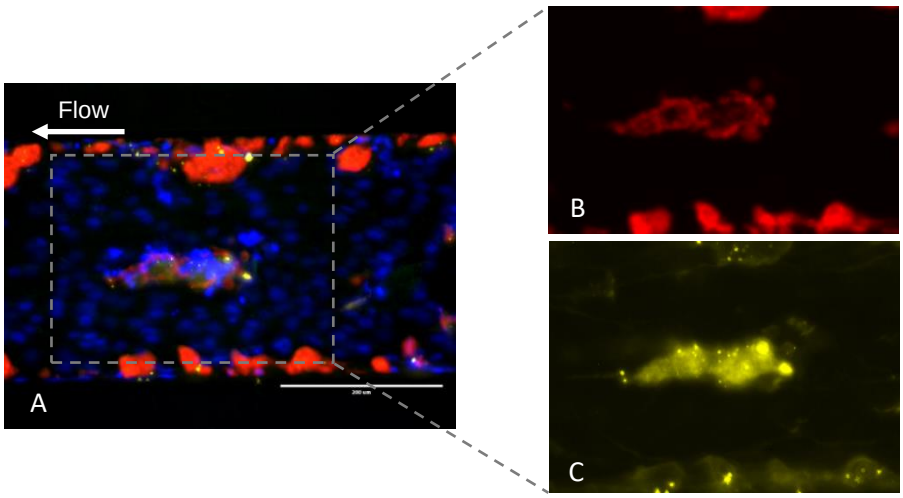

Figure 33 - Fluorescent staining of a treated hiPSC-EC channel after blood perfusion for 20 minutes. The filter channels of the original image (A) were split into the RPF (B) and Cy5 (C) to allow visualisation of the clot composition. Nuclei stained in blue (DAPI), fibrin in yellow (AlexaFluor 647, Cy5) and platelets' CD41 in red (PE, RFP). Scale bar, 200 µm.

As stated, images of the clots (fig. 33) indicate that they were largely composed of platelets and fibrin. This is a recognised and reported characteristic of *in vivo* and *in vitro* arterial blood clots[37].

Moreover, the presence of a network of fibrin on and around the clots also indicates that hiPSC-ECs in the microchannels were still able to promote the conversion of fibrinogen to fibrin, retaining the ECs' natural ability to trigger the coagulation cascade in response to injury (see section 2.3 of the Introduction). This is a critical step of the *in vivo* secondary haemostasic mechanism and, together with the data previously presented, demonstrating the activation of platelets, supports the hypothesis that

full haemostasis (including the primary and secondary stages) is taking place in the microfluidic device, leading to the desired thrombotic events.

Although it was not the focus of the experiment, a high density of apparently smaller nuclei located in the zone of the clot is also noticeable in fig. 33A. One possible explanation is that those nuclei belong to ECs altered by the induced injury. However, this was not expected to alter nuclear configuration. Another possible explanation is that the nuclei correspond to leukocytes that were recruited to the site of the injury. Leukocytes (10-15 µm) are reported to be larger than platelets (~2 µm) but smaller than *in vivo* arterial endothelial cells (usually > 20 µm)[129]. Considering the differences in size and the fact that the endothelial cells are activated (their surface receptors, such as ICAM-I, which interact with leukocytes, are expected to be upregulated), it is indeed deemed possible that leukocytes were being recruited to the site and that their nuclei were unintentionally stained with DAPI (NucBlue). Although no more experiments were performed to confirm or deny the veracity of this hypothesis yet, this may be an interesting target for future tests.

If further experiments prove this hypothesis that leukocyte recruitment and adhesion to sites of injury are being triggered in the channel, the potential of this *in vitro* model to study thrombosis will be reinforced.

7. Quantitative analysis of platelet coverage and average clot size in the thrombosis-on-a-chip device

After experiments indicating the adaptability of hiPSC-ECs to the BIOS thrombosis-on-a-chip device and the adequacy and utility of the model to reproduce thrombogenesis *in vitro*, the characteristics of the induced thrombotic events were accessed and compared to those occurring with an endothelium of HUVECs (fig. 34). These characteristics were evaluated through two parameters: platelet coverage in the channel (after blood perfusion) and average clot size (the area occupied). Differences between treated and untreated endothelium were also studied.

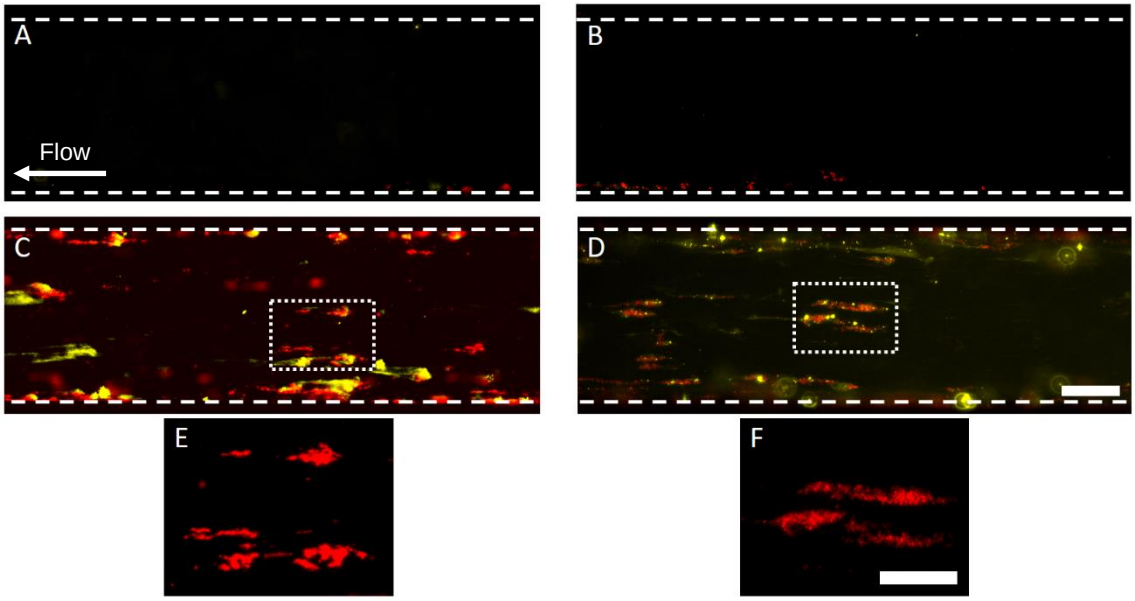

Figure 34 - Fluorescent staining of untreated and treated HUVEC channels (A and C, respectively) and untreated and treated hiPSC-EC channels (B and D) after 20 min blood perfusions. Clots corresponding to the white marked areas are represented in E and F. Platelets' CD41 are stained in red (PE, RFP filter) and fibrin in yellow (AlexaFluor 647, Cy5). Scale bars, 100 µm (A, B, C and D) and 50 µm (E and F).

Several sets of endpoint pictures taken of each channel with hiPSC-ECs and HUVECs, healthy and TNF-α treated, after blood perfusion experiments (e.g. the set displayed in fig. 34), were automated and turned into black and white pictures (not shown). The images were analysed for platelet coverage on the channel. As expected, platelet coverage values of untreated, healthy channels were low, in comparison with the ones obtained for treated endothelium (fig. 35). However, high variability was observed among sets from different days of blood perfusion experiments. This variability was considered to be mainly related to the intrinsic blood-variability. Even with the attempted minimisation of this factor (e.g. using the blood in the first 5 h after being drawn to avoid platelet activation and blood degradation), blood and donor-variability are well-documented causes of unpredictability in blood perfusion experiments[92] and can lead to different responses of circulating cells and of the endothelium to the tested conditions.

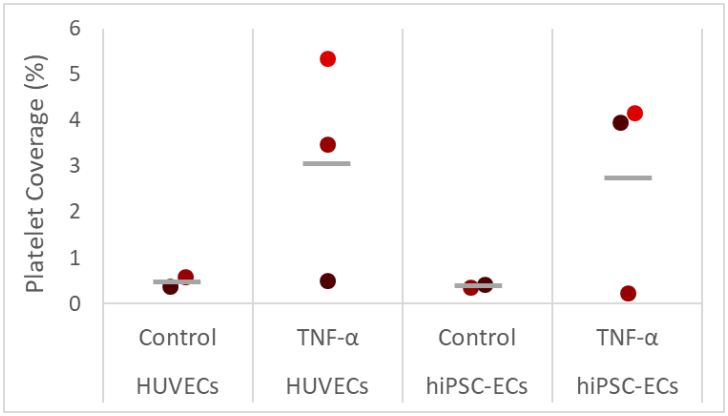

Figure 35 - Representation of the platelet coverage (%) in the experiments with treated and untreated HUVECs and hiPSC-ECs. Each point's colour represents a different day of experiments (n=2 for untreated and n=3 for treated endothelium). The average (mean) of the values is represented as horizontal grey lines.

After automated image analysis, the average platelet coverages in untreated hiPSC-ECs and HUVECs channels were estimated as 0.4 % and 0.5 %, respectively. Treated channels, however, showed an average of 2.8 % and 3.1 % of platelet coverage for hiPSC-ECs and HUVECs, respectively. These results suggested that a difference between average platelet coverage of different cell lines existed and that the HUVECs inflamed endothelium demonstrated higher tendency for platelet attachment than the hiPSC-EC endothelial layer. Furthermore, a difference in average clot size was also verified: while hiPSC-EC presented an average clot size of 38 μm^2, HUVECs' was estimated as 44 μm^2. However, no statistically significant difference between the independent values of platelet coverage obtained for hiPSC-ECs and HUVECs was verified (P-value=0.77, Student's *t*-test).

Although further testing is needed, differences between the two cell lines were to be expected, taking into consideration the previously published different nature and characteristics of these cell lines. HiPSC-EC have been reported by Halaidych et al. (2018)[34] to present lower basal levels of vWF and lower expression levels of pro-inflammatory adhesive receptors (both relevant in haemostasis) than HUVECs. These authors also demonstrated that HUVECs promote more leukocyte attachment than hiPSC-EC after treatment with TNF-α (in *in vitro* experiments under flow). Thus, differences in reaction to *in vitro* induced thrombogenesis were expectable, and more clot formation and platelet coverage in HUVECs. In the future, more experiments must be performed to reduce variability and before more precise and reliable conclusions regarding platelet coverage in both type of endothelium can be drawn

IV. Conclusions and future work

In this work, successful implementation of an *in vitro* endothelium of hiPSC-ECs in thrombosis-on-a-chip devices was achieved. In contrast with HUVECs' cobblestone morphology, hiPSC-ECs displayed an elongated, spindle-like morphology in static and dynamic conditions, and observations of cell and nuclei alignment in the channel suggested high plastic responsiveness to shear.

A proof-of-concept experiment of human blood perfusion and *in vitro* thrombosis induction with hiPSC-ECs was also performed in the microchip. *In vivo*-like primary and secondary haemostatic mechanisms were triggered, since platelet activation and aggregation and fibrin deposition were observed in treated channels. During blood perfusion, HUVECs presented higher platelet coverage and larger clots than hiPSC-ECs. This is in line with recent findings that pointed at higher basal levels of pro-inflammatory adhesive receptors and coagulation-related molecules (vWF) in HUVECs[34]. However, statistical significance was not proved, and further testing will be performed.

The use of microfluidics together with the hiPSC technology brings a promising approach to *in vitro* targeting of vascular diseases. HiPSC-ECs have been reported to behave and reproduce mechanisms of primary cells, from the physiologic morphology of endothelial cells[120] and arterial phenotypic adaptations to shear[97], to the ability to form vessel-like networks[100] and present integral barrier function, with upregulation of markers of injury and inducers of inflammation[34]. Here, we conclude that they can also be used to efficiently line the walls of thrombosis-on-a-chip microfluidic devices as an *in vitro* endothelium and be tested for response to mechanisms of thrombogenesis with comparable realism to established primary cell lines (HUVECs). Further experiments involving the use of healthy and diseased patients' hiPSC-ECs and blood in thrombosis-on-a-chip setups will allow for patient-specific drug testing and the development of the personalised medicine paradigm.

.

V. References

1. World Health Organization. The top 10 causes of death. *Fact sheet No 310* (2017). Available at: http://www.who.int/mediacentre/factsheets/fs310/en/. (Accessed: 13th February 2018)

2. Colman, R. W. Are hemostasis and thrombosis two sides of the same coin? *J. Exp. Med.* **203,** 493–495 (2006).

3. Badimon, L., Vilahur, G. & Padro, T. Atherosclerosis and thrombosis: Insights from large animal models. *J. Biomed. Biotechnol.* **2011,** 1-12 (2011).

4. Pandian, N. K. R., Mannino, R. G., Lam, W. A. & Jain, A. Thrombosis-on-a-chip: Prospective impact of microphysiological models of vascular thrombosis. *Curr. Opin. Biomed. Eng.* **5,** 29–34 (2018).

5. Westein, E., van der Meer, A. D., Kuijpers, M. J. E., Frimat, J.-P., van den Berg, A. & Heemskerk, J. W. M. Atherosclerotic geometries exacerbate pathological thrombus formation poststenosis in a von Willebrand factor-dependent manner. *Proc. Natl. Acad. Sci.* **110,** 1357–1362 (2013).

6. Costa, P. F., Albers, H. J., Linssen, J. E. A., Middelkamp, H. H. T., van der Hout, L., Passier, R., van den Berg, A., Malda, J. & van der Meer, A. D. Mimicking arterial thrombosis in a 3D-printed microfluidic *in vitro* vascular model based on computed tomography angiography data. *Lab Chip* **17,** 2785–2792 (2017).

7. Cao, Y., Gong, Y., Liu, L., Zhou, Y., Fang, X., Zhang, C., Li, Y. & Li, J. The use of human umbilical vein endothelial cells (HUVECs) as an *in vitro* model to assess the toxicity of nanoparticles to endothelium: a review. *J. Appl. Toxicol.* **37,** 1359–1369 (2017).

8. Cochrane, A., Albers, H. J., Passier, R., Mummery, C. L., Van Den Berg, A., Orlova, V. V & Van Der Meer, A. D. Advanced *in vitro* models of vascular biology: Human induced pluripotent stem cells and organ-on-chip technology. *Adv. Drug Deliv. Rev.* (2018), in press.

9. Passier, R., Orlova, V. & Mummery, C. Review Complex Tissue and Disease Modeling using hiPSCs. *Stem Cell* **18,** 309–321 (2016).

10. Jain, A., van der Meer, A. D., Papa, A. L., Barrile, R., Lai, A., Schlechter, B. L., Otieno, M. A., Louden, C. S., Hamilton, G. A., Michelson, A. D., Frelinger, A. L. & Ingber, D. E. Assessment of whole blood thrombosis in a microfluidic device lined by fixed human endothelium. *Biomed. Microdevices* **18,** 1–7 (2016).

11. Witzleb, E. Functions of the Vascular System. in *Human Physiology* (eds. Schmidt, R. & Thews, G.) 480–481 (Springer, 1989).

12. National Cancer Institute. Introduction to the Cardiovascular System | SEER Training. Available at: https://training.seer.cancer.gov/anatomy/cardiovascular/. (Accessed: 6th June 2018)

13. Johns Hopkins Medicine. Overview of the Vascular System. 2–4 (2018). Available at: https://www.hopkinsmedicine.org/healthlibrary/conditions/cardiovascular_diseases/overview_of_the_vascular_system_85,P08254. (Accessed: 13th February 2018)

14. The Cardiovascular System: Blood Vessels : *Anatomy & Physiology - a learning initiative* (2013). Available at: http://anatomyandphysiologyi.com/cardiovascular-system-blood-vessels/. (Accessed: 13th September 2018)

15. Hathcock, J. J. Flow Effects on Coagulation and Thrombosis. *Arter. Thromb Vasc Biol* **26,** 1729–1737 (2006).

16. Goncharov, N. V., Nadeev, A. D., Jenkins, R. O. & Avdonin, P. V. Markers and Biomarkers of Endothelium: When Something Is Rotten in the State. *Oxid. Med. Cell. Longev.* **2017,** (2017).

17. Michiels, C. Endothelial cell functions. *J. Cell. Physiol.* **196,** 430–443 (2003).

18. Bierhansl, L., Conradi, L.-C., Treps, L., Dewerchin, M. & Carmeliet, P. Central Role of Metabolism in Endothelial Cell Function and Vascular Disease. *Physiology* **32,** 126–140 (2017).

19. Rajendran, P., Rengarajan, T., Thangavel, J., Nishigaki, Y., Sakthisekaran, D., Sethi, G. & Nishigaki, I. The vascular endothelium and human diseases. *Int. J. Biol. Sci.* **9,** 1057–1069 (2013).

20. Douglas B. Cines, Eleanor S. Pollak, Clayton A. Buck, Joseph Loscalzo, Guy A. Zimmerman, Rodger P. McEver, Jordan S. Pober, Timothy M. Wick, Barbara A. Konkle, Bradford S. Schwartz, Elliot S. Barnathan, Keith R. McCrae, Bruce A. Hug, Ann-Marie Schmidt, and D. M. S. Endothelial Cells in Physiology and in the Pathophysiology of Vascular Disorders. *Blood* **92,** 3527–3562 (1998).

21. Yuan, S. & Rigor, R. The Endothelial Barrier. in *Regulation of Endothelial Barrier Function* (Morgan & Claypool Life Sciences, 2011).

22. Dejana, E., Orsenigo, F., Molendini, C., Baluk, P. & McDonald, D. M. Organization and signaling of endothelial cell-to-cell junctions in various regions of the blood and lymphatic vascular trees. *Cell Tissue Res.* **335,** 17–25 (2009).

23. Aghajanian, A., Wittchen, E. S., Allingham, M. J., Garrett, T. A. & Burridge, K. Endothelial cell junctions and the regulation of vascular permeability and leukocyte transmigration. *J. Thromb. Haemost.* **6,** 1453–60 (2008).

24. Monteiro, G. Cell and Tissue Biology - Part I. *Cell & Tissue Engineering lectures, Instituto Superior Técnico, University of Lisbon* 62–63 (2016).

25. Hoelzle, M. K. & Svitkina, T. The cytoskeletal mechanisms of cell-cell junction formation in endothelial cells. *Mol. Biol. Cell* **23,** 310–23 (2012).

26. Vivas, A. G. de S. Optimization of a microfluidic device towards a self- assembled BBB-on-a-

chip. (Instituto Superior Técnico, University of Lisbon, 2017).

27. Mitchell, L. A., Ward, C., Kwon, M., Mitchell, P. O., Quintero, D. A., Nusrat, A., Parkos, C. A. & Koval, M. Junctional adhesion molecule a promotes epithelial tight junction assembly to augment lung barrier function. *Am. J. Pathol.* **185,** 372–386 (2014).

28. Dvorak, A. M., Kohn, S., Morgan, E. S., Fox, P., Nagy, J. A. & Dvorak, H. F. The vesiculo-vacuolar organelle (VVO): a distinct endothelial cell structure that provides a transcellular pathway for macromolecular extravasation. *J. Leukoc. Biol.* **59,** 100–115 (1996).

29. Dvorak, A. M. Vesiculo-Vacuolar Organelles and the Regulation of Venule Permeability to Macromolecules By Vascular Permeability Factor , Histamine , and Serotonin. *J. Exp. Med* **183,** 1981-1986 (1996).

30. Wu, C. Focal Adhesion. *Cell Adh. Migr.* **1,** 13–18 (2007).

31. Lodish, H., Berk, A., Zipursky, S. L., Matsudaira, P., Baltimore, D. & Darnell, J. Cell-Matrix Adhesion. in *Molecular Cell Biology* (W. H. Freeman, 2000).

32. Goodwin, K., Lostchuck, E. E., Cramb, K. M. L., Zulueta-Coarasa, T., Fernandez-Gonzalez, R. & Tanentzapf, G. Cell-cell and cell-extracellular matrix adhesions cooperate to organize actomyosin networks and maintain force transmission during dorsal closure. *Mol. Biol. Cell* **28,** 1301–1310 (2017).

33. Müller, A. M., Hermanns, M. I., Skrzynski, C., Nesslinger, M., Müller, K.-M. & Kirkpatrick, C. J. Expression of the Endothelial Markers PECAM-1, vWf, and CD34 *in Vivo* and *in Vitro*. *Exp. Mol. Pathol.* **72,** 221–229 (2002).

34. Halaidych, O. V., Freund, C., van den Hil, F., Salvatori, D. C. F., Riminucci, M., Mummery, C. L. & Orlova, V. V. Inflammatory Responses and Barrier Function of Endothelial Cells Derived from Human Induced Pluripotent Stem Cells. *Stem Cell Reports* **10,** 1642–1656 (2018).

35. Fleming, W. H., Breviario, F., Caveda, L., Berthier, R., Schnürch, H., Gotsch, U., Vestweber, D., Risau, W. & Dejana, E. Endothelial cell-specific markers: going... going... gone. *Blood* **106,** 769–769 (2005).

36. Metcalf, D. J., Nightingale, T. D., Zenner, H. L., Lui-Roberts, W. W. & Cutler, D. F. Formation and function of Weibel-Palade bodies. *J. Cell Sci.* **121,** 19–27 (2008).

37. Gale, A. J. Continuing Education Course #2: Current Understanding of Hemostasis. *Toxicol. Pathol.* **39,** 273–280 (2011).

38. Starke, R. D., Ferraro, F., Paschalaki, K. E., Dryden, N. H., Mckinnon, T. A. J., Sutton, R. E., Payne, E. M., Haskard, D. O., Hughes, A. D., Cutler, D. F., Laffan, M. A. & Randi, A. M. Endothelial von Willebrand factor regulates angiogenesis. *Blood* **117,** 1071–1080 (2011).

39. Kalinowska, A. & Losy, J. PECAM-1, a key player in neuroinflammation. *Eur. J. Neurol.* **13,** 1284–

1290 (2006).

40. Riccieri, V., Stefanantoni, K., Vasile, M., Macrì, V., Sciarra, I., Iannace, N., Alessandri, C. & Valesini, G. Abnormal plasma levels of different angiogenic molecules are associated with different clinical manifestations in patients with systemic sclerosis. *Clin. Exp. Rheumatol.* **29,** S46-52 (2011).

41. Granger, D. N. & Senchenkova, E. Leukocyte–Endothelial Cell Adhesion. in *Inflammation and the Microcirculation* (Morgan & Claypool Life Sciences, 2010).

42. Falati, S., Gross, P., Merrill-Skoloff, G., Furie, B. C. & Furie, B. Real-time *in vivo* imaging of platelets, tissue factor and fibrin during arterial thrombus formation in the mouse. *Nat. Med.* **8,** 1175–1180 (2002).

43. Reininger, A. J. Function of von Willebrand factor in haemostasis and thrombosis. *Haemophilia* **14,** 11–26 (2008).

44. Ruggeri, Z. M. Platelet Adhesion Under Flow. *Microcirculation* **16,** 58–83 (2009).

45. Barg, A., Ossig, R., Goerge, T., Schneider, M. F., Schillers, H., Oberleithner, H. & Schneider, S. W. Soluble plasma-derived von Willebrand factor assembles to a haemostatically active filamentous network. *Thromb. Haemost.* **97,** 514–26 (2007).

46. Peyvandi, F., Garagiola, I. & Baronciani, L. Role of von Willebrand factor in the haemostasis. *Blood Transfus.* **9,** 3–8 (2011).

47. Litvinov, R. I. & Weisel, J. W. What Is the Biological and Clinical Relevance of Fibrin? *Semin. Thromb. Hemost.* **42,** 333–43 (2016).

48. Brown, A. E. X., Litvinov, R. I., Discher, D. E., Purohit, P. K. & Weisel, J. W. Multiscale Mechanics of Fibrin Polymer: Gel Stretching with Protein Unfolding and Loss of Water. *Science* **325,** 741–744 (2009).

49. Pugsley, M. K. & Tabrizchi, R. The vascular system: An overview of structure and function. *J. Pharmacol. Toxicol. Methods* **44,** 333–340 (2000).

50. Palta, S., Saroa, R. & Palta, A. Overview of the coagulation system. *Indian J. Anaesth.* **58,** 515–23 (2014).

51. Varga-Szabo, D., Braun, A. & Nieswandt, B. Calcium signaling in platelets. *J. Thromb. Haemost.* **7,** 1057–1066 (2009).

52. Rau, J. C., Beaulieu, L. M., Huntington, J. A. & Church, F. C. Serpins in thrombosis, hemostasis and fibrinolysis J. *J. Thromb. Haemost.* **5,** 102–115 (2007).

53. Huntington, J. A. Serpin structure, function and dysfunction. *J. Thromb. Haemost.* **9,** 26–34 (2011).

54. Stavenuiter, F., Bouwens, E. a M. & Mosnier, L. O. Down-regulation of the clotting cascade by the protein C pathway. *Hematol. Educ.* **7,** 365–374 (2013).

55. Carrell, R. W. & Huntington, J. A. How serpins change their fold for better and for worse. *Biochem. Soc. Symp.* **70**, 163–178 (2003).

56. Cesarman-Maus, G. & Hajjar, K. A. Molecular mechanisms of fibrinolysis. *Br. J. Haematol.* **129,** 307–321 (2005).

57. Chapin, J. & Hajjar, K. A. Fibrinolysis and the control of blood coagulation. *Blood Rev* **29,** 17–24 (2015).

58. Reininger, A. J., Heijnen, H. F. G., Schumann, H., Specht, H. M., Schramm, W. & Ruggeri, Z. M. Mechanism of platelet adhesion to von Willebrand factor and microparticle formation under high shear stress. *Blood* **107,** 3537–3545 (2006).

59. Norström, E. & Escolar, G. *Natural anticoagulants and thrombophilia*. *Blood and Bone Marrow Pathology* (Ed. Anna Porwit, Jeffrey McCullough and Wendy N. Erber) 588-589 (Elsevier Ltd, 2011).

60. Johns Hopkins Medicine. Thrombosis. 2–4 (2018). Available at: https://www.hopkinsmedicine.org/healthlibrary/conditions/hematology_and_blood_disorders/thrombosis_85,P00105. (Accessed: 13th February 2018)

61. National Heart, Lung, and Blood Institute, N. Venous Thromboembolism. Available at: https://www.nhlbi.nih.gov/health-topics/venous-thromboembolism. (Accessed: 9th September 2018)

62. Bagot, C. N. & Arya, R. Virchow and his triad: A question of attribution. *Br. J. Haematol.* **143,** 180–190 (2008).

63. Kyrle, P. A. & Eichinger, S. Is Virchow's triad complete? *Blood* **114,** 1138–9 (2009).

64. Souto, J. C., Almasy, L., Borrell, M., Blanco-Vaca, F., Mateo, J., Soria, J. M., Coll, I., Felices, R., Stone, W., Fontcuberta, J. & Blangero, J. Genetic susceptibility to thrombosis and its relationship to physiological risk factors: the GAIT study. Genetic Analysis of Idiopathic Thrombophilia. *Am. J. Hum. Genet.* **67,** 1452–9 (2000).

65. National Heart, Lung, and Blood Institute, N. Atherosclerosis. *Health Topics* Available at: https://www.nhlbi.nih.gov/health-topics/atherosclerosis. (Accessed: 10th September 2018)

66. Libby, P. Inflammation in atherosclerosis. *Arterioscler. Thromb. Vasc. Biol.* **32,** 2045–2051 (2012).

67. Nesbitt, W. S., Westein, E., Tovar-Lopez, F. J., Tolouei, E., Mitchell, A., Fu, J., Carberry, J., Fouras, A. & Jackson, S. P. A shear gradient-dependent platelet aggregation mechanism drives thrombus formation. *Nat. Med.* **15,** 665–673 (2009).

68. Previtali, E., Bucciarelli, P., Passamonti, S. M. & Martinelli, I. Risk factors for venous and arterial thrombosis. *Blood Transfus.* **9,** 120–138 (2011).

69. Jagadeeswaran, P., Cooley, B. C., Gross, P. L. & Mackman, N. Animal Models of Thrombosis from Zebrafish to Nonhuman Primates: Use in the Elucidation of New Pathologic Pathways and the Development of Antithrombotic Drugs. *Circ. Res.* **118,** 1363–1379 (2016).

70. Levi, M., Dörffler-Melly, J., Johnson, G. J., Drouet, L. & Badimon, L. Usefulness and limitations of animal models of venous thrombosis. *Thromb. Haemost.* **86,** 1331–1333 (2001).

71. Todd, M. E., McDevitt, E. & Goldsmith, E. I. Blood-Clotting Mechanisms of Nonhuman Primates. *J. Med. Primatol.* **1,** 132–141 (1972).

72. Fuster, V., Lie, J. T., Badimon, U., Rosemark, J. A., Badimon, J.-J. & Bowie, E. J. W. Spontaneous and Diet-Induced Coronary Atherosclerosis in Normal Swine and Swine with von Wiiiebrand Disease. *Arteriosclerosis.* **5,** 67–73 (1985).

73. Sachs, U. & Nieswandt, B. *In Vivo* Thrombus Formation in Murine Models. *Circ. Res.* **100,** 979–991 (2007).

74. Cooper, S., Dick, M., Emmott, A., Jonak, P., Rouleau, L. & Leask, R. L. *In Vitro* Leukocyte Adhesion in Endothelial Tissue Culture Models Under Flow. in *Biomedical Science, Engineering and Technology* (ed. Dhanjoo N. Ghista) 191–208 (IntechOpen, 2012).

75. Roest, M., Reininger, A., Zwaginga, J. J., King, M. R. & Heemskerk, J. W. M. Flow chamber-based assays to measure thrombus formation *in vitro*: Requirements for standardization. *J. Thromb. Haemost.* **9,** 2322–2324 (2011).

76. Van Kruchten, R., Cosemans, J. M. E. M. & Heemskerk, J. W. M. Measurement of whole blood thrombus formation using parallel-plate flow chambers a practical guide. *Platelets* **23,** 229–242 (2012).

77. Girdhar, G. & Bluestein, D. Biological effects of dynamic shear stress in cardiovascular pathologies and devices. *Expert Rev. Med. Devices* **5,** 167–81 (2008).

78. Tran, R., Myers, D. R., Ciciliano, J., Trybus Hardy, E. L., Sakurai, Y., Ahn, B., Qiu, Y., Mannino, R. G., Fay, M. E. & Lam, W. A. Biomechanics of haemostasis and thrombosis in health and disease: from the macro- to molecular scale. *J. Cell. Mol. Med.* **17,** 579–596 (2013).

79. Whitesides, G. M. The origins and the future of microfluidics. *Nature* **442,** 368–373 (2006).

80. Duffy, D. C., McDonald, J. C., Schueller, O. J. A. & Whitesides, G. M. Rapid prototyping of microfluidic systems in poly(dimethylsiloxane). *Anal. Chem.* **70,** 4974–4984 (1998).

81. Xia, Y. & Whitesides, G. M. Soft lithography. *Annu. Rev. Mater. Sci.* **28,** 153–184 (1998).

82. Pasirayi, G., Auger, V., M. Scott, S., K.S.M. Rahman, P., Islam, M., O'Hare, L. & Ali, Z. Microfluidic Bioreactors for Cell Culturing: A Review. *Micro Nanosyst.* **3,** 137–160 (2011).

83. Zhao, B., Cui, X., Ren, W., Xu, F., Liu, M. & Ye, Z.-G. A Controllable and Integrated Pump-enabled Microfluidic Chip and Its Application in Droplets Generating. *Sci. Rep.* **7,** 1-8 (2017).

84. Jain, A., Barrile, R., van der Meer, A. D., Mammoto, A., Mammoto, T., De Ceunynck, K., Aisiku, O., Otieno, M. A., Louden, C. S., Hamilton, G. A., Flaumenhaft, R. & Ingber, D. E. Primary Human Lung Alveolus-on-a-chip Model of Intravascular Thrombosis for Assessment of Therapeutics. *Clin. Pharmacol. Ther.* **103,** 332–340 (2018).

85. Mcdonald, J. C., Duffy, D. C., Anderson, J. R. & Chiu, D. T. Fabrication of microfluidic systems in poly (dimethylsiloxane). *Electrophoresis* **21,** 27–40 (2000).

86. Byrnes, J. R. & Wolberg, A. S. New findings on venous thrombogenesis. *Hamostaseologie* **37,** 25–35 (2017).

87. Wrobleski, S. K., Farris, D. M., Diaz, J. A., Myers, D. D. & Wakefield, T. W. Mouse complete stasis model of inferior vena cava thrombosis. *J. Vis. Exp.* **52,** 2738 (2011).

88. Diaz, J. A., Farris, D. M., Wrobleski, S. K., Myers, D. D. & Wakefield, T. W. Inferior vena cava branch variations in C57BL/6 mice have an impact on thrombus size in an IVC ligation (stasis) model. *J. Thromb. Haemost.* **13,** 660–664 (2015).

89. Brill, A., Fuchs, T. A., Chauhan, A. K., Yang, J. J., De Meyer, S. F., Kollnberger, M., Wakefield, T. W., Lammle, B., Massberg, S. & Wagner, D. D. von Willebrand factor-mediated platelet adhesion is critical for deep vein thrombosis in mouse models. *Blood* **117,** 1400–1407 (2011).

90. Payne, H. & Brill, A. Stenosis of the Inferior Vena Cava: A Murine Model of Deep Vein Thrombosis. *J. Vis. Exp.* **130***,* 56697 (2017).

91. Diaz, J. A., Wrobleski, S. K., Hawley, A. E., Lucchesi, B. R., Wakefield, T. W., Myers, D. D. & Jr. Electrolytic inferior vena cava model (EIM) of venous thrombosis. *J. Vis. Exp.* **53***,* e2737 (2011).

92. Barrile, R., van der Meer, A. D., Park, H., Fraser, J. P., Simic, D., Teng, F., Conegliano, D., Nguyen, J., Jain, A., Zhou, M., Karalis, K., Ingber, D. E., Hamilton, G. A. & Otieno, M. A. Organ-on-Chip Recapitulates Thrombosis Induced by an anti-CD154 Monoclonal Antibody: Translational Potential of Advanced Microengineered Systems. *Clin. Pharmacol. Ther.* **00,** 1–9 (2018).

93. Palladino, M. A., Bahjat, F. R., Theodorakis, E. A. & Moldawer, L. L. Anti-TNF-α therapies: The next generation. *Nat. Rev. Drug Discov.* **2,** 736–746 (2003).

94. Liu, Z. Molecular mechanism of TNF signaling and beyond. *Cell Res.* **15,** 24–27 (2005).

95. Baudin, B., Bruneel, A., Bosselut, N. & Vaubourdolle, M. A protocol for isolation and culture of human umbilical vein endothelial cells. *Nat. Protoc.* **2,** 481–485 (2007).

96. Ganguly, A., Zhang, H., Sharma, R., Parsons, S. & Patel, K. D. Isolation of human umbilical vein endothelial cells and their use in the study of neutrophil transmigration under flow conditions. *J.*

Vis. Exp. **66,** e4032 (2012).

97. Smith, Q., Macklin, B., Chan, X. Y., Jones, H., Trempel, M., Yoder, M. C. & Gerecht, S. Differential HDAC6 Activity Modulates Ciliogenesis and Subsequent Mechanosensing of Endothelial Cells Derived from Pluripotent Stem Cells. *Cell Rep.* **24,** 895–908 (2018).

98. Heiss, M., Hellström, M., Kalén, M., May, T., Weber, H., Hecker, M., Augustin, H. G. & Korff, T. Endothelial cell spheroids as a versatile tool to study angiogenesis *in vitro*. *FASEB J.* **29,** 3076–3084 (2015).

99. van der Meer, A. D., Orlova, V. V., ten Dijke, P., van den Berg, A. & Mummery, C. L. Three-dimensional co-cultures of human endothelial cells and embryonic stem cell-derived pericytes inside a microfluidic device. *Lab Chip* **13,** 3562 (2013).

100. Bezenah, J. R., Kong, Y. P. & Putnam, A. J. Evaluating the potential of endothelial cells derived from human induced pluripotent stem cells to form microvascular networks in 3D cultures. *Sci. Rep.* **8,** 1–10 (2018).

101. Setyawati, M. I., Tay, C. Y., Docter, D., Stauber, R. H. & Leong, D. T. Understanding and exploiting nanoparticles' intimacy with the blood vessel and blood. *Chem. Soc. Rev.* **44,** 8174–99 (2015).

102. Takahashi, K. & Yamanaka, S. Induction of Pluripotent Stem Cells from Mouse Embryonic and Adult Fibroblast Cultures by Defined Factors. *Cell* **126,** 663–676 (2006).

103. Malik, N. & Rao, M. S. A Review of the Methods for Human iPSC Derivation. *Methods Mol. Biol.* **997,** 23–33 (2013).

104. Lin, Y., Gil, C.-H. & Yoder, M. C. Differentiation, Evaluation, and Application of Human Induced Pluripotent Stem Cell–Derived Endothelial Cells. *Arterioscler. Thromb. Vasc. Biol.* **37,** 2014-2025 (2017).

105. Choi, K.-D., Yu, J., Smuga-Otto, K., Salvagiotto, G., Rehrauer, W., Vodyanik, M., Thomson, J. & Slukvin, I. Hematopoietic and endothelial differentiation of human induced pluripotent stem cells. *Stem Cells* **27,** 559–567 (2009).

106. Sahara, M., Hansson, E. M., Wernet, O., Lui, K. O., Später, D. & Chien, K. R. Manipulation of a VEGF-Notch signaling circuit drives formation of functional vascular endothelial progenitors from human pluripotent stem cells. *Cell Res.* **24,** 820–841 (2014).

107. Prasain, N. *et al.* Differentiation of human pluripotent stem cells to cells similar to cord-blood endothelial colony-forming cells. *Nat. Biotechnol.* **32,** 1151–1157 (2014).

108. White, M. P., Rufaihah, A. J., Liu, L., Ghebremariam, Y. T., Ivey, K. N., Cooke, J. P. & Srivastava, D. Limited Gene Expression Variation in Human Embryonic Stem Cell and Induced Pluripotent Stem Cell Derived Endothelial Cells. *Stem Cells* **31,** 92–103 (2013).

109. Ohtani-Kaneko, R., Sato, K., Tsutiya, A., Nakagawa, Y., Hashizume, K. & Tazawa, H. Characterisation of human induced pluripotent stem cell-derived endothelial cells under shear stress using an easy-to-use microfluidic cell culture system. *Biomed. Microdevices* **19,** 91 (2017).

110. Ikuno, T., Masumoto, H., Yamamizu, K., Yoshioka, M., Minakata, K., Ikeda, T., Sakata, R. & Yamashita, J. K. Efficient and robust differentiation of endothelial cells from human induced pluripotent stem cells via lineage control with VEGF and cyclic AMP. *PLoS One* **2,** 1–18 (2017).

111. Tan, K. S., Tamura, K., Lai, M. I., Veerakumarasivam, A., Nakanishi, Y., Ogawa, M. & Sugiyama, D. Molecular Pathways Governing Development of Vascular Endothelial Cells from ES/iPS Cells. *Stem Cell Rev. Reports* **9,** 586–598 (2013).

112. Vogenberg, F. R., Isaacson Barash, C. & Pursel, M. Personalized medicine - part 1: evolution and development into theranostics. *Pharm. Ther.* **35,** 560–76 (2010).

113. Runyon, M. K., Kastrup, C. J., Johnson-Kerner, B. L., Van Ha, T. G. & Ismagilov, R. F. Effects of Shear Rate on Propagation of Blood Clotting Determined Using Microfluidics and Numerical Simulations. *J. Am. Chem. Soc.* **130,** 3458–3464 (2008).

114. Neeves, K. B., Maloney, S. F., Fong, K. P., Schmaier, A. A., Kahn, M. L., Brass, L. F. & Diamond, S. L. Microfluidic focal thrombosis model for measuring murine platelet deposition and stability: PAR4 signaling enhances shear-resistance of platelet aggregates. *J. Thromb. Haemost.* **6,** 2193–2201 (2008).

115. Charles, R. G. & Epstein, E. J. Diagnosis of coronary embolism: a review. *J. R. Soc. Med.* **76,** 863–869 (1983).

116. Nesbitt, W. S., Mangin, P., Salem, H. H. & Jackson, S. P. The impact of blood rheology on the molecular and cellular events underlying arterial thrombosis. *J. Mol. Med.* **84,** 989–995 (2006).

117. Ni, H., Denis, C. V, Subbarao, S., Degen, J. L., Sato, T. N., Hynes, R. O. & Wagner, D. D. Persistence of platelet thrombus formation in arterioles of mice lacking both von Willebrand factor and fibrinogen. *J. Clin. Invest.* **106,** 385–92 (2000).

118. Rossi, F., Rossi, E., Pareti, F. I., Colli, S., Tremoli, E. & Gallo, L. *In vitro* measurement of platelet glycoprotein IIb/IIIa receptor blockade by abciximab: interindividual variation and increased platelet secretion. *Haematologica* **86,** 192–8 (2001).

119. Orlova, V. V, van den Hil, F. E., Petrus-Reurer, S., Drabsch, Y., ten Dijke, P. & Mummery, C. L. Generation, expansion and functional analysis of endothelial cells and pericytes derived from human pluripotent stem cells. *Nat. Protoc.* **9,** 1514–1531 (2014).

120. Belt, H., Koponen, J. K., Kekarainen, T., Puttonen, K. A., Mäkinen, P. I., Niskanen, H., Oja, J., Wirth, G., Koistinaho, J., Kaikkonen, M. U. & Ylä-Herttuala, S. Temporal Dynamics of Gene Expression During Endothelial Cell Differentiation From Human iPS Cells: A Comparison Study of Signalling Factors and Small Molecules. *Front. Cardiovasc. Med.* **5,** 1–15 (2018).

121. Orlova, V. V., Van Den Hil, F. E., Petrus-Reurer, S., Drabsch, Y., Ten Dijke, P. & Mummery, C. L. Generation, expansion and functional analysis of endothelial cells and pericytes derived from human pluripotent stem cells. *Nat. Protoc.* **9,** 1514–1531 (2014).

122. Stevenson, M. D., Sieminski, A. L., McLeod, C. M., Byfield, F. J., Barocas, V. H. & Gooch, K. J. Pericellular conditions regulate extent of cell-mediated compaction of collagen gels. *Biophys. J.* **99,** 19–28 (2010).

123. Dartsch, P. C. & Betz, E. Response of cultured endothelial cells to mechanical stimulation. *Basic Res. Cardiol.* **84,** 268–281 (1989).

124. Sivarapatna, A., Ghaedi, M., Xiao, Y., Han, E., Aryal, B., Zhou, J., Fernandez-Hernando, C., Qyang, Y., Hirschi, K. K. & Niklason, L. E. Engineered Microvasculature in PDMS Networks Using Endothelial Cells Derived from Human Induced Pluripotent Stem Cells. *Cell Transplant.* **26,** 1365–1379 (2017).

125. Sivarapatna, A., Ghaedi, M., Le, A. V, Mendez, J. J., Qyang, Y. & Niklason, L. E. Arterial specification of endothelial cells derived from human induced pluripotent stem cells in a biomimetic flow bioreactor. *Biomaterials* **53,** 621–33 (2015).

126. Sivarapatna, A., Ghaedi, M., Xiao, Y., Han, E., Aryal, B., Zhou, J., Fernandez-Hernando, C., Qyang, Y., Hirschi, K. K. & Niklason, L. E. Engineered Microvasculature in PDMS Networks Using Endothelial Cells Derived from Human Induced Pluripotent Stem Cells. *Cell Transplant.* **26,** 1365–1379 (2017).

127. Santaguida, S., Janigro, D., Hossain, M., Oby, E., Rapp, E. & Cucullo, L. Side by side comparison between dynamic versus static models of blood–brain barrier *in vitro*: A permeability study. *Brain Res.* **1109,** 1–13 (2006).

128. George, R., Bhatt, A., Narayani, J., Thulaseedharan, J. V., Sivadasanpillai, H. & Tharakan, J. A. Enhanced P-selectin expression on platelet-a marker of platelet activation, in young patients with angiographically proven coronary artery disease. *Mol. Cell. Biochem.* **419,** 125–133 (2016).

129. Freitas Jr, R. A. Cytometrics. in *Nanomedicine, Volume I: Basic Capabilities,* 247 (Landes Bioscience, 1999).

130. Salipante, P. F., Little, C. A. E. & Hudson, S. D. Jetting of a shear banding fluid in rectangular ducts. *Phys. Rev. Fluids* **2,** 1–25 (2017).

131. Dela Paz, N. G., Walshe, T. E., Leach, L. L., Saint-Geniez, M. & D'amore, P. A. Role of shear-stress-induced VEGF expression in endothelial cell survival. *J. Cell Sci.* **125,** 831–843 (2012).

VI. Appendices

Appendix I. Estimation of shear stress after medium replacement

Shear stress, the stress created by a tangential force on a surface, represents the friction which a certain fluid will impose to the cells in contact with it. For Newtonian fluids and laminar flow, shear stress increases with velocity and viscosity. The simplified relationship between shear stress (dyne/cm^2), τ, and shear rate (s^{-1}), γ, influenced by the dynamic viscosity of the fluid, (dyne.s/cm^2), η, is given by equation 1[15]:

$$\tau = \eta \times \gamma \quad (1)$$

The analytical methods do accurately calculate flow and shear stress in complex microfluidic setups would involve the resolution of the Navier-Stokes equation. However, for simple designs, such as straight, rectangular-shaped channels, and assuming an incompressible fluid, an equation for shear rate can be derived as a function of the volumetric flow rate, Q, and the channel dimensions (width, w, and height, h)[130]:

$$\gamma = \frac{6Q}{h^2 w} \quad (2)$$

or

$$\tau = \frac{6\eta Q}{h^2 w} \quad (3)$$

To simplify the estimation of the flow rate at the channel after medium replacement, two approximations had to be done: the flow was considered to be constant from the moment both pipette tips (one empty and one full) were introduced in the reservoirs until the moment an equilibrium was reached; the elapsed time between those two time points was approximately 1 hour (from estimations done during experiments). Since the pipette tip was filled with 200 µl of fresh medium and considering that the small volume located inside the channel at a certain moment is not significant, it was considered that the equilibrium was reached when both pipette tips had 100 µl:

$$Q = \frac{V}{t} = \frac{100}{3600} = 2.83 \times 10^{-2} \frac{\mu l}{s} = 2.83 \times 10^{7} \frac{\mu m^3}{s}$$

Shear rate can then be estimated with equation (2):

$$\gamma = \frac{6 \times 2.83 \times 10^7}{50^2 \times 300} = 226.4\, s^{-1}$$

Or, using equation 3 and considering a reported value of dynamic viscosity of EGM-2 culture medium[131] of 7.50 x 10^{-3} dyne.s/cm^2, we can estimate a shear stress value of approximately 1.70 dyne/cm^2.

Since, as described in section 1.2 of the Introduction, shear rate value up to 250 s^{-1} are representative of venous environment and Hathcock[15] consider venous wall shear stress values ranging from 1 to 10 dyne/cm^2, values obtained during medium replenishing in the channels are deemed of relevance for exposed cells.

Appendix II. TNF-α molecules in microwells and microfluidic channels

The concentration of TNF-α used in experiments with microwells and with the microfluidic devices was 10 ng/mL. However, the response of the cells was exacerbated in microwells. The hypothesis was that, although the concentration was the same, cells would be exposed more intensively to molecules of the inflammatory agents in microwells.

For the microfluidic channels, the volume of medium in the channel, considering its dimensions, would be:

$$V_{channel} = w \times h \times l \tag{4}$$

$$= 300 \times 50 \times 1.0 \times 10^4 = 1.5 \times 10^8 \mu m^3 = 1.5 \times 10^{-1}\ \mu L$$

Since the seeding density was around 15 x 10^6 cells/mL, and considering 100% viability and attachment of the cells in the channel, then:

$$Viable\ cells\ per\ channel = C_{cells} \times V_{channel} \tag{5}$$

$$= 15 \times 10^6 \times 1.5 \times 10^{-4} = 2250\ viable\ cells/channel$$

On the other hand, the mass of TNF-α per each cell in the channel can be given by:

$$TNF\ mass\ per\ cell = \frac{C_{TNF} \times V_{channel}}{Cells\ in\ the\ channel} \tag{6}$$

$$= \frac{10 \times 1.5 \times 10^{-4}}{2250} = 6.7 \times 10^{-7}\ ng/cell$$

Considering the molar mass of soluble TNF-α (17 kDa) the number of TNF-α molecules per cell can be estimated:

$$TNF\ molecules\ per\ cell = \frac{Mass\ TNF\ per\ cell}{Molar\ mass\ of\ TNF} \times \frac{Molecules}{mol} \tag{7}$$

$$= 6.7 \times 10^{-7} \frac{ng}{cell} \times 10^{-9} \frac{g}{ng} \times (1.7 \times 10^4)^{-1} \frac{mol}{g} \times 6.022 \times 10^{23} \frac{molecules}{mol} = 2.4 \times 10^4\ molecules/cell$$

In a microwell, considering 200 µl of medium were used and that the seeding density was around 5 x 10^4 cells/mL (and the same viability and attachment), using equation 5:

$$C_{cells} \times V_{channel} = 5 \times 10^4 \times 200 \times 10^{-3} = 10000\ cells/microwell$$

And the mass and number of molecules of TNF-α per each cell can be given by equations 6 and 7:

$$\frac{C_{TNF} \times V_{channel}}{Cells\ in\ the\ channel} = \frac{10 \times 200 \times 10^{-3}}{10000} = 2.0 \times 10^{-4}\ ng/cell$$

$$\frac{Mass\ TNF\ per\ cell}{Molar\ mass\ of\ TNF} \times \frac{Molecules}{mol} = 7.1 \times 10^6\ molecules/cell$$

These estimations indicate that each cell in the microwell platform was exposed to a higher number of molecules of the inflammatory agent. To compare these amounts, the ratio between the number of TNF-α molecules per each cell in a microwell and a microfluidic channel was calculated as:

$$\frac{7.1 \times 10^6}{2.4 \times 10^4} = 296$$

This means that each cell in the microwell was exposed to 296 times more molecules of the inflammatory agent than each cell in the microfluidic channel.